Identification and Characterization of G Protein Signaling Networks by Proximity Labeling-Coupled Proteomics

by

Naincy Chandan

A dissertation submitted in partial fulfillment
of the requirements for the degree of
Doctor of Philosophy
(Pharmacology)
in the University of Michigan
2021

Doctoral Committee:

Professor Alan V. Smrcka, Chair
Professor Alexey Nesvizhskii
Professor Carole Parent
Associate Professor Manojkumar Puthenveedu
Associate Professor Gregory Tall

Naincy Ramniklal Chandan

nchandan@umich.edu

ORCID ID: 0000-0001-8097-1867

Dedication

Dedicated to my Mummy ***(Pratima Chandan)****, my Pappa* ***(Ramnik Chandan)****, and my alter ego-*

my younger brother ***(Viral Chandan)***

whose love and support have made this possible.

Acknowledgements

Starting from the engineering of super cool light-activatable G protein to embarking on the journey of finding new interactors for many G protein subtypes, my journey in the Smrcka lab is beyond my imagination. First and foremost, I would like to express my sincere thanks to my mentor, Dr. Alan Smrcka. His guidance, incessant encouragement, and prudent suggestions with sound perception. He is a constant source of knowledge and new ideas in the frontiers of the research world. All his suggestions, intelligent planning, valuable advice, and trust in me were the backbone of this work. His love and passion for science are contagious, and if I can retain half of the enthusiasm he has at this age, I would consider it my lifetime achievement. Thank you, Alan, for giving me a great deal of freedom to pursue my ideas. Though not always fruitful, all these experiences have truly shaped how I think about and conduct science. Second, I want to thank the members of my thesis committee: Drs. Alexey Nesvizhskii, Carole Parent, Manojkumar Puthenveedu, and Gregory Tall. You all have been very influential in advancing my research project; thank you for your efforts.

Best teachers teach from the heart, not from the book. My research mentor Dr. Sundeep Malik is one such. Words can’t express my gratitude towards him, whose help was always a call away. He is the first one who comes to my mind when I think about any research problem or seek advice regarding anything and everything in the lab. His words, “I wanted to do all the experiments yesterday”, inspires me to work harder every day. Besides my research mentor, he is my friend and support. I would like to express my deepest appreciation and gratitude to Dr. Jorge A. Iñiguez-Lluhí for inculcating a love of Pharmacology in me and generously volunteering the time to discuss

my research ideas, troubleshoot my experiments, and pushing me to think about my research from a different perspective.

I wish to thank all current and past members in the Smrcka laboratory at UM including, Dr. Saji Abraham, Wenhui Wei, Dr. Hoa Phan, Nathalie Momplaisir, Joseph Loomis, Tyler Lefevre, Michael Burroughs, Gissell Sanchez, as well as past members Jesi To, Rafael Gil de Rubio, and Isaac Fisher for discussing the data, experimental procedures, and their wisdom. They not only provided suggestions, guidance and feedback on my research project but also made the Smrcka lab fun and stimulating environment. In addition to lab mates, I have found lifetime friends in Saji and Wenhui. They have been my constant supports during all the hard times in my professional and personal life. I have celebrated all our tiniest excitements and cried on their shoulders during failures. I owe them for life. Thank you, Amanda Smrcka, for taking the time for organizing all the Smrcka lab retreats and hosting us for countless dinners and lunches. Thank U of M Pathology core, especially Venkatesha Barsur, Alexey Nesvizhskii, and Kevin Conlon for running mass spec samples as well as for advice on the data analysis.

I am grateful to Dr. Mathew Brody and his postdoc Dr. Kobina Essandoh for all scientific discussions, sharing reagents, help in troubleshooting, and friendship. Special thanks to Parent lab member Dr. Shuvasree SenGupta for sharing her knowledge on neutrophils and isolated neutrophils. Thank you to Srilakshmi Yalavarthi and Dr. Gautam Sule for all the help during neutrophils experiments and for providing isolated neutrophils during the optimization experiments. I am very grateful that I was assigned as a GSI MC600 for Dr. Mustapha Beleh's course. In addition to a mentor, I found a friend in him.

In the Pharmacology Department, I want to thank Drs. Lori Isom and Margret Gnegy for their great leadership. I sincerely thank Drs. Steve Fisher, Yoichi Osawa, and Ronald Holz for the

valuable advice during seminar practice sessions. I want to express my appreciation to the office staff for all the help on everything, including Elizabeth Oxford, Josh Daniels, Ingrid Shriner-Ward, Dar-Weia Liao, Audrey Morton-Dziekan, and Lisa Garber.

I would like to express my utmost gratitude to my parents, Ramnik and Pratima Chandan, for their encouragement, above and beyond love, immense support, and all their sacrifices. Thank you for allowing me the freedom to truly be myself and to follow my own dreams. I am very thankful to my younger brother and my most favorite person, Viral Chandan, who has always been with me through his prayers, endowed me with tremendous encouragement and inspiration. Thank you for being there while I was dreaming about pursuing PhD until I finish writing this thesis and beyond. Thank you for remembering our time difference, assignments' deadlines, food schedule, our virtual birthday celebrations, sending packages during festival times, piano sessions, and whatnot. They keep me grounded, and if it weren't for their prayers, encouragement, and faith in me, I wouldn't have been able to achieve anything. I consider it a privilege to express my gratitude to my fiancé Dr. Sunny Trivedi, for always being like a candle that enlightened my mind during the darkest moments, not only during work but also in the walk of life. He has been a constant strength, and I am forever indebted to him for his support throughout this process. Thank you for having faith in me when I didn't have it in myself. Thank you to my in-laws, especially my mother-in-law, Harsha Trivedi, for countless acts of love and support during the course. My sincere thanks go to my cousins, Palak, Falguni, Bhavna, Kishan, Khushboo, Sara, Harshal, Parin, Vishal, Pooja, Jinal, for always remembering me in every celebration and for warmly welcoming me with much love every time I come home. My niece and nephews Vansh, Nivaan, Aaraya, Vihaan, Hayan, Angel, Dhyana, Yashi, and Vritee for being the cutest and sweetest they are. I am thankful to my extended family for countless acts of trust, understanding and kindness in difficult times.

I am thankful to Dr. Disheet Shah for always bringing a new perspective to science and life, teaching me great life lessons, and inspiring me even on a Sunday! I am very thankful to have found badminton buddies who became close friends, who helped me manage my work-life balance. Thank you, Dinesh Kommireddi, Anvesh Tavva, Sudeep Manjunath, Kush Goliya, Shashank Nair, Partha Dutta, Yakshita Malhotra, and Masthan Sayed, for amazing badminton, board-game, and cooking sessions. Special thanks to Dinesh for all the bio and non-bio information exchange sessions, sharing good laughs, and great philosophical discussions. I am very grateful to my friend Tavva for countless lessons of wisdom and advice, including "don't look at the problems as you look at the cells in the microscope" to "life is short, Nanba, always be happy". Thank you for lightninging my mood during stressful times, for all the reminders for errands, and for feeding me countless times during this period. I am very thankful to Drs. Palak Shah, Nabanita Saha, Seema Chugh, Pankaj Vats and Jaya Priyadidi, who make me feel like a home away from home. Thanks to my friends from Rochester, especially Dr. Sutirtha Chowdhury, Dr. Rakesh Chatrikihi and Somjit Bhar, and Arjun Uthamaraj, who have always been there irrespective of distance. Thanks to all my amazing flatmates and friends, Drs. Jesi To, Tanvi Gujarati, Pooja Panwalkar, Sanjima Pal and Prachi Atmasiddha.

The Universe has been most beneficent and merciful to me and has provided me strength during the research efforts and blessed me with the presence of many people who have helped me in this journey. Apart from my efforts, the success of this thesis largely depends on the encouragement and guidance of many others, who directly or indirectly contributed to my growth, and influenced thinking, behavior. And last but not least, thank you to all the scientists for their tireless efforts and research papers, which definitely is inseparable part of my research endeavors.

Table of Contents

List of Figures

List of Tables

Abstract

Cell signaling networks control the ability of the cells to function and maintain equilibrium with intracellular and extracellular milieus. These networks are highly complex and tightly regulated, as they control essential functions in the body. Dysregulation of any of the pathways can lead to various pathophysiological disorders. Cell migration and adhesion are fundamental biological processes regulated by chemokine G-protein-coupled receptors (GPCRs). Chemokine receptors primarily couple to the Gi/o family of G proteins, composed of $G\alpha_i$ and $G\beta\gamma$ subunits. In the inactive form, $G\alpha_i$ is bound to GDP and $G\beta\gamma$. Receptor activation triggers the exchange of GDP for GTP on $G\alpha_i$, leading to its dissociation from the receptor and the $G\beta\gamma$ complex.

The role of $G\beta\gamma$ subunits released from G_i heterotrimers in chemokine signaling has been well characterized and is thought to be the major signal transducer. Lack of tools to manipulate $G\alpha_i$ signaling lead to the conclusion that it has no signaling role other than to regulate the release of $G\beta\gamma$. By developing the selective activator of $G\beta\gamma$, without $G\alpha_i$ activation; our recent work has discovered novel roles for $G\alpha_i$ in migration of neutrophils and fibrosarcoma cells, downstream of chemoattractant receptors. However, the molecular targets of $G\alpha_i$ in these processes remain to be identified. Driven by the possibility that multiple targets of G_i-coupled receptors remain to be identified, we adopted an intact cell proximity-based labeling approach using BioID2 (promiscuous biotin ligase enzyme)-coupled to mass spectrometry (MS).

We screened for proteins that are differentially labeled in $G\alpha_{i1}$-WT (inactive) vs $G\alpha_{i1}$-QL (constitutively active), expressing cells. We confirmed that BioID2 fused $G\alpha_{i1}$ performs unaltered signaling functions and localizes to the PM in HT1080 fibrosarcoma cells. Tandem mass tag

(TMT)-MS with BioID2-fused $G\alpha_{i1}$, $G\alpha_{i1}$-QL and BioID2-CaaX (as a membrane- targeted control) was performed and known interactors of G protein α subunits including GPCRs, Gβ and Gγ, adenylate cyclase (AC), Resistance to inhibitors of cholinesterase 8A (Ric8A), and others were identified. Following the success of the BioID2-$G\alpha_i$ screen, we performed proximity-based labeling coupled MS screen for another G proteins subtype, $G\alpha_q$. This was done using TurboID, an improved enzyme with faster labeling kinetics. Multiple known interactors, including PLCβ isoforms 1,3 and 4, RhoGEF; Trio, Kalirin, and p63RhoGEF, were selectively enriched in the TurboID-$G\alpha_q$-QL samples relative to TurboID-$G\alpha_q$.

In our screen, multiple potential candidate interactor proteins were identified and validated for selective biotinylation by BioID2-$G\alpha_{i1}$-QL. This suggests a previously unappreciated network of interactions for activated $G\alpha_i$ proteins in intact cells. Extensive characterization of one candidate protein, PDZ-RhoGEF (PRG), using *in vitro* cell-based and biochemical assays revealed that active $G\alpha_{i1}$ strongly activates and interacts with PRG. Strikingly, large differences in the ability of $G\alpha_{i1,}$ $G\alpha_{i2,}$ and $G\alpha_{i3}$ isoforms to activate PRG were observed despite over 85% sequence identity. We also demonstrate the functional relevance of the interaction between active $G\alpha_i$ and PRG in primary human neutrophils. Besides, we identified a number of RasGAP proteins in MS, which we validated by co-immunoprecipitation and are currently characterizing it.

Given the ubiquitous presence of Gi and Gq-coupled receptors and G proteins, identification, and characterization of their binding partners both individually and in networks provides insights that will unravel multiple novel physiological roles of these receptors. In addition, it can identify novel therapeutic targets and contribute to understanding the on and off-target effects of drugs that directly target GPCRs leading to the development of safer drugs.

Chapter-1

General Introduction

1.1 Cellular signaling

Signal transduction, or cell signaling, is a basic process of information transmission between cells or cells and the environment. All cells receive, process, and respond to environmental cues to survive, grow, and reproduce. The cues can be electrical, mechanical, or chemical in nature. Electrical signals depend on the change in the ionic potential of the cells, whereas mechanical signals include shear stress or pressure, stretching, compression, sound, etc. A plethora of molecules, including proteins, amino acids, nucleotides, fatty acids, lipids, ions or even gases, are classified as chemical signals. Signals can trigger a response in neighboring or distant cells, and the mechanisms to achieve the response, at a fundamental level, involve receiver proteins called receptors.

Most receptors are on the cell surface, while some are intracellular. G protein-coupled receptors (GPCRs), enzyme-linked protein receptors, and ion channel-coupled receptors are three major classes of cell surface receptors. GPCRs bind a ligand and activate membrane-associated G proteins. Enzyme-linked receptors associate with an enzyme intracellularly or are enzymes themselves. Ligand-gated ion channels, upon activation, bind a ligand and briefly open a channel through the membrane that allows specific ions to pass through.

Receptors have three main domains: an extracellular ligand-binding domain, a hydrophobic transmembrane domain, and an intracellular domain. Intracellular receptors are

typically present in the cytoplasm, nucleus, or intracellular membranes and bind to hydrophobic ligand molecules that can diffuse directly across the plasma membrane (PM) [1-4].

Upon receptor activation, the signal is transduced inside the cell via activation, inactivation, or recruitment of multiple specific intracellular signaling and effector proteins to execute a cellular response (Fig. 1.1). Thus, activation of a few receptors results in multiple catalytic second messenger production, thereby amplifying the initial signal. Signal amplification of the small stimulus to larger physiological changes allows precise and appropriate control of the physiological responses. These processes are dynamically regulated with changing environmental cues. The speed of signal transduction depends on the type of response exerted by the ligand. Changes in the electrical potential by ion movement or a change in the signaling activity of the proteins already present in the cell generally takes milliseconds to seconds. In contrast, the involvement of gene transcription and protein translation steps require minutes to hours.

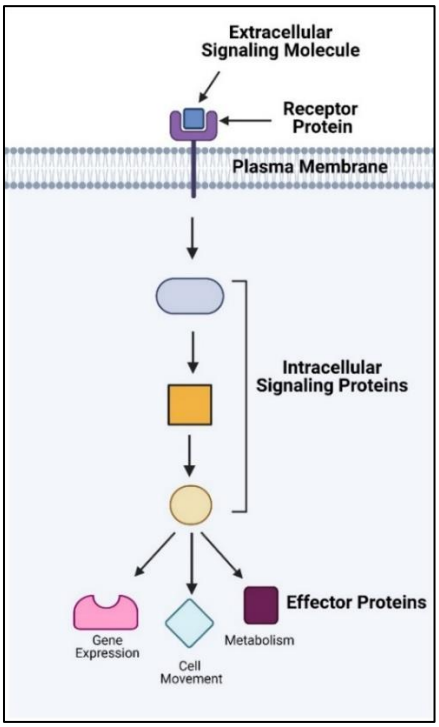

Figure 1.1: Schematic representation of a basic cellular signaling process.
The binding of extracellular signaling molecules initiates activation of a receptor protein, which transduces signals to intracellular proteins leading to signal amplification to generate the desired response. Adapted from [5]. Created with Biorender.com

Cell signaling processes are highly complex and regulate all aspects of cellular behavior, including survival, division, differentiation, movement, and metabolism, to name a few. Tight regulation of these signaling cascades is essential for the body's normal functions; therefore, dysregulation of signaling pathways can lead to various pathophysiological disorders. Therefore, understanding the signaling processes regulated by receptors is critical not only for the basic understanding of biology and the development of new pharmaceuticals, but also for understanding how existing drugs exert their therapeutic functions. This thesis will focus on signaling pathways downstream of GPCRs.

1.2 G protein-coupled receptors (GPCRs)

G protein-coupled receptors (GPCRs) are among the largest and most diverse family of cell surface receptors. GPCRs constitute ~1000 annotated genes corresponding to ~4% of all the genes and up to 1-5% of the total proteins in a cell [6-9]. Around 35% of all drugs approved by the US Food and Drug Administration (FDA) target GPCRs. Currently, ~110 out of ~800 known GPCRs are targeted by drugs, which only constitutes ~14% of the total receptors [10, 11]. Hence, discovering the signaling pathways of these receptors may open the doors for designing new therapies.

GPCRs regulate diverse processes in the body where they play major roles in the normal functioning of the nervous, cardiovascular, endocrine, and immune systems. Dysregulation of GPCR signaling can lead to a range of diseases such as cardiovascular diseases, rheumatoid arthritis, diabetes, asthma, and cancer [12-15]. Therefore, detailed elucidation of the molecular components of GPCR signaling pathways is important to improve our understanding of the biology

and pathophysiology regulated by these pharmacologically important receptors and aid in the identification of novel, alternative therapeutic targets. In addition, a comprehensive understanding of the signaling pathways regulated by the drug targets will not only aid in developing safer drugs but also understand the off-target effects or on-target side effects of existing drugs [16].

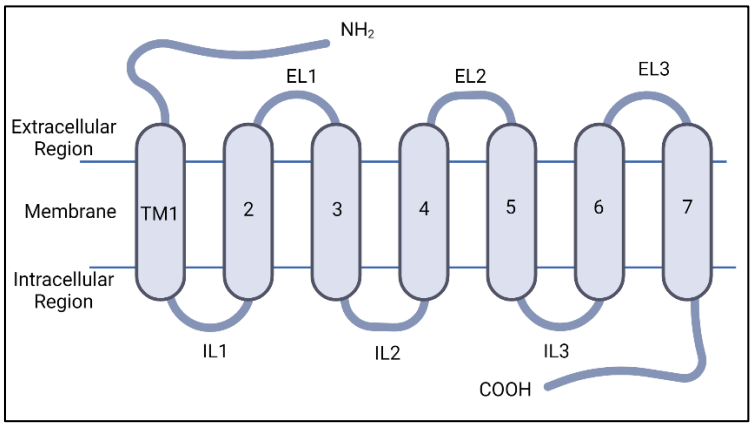

Figure 1.2: Topological representation of GPCR structure showing seven transmembrane domains (TM1-7) and EL1-3 and IL1-3 loops.
Adapted from [17]

GPCRs are named for their ability to bind and activate guanine-nucleotide binding proteins (G proteins). They are seven-transmembrane (7-TM) receptors, characterized by an extracellular amino-terminus (N-terminus) and intracellular carboxy-terminus (C-terminus) connected by seven membrane-spanning α helical bundles. These TM1-7 are connected by six interhelical loops- three extracellular (EL1-3) and three intracellular (IL1-3) loops (Fig. 1.2). GPCRs are classified by sequence homology into 5 families: Rhodopsin (Family A), Secretin (Family B), Glutamate (Family C), Frizzled/Taste2, and Adhesion [18]. Family A receptors are the largest and by far the most studied GPCR class, which include adrenergic, dopamine, serotonin, opioid, and chemokine receptors.

GPCRs can bind to a plethora of chemically diverse molecules, including lipids, peptides, proteins, biogenic amines, sugar, hormones, amino acids, nucleotides, chemokines, sensory stimuli such as odor, taste and even light! In the basal state, receptors are in dynamic equilibrium between

active and inactive states. Agonist or partial agonist binding to the orthosteric site (endogenous agonist binding site) on the receptor stabilizes the active state of the receptor and increases receptor Guanine Nucleotide Exchange Factor (GEF) activity. Increased GEF activity facilitates the exchange of GDP for GTP on G proteins. Allosteric modulators bind to allosteric sites, sites distinct from the orthosteric site, and promote distinct conformation states that changes the intrinsic properties of the receptor toward the orthosteric ligand [19]. Depending on the G protein subtype the receptor is coupled to, a variety of downstream signaling pathways can be activated.

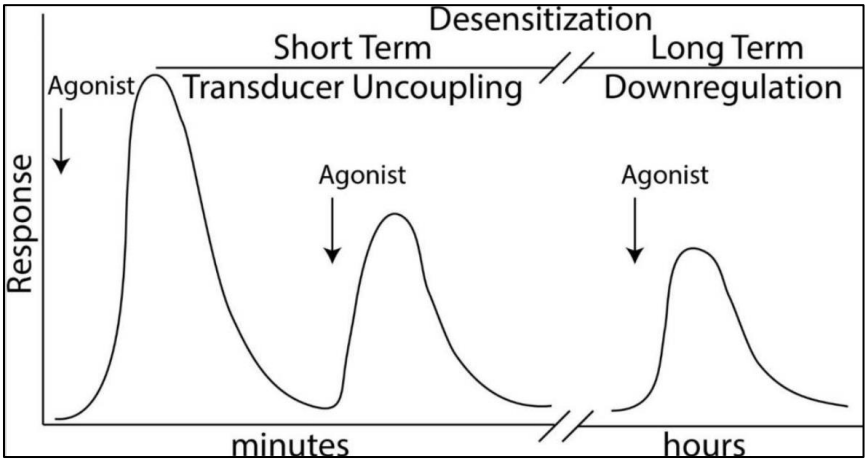

Figure 1.3: Short and long-term receptor stimulation and desensitization mechanism.
Adapted from [20].

GPCR signaling can be attenuated by ligand occupied receptor phosphorylation by second-messenger kinases such as protein kinase A (PKA) and protein kinase C (PKC), or by G protein receptor kinases (GRKs) within sec to mins of agonist stimulation. Phosphorylation of the receptor by GRK leads to β-arrestin recruitment and receptor endocytosis via clathrin-coated vesicles [21-27]. Receptor phosphorylation is reversed by phosphatases present in intracellular vesicles, and thus the internalized receptors can be recycled back to the PM following removal of the agonist [28-32]. Repeated receptor activation results in a decreased response compared to the initial response, and this process is referred to as desensitization (Fig. 1.3). Prolonged stimulation of the

receptor for several hours results in decreased receptor expression at the PM and receptor downregulation, mostly by proteolytic degradation and proteolysis of the receptor often carried out in lysosomes [20, 33-37].

1.3 Heterotrimeric G proteins: Transducers of GPCR signaling

G proteins are named for their ability to bind phosphorylated guanosine nucleotides. G proteins are heterotrimers made up of a large Gα subunit of 39-52 kDa and the obligate Gβγ heterodimer dimer of 35-36 and 8 kDa. The evolution of numerous subtypes of G proteins accounts for a massive number of potential combinations and the functional versatility of G protein signaling [38, 39].

They are members of a diverse GTPase superfamily that includes the Ras superfamily of small GTPases and the family of initiation and elongation factors (EF-Tu) [40]. In humans, there are 20 Gα subunits, 6 Gβ subunits, and 12 Gγ subunits [41, 42]. The Gα subunit, in its inactive form, binds to GDP, and upon activation, exchanges GDP for GTP. G proteins have Kd values between 10^{-11} and 10^{-7} M for the nucleotides to ensure stable binding and to prevent the spontaneous exchange of one nucleotide for the other [43].

At the molecular level, binding of the agonist to the extracellular side of a GPCR causes conformational changes in the receptor and subsequent binding of the heterotrimeric G protein to the cytoplasmic side of the receptor [44, 45]. In some cases, G proteins are pre-coupled to the receptor before the receptor is activated [46, 47]. The activated receptor acts as a GEF, which promotes the release of GDP from the Gα subunit. As the cytoplasmic concentration of GTP ($>10^{-4}$ M) is 10 times higher than GDP ($>10^{-5}$ M), upon GDP release, GTP rapidly binds to the Gα subunit [44]. GTP binding causes conformational changes in the Gα subunit, resulting in the

disassociation of the Gα subunits from the activated GPCR and Gβγ subunit. GTP bound Gα and Gβγ can then interact with multiple signaling molecules. The Gα subunit has intrinsic GTPase activity, and hydrolysis of GTP to GDP leads to reassociation of Gα-GDP and Gβγ into the inactive heterotrimeric G protein. This restricts the lifetime of the signaling and allows G proteins to be ready for another round of signaling (Fig. 1.4).

Regulators of G protein signaling (RGS) proteins serve as GTPase activating proteins (GAPs) and bind to GTP bound Gα subunits and enhance the intrinsic GTPase activity of most Gα subunits [48-53]. There are ~30 RGS proteins encoded in the human genome, each of which interacts with a particular set of G proteins.

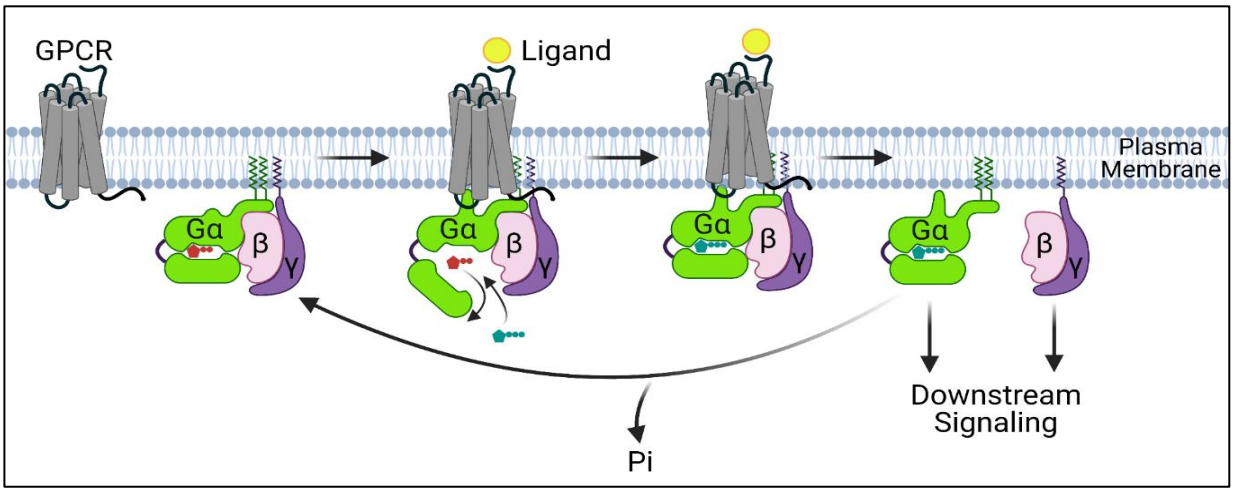

Figure 1.4: G protein activation cycle.
Ligand binding to the GPCR leads to its activation, recruitment of the heterotrimer G protein and catalysis of the exchange of GDP for GTP on Gα subunits. GTP binding destabilizes the heterotrimer releasing Gα-GTP and Gβγ subunits. G protein signaling is terminated upon hydrolysis of GTP to GDP on the Gα subunit and reassociation of the trimer.

In addition to the classical signaling paradigm, which involves GPCR dependent activation of heterotrimeric G proteins, non-GPCR proteins such as activators of G protein signaling (AGS) proteins can also mediate activation [54]. AGS proteins are classified into three groups based on their postulated mechanism of action [55-58]. AGS1 is the only protein classified in Group I that acts as a GEF for $G\alpha_{i/o}$ [59]. Group II is characterized by their G protein regulatory (GPR) or

GoLoco motifs and act as a guanine-nucleotide dissociation inhibitor (GDI) by specifically binding and stabilizing Gα-GDP, free of Gβγ [60]. AGS3-6, AGS3 (GPSM1), AGS4 (GPSM3), AGS5 (GPSM2), AGS6 (RGS12) proteins are members of Group II [61]. Group III directly binds to Gβγ, but not Gα, and activates Gβγ signaling. Resistance to inhibitors of cholinesterase 8 (Ric8) or synembryn is a non-receptor GEF that activates monomeric Gα subunits and not the G protein heterotrimer. It also acts as a chaperone for the Gα subunit by regulating the folding of the nascent Gα subunit and its processing during biosynthesis [62-65].

1.4 Gα subunits

1.4.1 Secondary structure

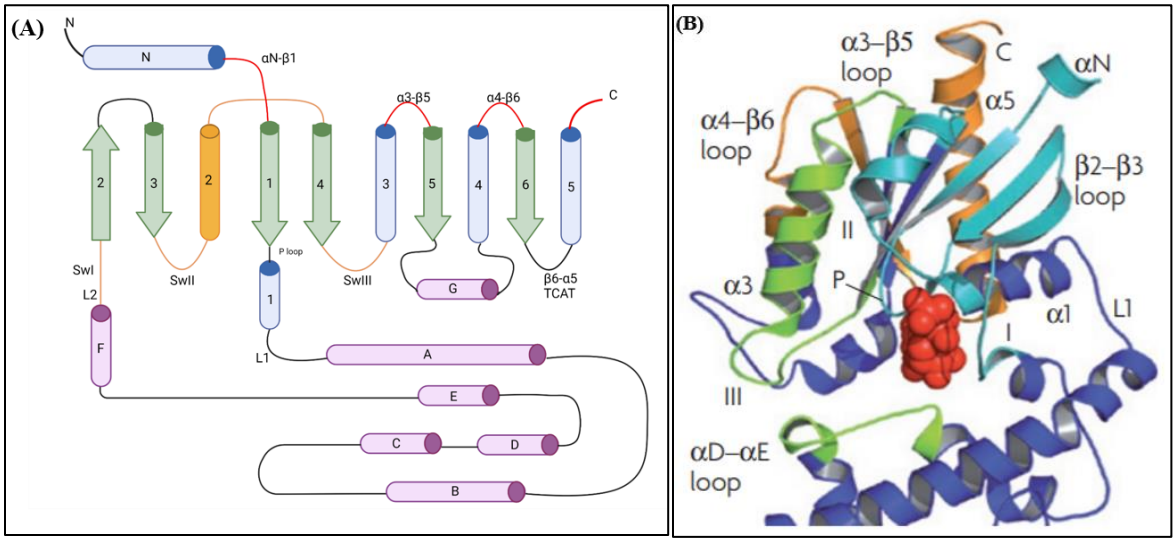

Figure 1.5: Secondary structure of Gα.
(A) Depicted is a schematic diagram of Gα subunit showing α-helix as cylinders and β-sheets as arrows. Seven helices of the helical domain (purple) are in seven letters A-F. L1 and L2 linkers connect the helical domain to the GTPase domain. Switch regions are in orange, Gβγ subunit binds to switch II region on Gα. Receptors contact sites are in red, TCAT is guanine ring-binding motif, and P look is nucleotide phosphate-binding loop. **(B)** The α5 helix and β6 strand (orange) connect the C terminus and the α4–β6 loop to the nucleotide-binding pocket at the β6–α5 loop, which contains the TCAT motif (orange). The α3–β5 loop is connected to switch III (III) by the α3 helix (light green). The αN helix is connected to the nucleotide phosphate binding (P) loop and two switches I and II (I; II) through its interactions with β strands 1–3 (cyan). Additionally, these β strands also interact with the α5 helix (orange). Adapted from [45].

Gα subunits are composed of a GTPase domain and a helical domain. The GTPase domain is conserved in all members of the G protein superfamily, whereas the helical domain is unique to Gα proteins. GTPase domain is composed of six-stranded β-sheets and five α-helices (Figure 1.5). It hydrolyses GTP and has binding sites for GPCRs, the Gβγ dimer, and effector proteins [45]. It contains three flexible loops, named switch I, II and III, that undergo structural changes upon activation, and the largest structural differences between the GDP and GTPγS-bound conformations of Gα have been identified in these regions by X-ray crystallography [66-69]. The C terminus of the Gα subunit is important for receptor engagement as well as for determining G protein-receptor coupling specificity [70, 71]. The helical domain is unique to each Gα subtype and is composed of six α-helix bundles [67-69, 72].

1.4.2 Gα subunit subtypes

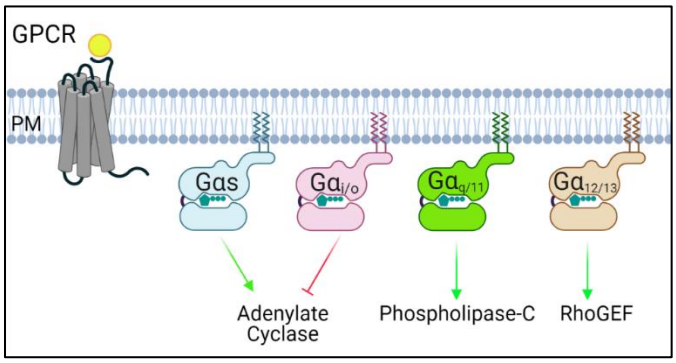

Figure 1.6: Different subtypes of Gα subunits and their classical effectors.
There are four different Gα subtypes. $G\alpha_s$ activates AC whereas $G\alpha_i$ is primarily known for its inhibitory effect on AC, $G\alpha_q$ activates PLC, and $G\alpha_{12/13}$ primarily activate RhoGEFs.

Based on sequence and functional similarities, Gα proteins are grouped into four subfamilies: $G\alpha_s$, $G\alpha_{i/o}$, $G\alpha_{q/11}$, and $G\alpha_{12/13}$ and share 35-95% sequence identity (Figure 1.6) [41]. $G\alpha_s$ and $G\alpha_i$ proteins are classically associated with stimulation and inhibition of AC. AC generates 3',5'-cyclic adenosine monophosphate (cAMP) from ATP to regulate effectors such as PKA and

exchange protein activated by cAMP (EPAC). GPCRs coupled to $G\alpha_s$ and $G\alpha_i$ in a single cell can precisely regulate intracellular cAMP levels and mediate subsequent downstream effects through the additive effects. $G\alpha_{q/11}$ proteins activate phospholipase Cβ (PLCβ), which cleaves PIP_2 to generate intracellular second messengers inositol triphosphate (IP3) and diacylglycerol (DAG), resulting in the activation of PKC and calcium signaling [73]. $G\alpha_{12/13}$ proteins activate Rho via activation of RhoGEFs [74-81].

Each family consists of various members that often show very specific expression patterns (Table 1.1). Members of each family are structurally similar and often share functional properties. GPCRs are characterized by the specific subtype of the G protein it couples to, which allows activation of unique sets of intracellular signaling pathways. Though the signal transduction is initiated by diverse GPCRs, they couple to a modest number of G protein subtypes to regulate intracellular signaling [82].

Table 1-1: Tissue distribution of different subtypes of Gα subunits
Adapted from [38].

Name	Gene	Expression
α-Subunits		
$G\alpha_s$ class		
$G\alpha_s$	*GNAS*	Ubiquitous
$G\alpha_{sXL}$	(*GNASXL*)	Neuroendocrine
$G\alpha_{olf}$	*GNAL*	Olfactory epithelium, brain
$G\alpha_{i/o}$ class		
$G\alpha_{i1}$	*GNAI1*	Widely distributed
$G\alpha_{i2}$	*GNAI2*	Ubiquitous
$G\alpha_{i3}$	*GNAI3*	Widely distributed
$G\alpha_o$	*GNAO*	Neuronal, neuroendocrine
$G\alpha_z$	*GNAZ*	Neuronal, platelets
$G\alpha_{gust}$	*GNAT3*	Taste cells, brush cells
$G\alpha_{t-r}$	*GNAT1*	Retinal rods, taste cells
$G\alpha_{t-c}$	*GNAT2*	Retinal cones
$G\alpha_{q/11}$ class		
$G\alpha_q$	*GNAQ*	Ubiquitous
$G\alpha_{11}$	*GNA11*	Almost ubiquitous
$G\alpha_{14}$	*GNA14*	Kidney, lung, spleen
$G\alpha_{15/16}$	*GNA16* (*Gna15*)	Hematopoietic cells
$G\alpha_{12/13}$ class		
$G\alpha_{12}$	*GNA12*	Ubiquitous
$G\alpha_{13}$	*GNA13*	Ubiquitous

1.4.3 Lipid modifications

Gα proteins are anchored to the membrane by fatty-acid modifications. Most Gα subunits (excluding $G\alpha_t$) are modified with saturated 16-carbon fatty acid palmitate near the N-terminus. S-palmitoylation is a reversible post-translational modification, which forms a thioester bond with cysteines. $G\alpha_q$, $G\alpha_{11}$, $G\alpha_{14}$ and $G\alpha_{16}$ are palmitoylated at multiple cysteine residues. $G\alpha_s$ is dually palmitoylated and not myristoylated. $G\alpha_i$, $G\alpha_o$, $G\alpha_z$, and $G\alpha_t$ are irreversibly modified with amide saturated 14-carbon fatty acid myristate at the N-terminal glycine following removal of start codon methionine [83-90].

1.5 Gβγ subunits

1.5.1 Secondary structure

The Gβγ subunit dimers are functionally monomeric proteins that can only be dissociated under denaturing conditions [91]. The Gβ subunit is composed of N-terminal α helix region, and a seven-bladed β-propeller structure composed of seven WD40 sequence repeats, each comprised of 4 antiparallel β sheets [92]. Gβ forms a constitutive dimer with Gγ through the N-terminal α helix region and forms a coiled-coiled interaction with N-terminal α-helix of the Gγ subunit. Gβ-Gγ assembly is required for proper folding of the Gβ subunit.

1.5.2 Gβγ subunit subtypes

To date, 5 Gβ and 12 Gγ proteins have been identified [93-97]. Gβ1-Gβ4 subunits are ~80-90% similar, while Gβ5 does not participate in classic G protein heterotrimer signaling, but rather associates with RGS proteins. Gγ subunits are more diverse with 30-80% sequence identity [98-102]. Although most Gβ subunits dimerize with most Gγ subunits, not all of the 72 possible dimer

combinations occur [103]. Different Gβγ dimers show highly tissue-specific expression patterns, which suggests specialized roles of distinct dimer combinations in the signal transduction pathway; however, the functional significance of individual Gβγ subunit combinations is not well understood [101]. In addition, tissue-specific expression, cellular localization, and pre-coupling of the G protein and effectors could also determine specificity. Overall, Gβγ can activate PLC, phosphatidylinositol 3-kinase (PI3K), AC, and inwardly rectifying potassium channels (GIRK), among many others [104-106]. Gβγ activation is coupled to recruitment GRKs to the PM to phosphorylate activated GPCRs.

1.5.3 Lipid modifications

The Gβγ subunit is anchored to the membrane through prenylation of γ subunits at their C-terminal CaaX motif (c-cysteine, a-aliphatic amino acid, X-any amino acid). The identity of the X amino acid determines whether the Gγ is modified with either a 15-carbon farnesyl or 20 carbon geranyl-geranyl moiety. Gγ is farnesylated if the X is serine, methionine, glutamine or alanine or geranylgeranylated if the residue is leucine [107]. Most γ subunits are modified by the 20-carbon geranylgeranyl moiety with the exceptions of γ1, γ11 and γ15, which are modified by 15-carbon farnesylation [108-110]. The nature of modification significantly affects the interaction between Gα and Gβγ or Gβγ subunit with effectors [111, 112].

1.5.4 Signaling by Gβγ dissociated from Gi-GPCRs

Most Gβγ mediated, GPCR-dependent processes are PTX sensitive, and only a few studies report otherwise [113-116]. One proposed reason is that $G\alpha_{i/o}$ are expressed at relatively high levels compared to other subtypes and have a relatively low affinity for AC. Therefore, $G\alpha_i$-activation

downstream of Gi-coupled GPCR results in the release of relatively high amounts of $G\alpha_i$ and Gβγ-complexes. Activation of Gi/o is therefore believed to be the major coupling mechanism that results in the activation of βγ-mediated signaling processes [101, 117].

1.6 Interfering with G protein function

Pharmacological manipulation of Gα subunits by two bacterial toxins, namely pertussis toxin (PTX) and cholera toxin (CT), enabled the mechanistic study of G protein functions and downstream signaling [118]. PTX catalyzes ADP ribosylation of Gi family members (except $G\alpha_z$) at a cysteine residue close to the C terminus [119]. As the C terminus interacts with the receptor, attachment of an ADP-ribose moiety sterically occludes coupling of the G protein to the receptor [44, 120, 121]. As a result, G protein remains in an inactive state. CT transfers ADP-ribose moiety from intracellular NAD^+ to an arginine residue on $G\alpha_s$. This arginine residue is involved in stabilizing the transition state during the hydrolysis of GTP to GDP, and the presence of a bulky ADP-ribose group at this position prevents GTP hydrolysis, causing it to remain constitutively active. In addition, nonhydrolyzable GTP analogs and $AlF4^-$ have been important tools for structural and functional characterization of G proteins. GTPγS is a nonhydrolyzable analog of GTP and prevents inactivation of the G protein. Similarly, aluminium fluoride binds with GDP to the active site as AlF4- or $AlF_3(OH)^-$ and adopts the position of the γ-phosphate of GTP [44, 122-124]. Thus, G proteins can be constitutively activated using GTPγS and $AlF4^-$.

In addition to biochemical modifications, genetic manipulation by site-directed mutagenesis showed that glutamine at position 204 of Gαi coordinates a hydrolytic water molecule during GTP hydrolysis to account for the GTPase activity of the Gα subunit. This glutamine is

highly conserved, and its mutation to leucine (QL) in Ras GTPases or Gα subunits leads to constitutive activation of the protein [69, 125-127].

This thesis will primarily be focused on signaling downstream of $G\alpha_q$ and $G\alpha_i$ coupled GPCRs and identification of novel downstream signaling pathways downstream of G proteins $G\alpha_i$ and $G\alpha_q$. Following is the detailed description of signaling components relevant to this thesis.

1.7 The $G\alpha_s$ family

$G\alpha_s$ is named stimulatory as it stimulates the activity of AC, an enzyme that generates cAMP from ATP [128-133]. Increased cAMP concentration can elicit a plethora of physiological effects by modulating the activity of multiple intracellular proteins. For example, activation of cAMP-dependent PKA by cAMP leads to phosphorylation of multiple intracellular proteins including, CREB, which binds to cAMP response elements (CRE) to modulate transcription of various genes [134]. cAMP also activates exchange protein activated by cAMP (EPAC), an exchange factor for Rap, which translocate to the PM following activation and produces a range of cell-specific responses.

Two members of the family, Gs, Gαs and Gαolf, are known. The Gαs gene gives rise to four splice variants, two short forms (Gαs-S) and two long forms, Gαs-L and XLαs [128, 135, 136]. Gαs is ubiquitously expressed, and all known AC isoforms are activated by Gαs [137]. XLαs expression is restricted adrenal gland, heart, pancreatic islets, brain, and pituitary gland [138].

1.8 The $G\alpha_q$ family

$G\alpha_q$ subunits activate PLCβ, an enzyme that hydrolyzes membrane phosphatidylinositol 4,5-bisphosphate (PIP2) into IP3 and DAG [73, 139]. DAG remains membrane-bound and

activates several PKC isoforms. PKC phosphorylates multiple intracellular proteins, including MAPK/ERK and NF-kB protein complexes. Regulation of gene expression downstream of these signaling pathways governs many physiological processes, including activation of pro-inflammatory and hypertrophic genes, etc. IP3 diffuses and binds to IP3 receptors on the surface of the endoplasmic reticulum (ER), leading to an increase in the intracellular calcium concentration, which regulates a wide variety of cellular processes.

1.9 The Gi family

$G\alpha_i$ is given its name, inhibitory, by its ability to inhibit AC proteins which is the best-described effector for most family members [119, 140-145]. The $G\alpha_i$ family is the largest and most diverse family, including $G\alpha_{i1}$, $G\alpha_{i2}$, $G\alpha_{i3}$, $G\alpha_{oA}$, $G\alpha_{oB,}$ $G\alpha_t$, $G\alpha_{gust}$, and $G\alpha_z$. The G proteins of the $G_{i/o}$ family are ubiquitously expressed (Fig. 1.7) [137]. $G\alpha_{gust}$ and $G\alpha_t$ are involved in sensory functions. $G\alpha_o$ is the most abundant Gα subunit and constitutes ~1% of membrane protein in the brain [146]. It weakly inhibits AC and has been shown to directly bind to Golgi-residing GTPases Rab1 and Rab3 and regulate neurite outgrowth [147]. Most of the effects downstream of Go are mediated by Gβγ subunits, and its direct function is still poorly understood [148].

GPCRs that couple to Gi subtypes include metabotropic glutamate (mGluR2, 3, 4, 6, 7, 8), muscarinic (M2 and M4), α_{2A}-adrenergic (α_{2A}, α_{2B}, α_{2C}), dopamine (D2, D3, D4), histamine (H_3 and H_4), melatonin (MT1, MT2, MT3), serotonin (5-$HT_{1A/B/D/E/F,}$ 5-$HT_{5A/B}$), ADP (P2Y12 and P2Y13), chemokine (CCR1, CCR2, CXCR, etc.) and multiple other receptors. They regulate important processes in the nervous, cardiovascular, endocrine, and immune systems. From all GPCRs, 21.9% couple exclusively to the $G_{i/o}$ subfamily, and the other 5% can couple to proteins of the $G_{i/o}$ and of other G subfamilies [149].

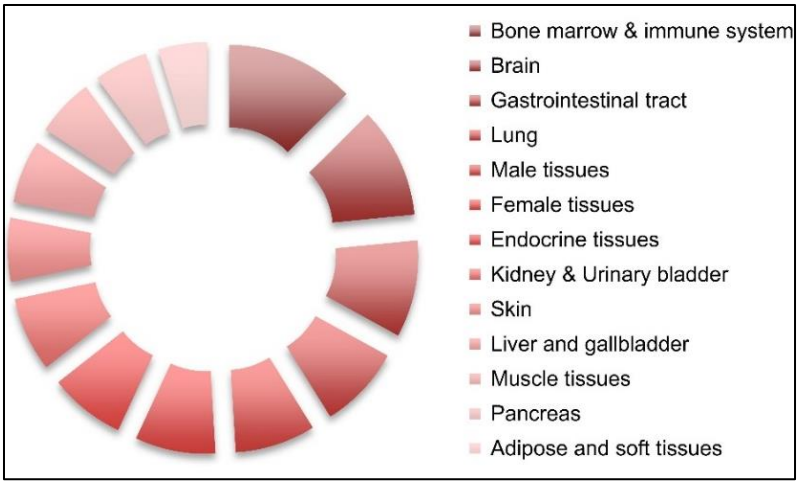

Figure 1.7: Pie chart showing relative tissue distribution of $G_{i/o}$ coupled GPCR.
Relative abundance in 13 human tissues was acquired from the Human Protein Atlas and quantitatively transformed (value 1=low, 2.5=medium and 3.5=high abundance), and the relative % of tissue distribution was calculated. The sum of all abundance values in all the 13 tissues was taken s as 100%. Adapted from [149].

1.9.1 Gi in chemotaxis

One of the processes regulated downstream of Gi-coupled GPCRs is chemotaxis. Chemotaxis is the migration of a cell toward a chemotactic stimulus. In almost all hematopoietic cells, chemotactic receptors are coupled to heterotrimeric Gi proteins [150]. The role of Gβγ in chemokine signaling has been well characterized and is thought to be the major transducer of chemotaxis [101]. Only a few interactors of $G\alpha_i$ are known [151-153]. $G\alpha_i$ has been proposed to function mostly passively through the release of Gβγ, and its direct signaling roles are underappreciated [154]. Determination of specific roles for downstream signaling by the $G\alpha_i$ subunit has been hampered by the fact that perturbations that inhibit $G\alpha_i$ signaling also inactivate Gβγ signaling. For example, the modification of $G\alpha_i$ by PTX blocks any interactions between the $G\alpha_i$-βγ heterotrimer and GPCRs, thereby inhibiting both Gα and Gβγ signaling. Similarly, knockout of specific G protein α subunits, either in mice or with specific short inhibitory RNAs (siRNAs) in cell culture, prevents signaling by both Gα and its associated Gβγ subunits.

Previous reports have shown the involvement of $G\alpha_i$ in the regulation of immune and cancer cell migration. Interaction of $G\alpha_{i2}$-GDP with mammalian Pins homolog (LGN/AGS3) leads to its localization at the pseudopod protrusion at the leading edge and interaction with a mammalian homolog of Inscuteable (mInsc) to maintain directionality of migrating neutrophils [155]. CXCR4, a chemokine receptor, is activated by stromal cell-derived factor-1 (SDF-1), also called CXCL12. Engulfment and cell motility (ELMO) is a scaffold protein and regulates the activity of PM and cytoplasmic proteins. CXCR4 triggered the interaction of two ELMO isoforms, ELMO1 and ELMO2, with $G\alpha_{i2}$-GTP regulate breast cancer and pancreatic cancer cell chemotaxis, migration and invasion, respectively [155, 156]. $G\alpha_{i2}$ with ZAP-70 mediate membrane localization of RasGRP1, a Ras guanine-nucleotide exchange factor, downstream of CXCR4 to regulate human T cell migration [157]. GTP-bound $G\alpha_i$ subunits activate c-Src kinase and Hck tyrosine kinases. This links Ras activation downstream of chemokine receptors via Shc, Grb2 and SOS. It also explains the activation of focal adhesion kinase (FAK), protein tyrosine kinase 2 (Pyk-2), and downstream effectors by chemokines [158]. However, the detailed molecular information on how these interactions lead to a functional readout or cell adhesion and migration hasn't been investigated.

Recent reports from our lab showed novel roles of $G\alpha_i$ in cell adhesion and migration. Our laboratory identified a small molecule, 12155, which displaces $G\beta\gamma$ from $G\alpha_i$-GDP, allowing investigation of $G\beta\gamma$ signaling independent of nucleotide exchange on the $G\alpha$ subunit or receptor activation (Fig. 1.8) [159]. Uniform treatment of neutrophils with 12155 on intracellular adhesion molecule 1 (ICAM-1) coated surfaces inhibited migration and enhanced adhesion.

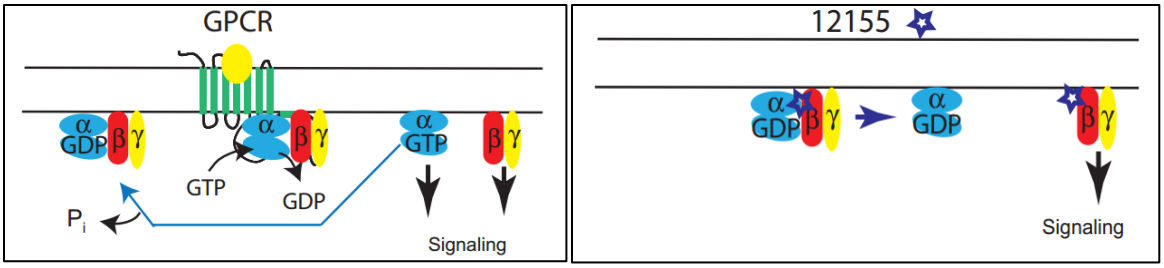

Figure 1.8: Schematic of canonical G protein regulation by GPCRs and mode of action of 12155.
Activation of the GPCR in the cells results in activation of Gα and Gβγ mediated signaling whereas 12155 treatment leads to signaling pathway downstream of Gβγ subunit. Adapted from [160].

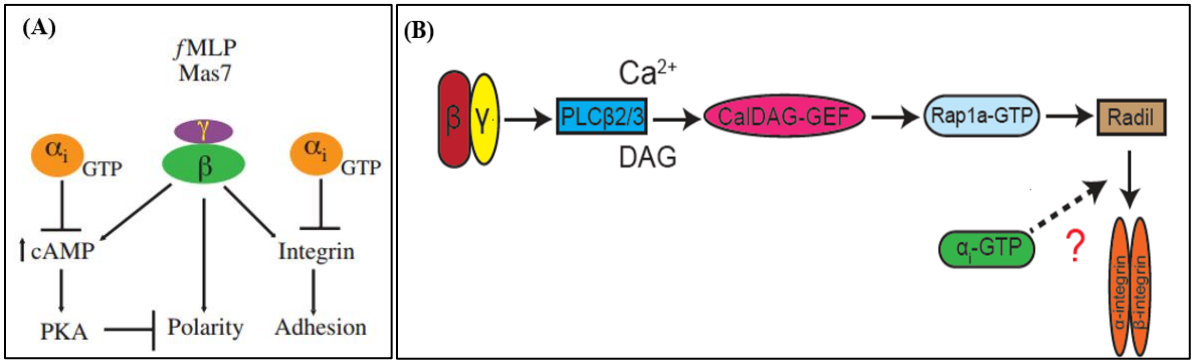

Figure 1.9: Schematic representation of a role of Gα$_i$ in cell adhesion and migration discovered in two previous studies from our group.
(A) Model depicting the role of Gi proteins in neutrophil migration. Adapted from [160]. **(B)** Schematic showing key components of the pathway regulating cell adhesion downstream of Gβγ and possible role of Gα$_i$ at the level downstream of Radil. Adapted from [161].

The decrease in cell adhesion by Gα$_i$-GTP was cAMP-independent and was shown to function downstream of or at the level of Radil in the Gβγ-PLCβ2/3-(CalDAG-GEF)-(Rap1a-GTP)-Radil axis [161]. Overexpression of Rap1a-GTP or Radil enhances uropod adhesion during cell migration on the fibronectin-coated surface, leading to elongated cell phenotype, which is reversed by Gα$_i$-QL but not Gα$_i$-WT. In addition, Gα$_i$-GTP mediated cell-deadhesion requires Rho signaling. This was the first evidence of dynamic cooperative regulation of adhesion and deadhesion by Gβγ and Gα$_i$-GTP, respectively [161]. These studies in neutrophils and fibrosarcoma cells identified a novel role of Gα$_i$ in cell adhesion and migration and demonstrated that Gβγ subunit signaling isn't sufficient to regulate this biology (Fig.1.9) [160, 161]. However,

the direct effector and molecular details of the signaling pathway by which $G\alpha_{i1}$ regulates these processes were not identified.

1.9.2 Other $G\alpha_i$ effectors

Other effectors such as RASA1 and RASA3 are shown to regulate different biological functions downstream of different Gi-coupled GPCRs. Ras-GTPase activating protein 3 (RASA3) has been shown to interact with $G\alpha_{i2}$ and $G\alpha_{i3}$ to mediate D2S-induced inactivation of the Ras-ERK1/2, MAPK pathway in neuroendocrine cells [162]. RasGTPase-activating protein 1 (RASA1), p120-GAP, is inhibited by fMLP induced FPR receptor activation in neutrophils [162]. $G\alpha_i$-GTP interacts with Rapl GTPase-activating protein rap1GAPII upon stimulation of the M2-muscarinic receptor [163]. $G\alpha_i$ has also been shown to interact with Gα-interacting vesicle-associated protein (GIV)/Girdin, and this interaction is proposed required for RTK mediated $G\alpha_i$ activation and is proposed to connect RTK signaling to G proteins [164].

1.9.3 Isoform-specific functions of $G\alpha_i$

Three Gαi isoforms, $G\alpha_{i1}$, $G\alpha_{i2}$, $G\alpha_{i3}$, share more than 85% identity, and they all inhibit AC to the same extent and potency [165]. Analysis of the kinetics of GTP binding and hydrolysis shows subtle differences among these isoforms [166-168]. However, no clear functional differences for these subtypes in preferential coupling to effectors have been defined. Mouse knockout (KO) studies showed differential roles for $G\alpha_i$ subtypes in immune cell function; $G\alpha_{i2}$ and $G\alpha_{i3}$ knockout inhibits neutrophil arrest, and have neutrophil chemotaxis defects, respectively upon CXCR2 stimulation which can't be explained based on Gβγ signaling [169]. In BALB/c 3T3 cells, it was reported that $G\alpha_{i2}$ mediates activation of mitogen-activated protein kinase (MAPK)

and DNA synthesis, whereas $G\alpha_{i3}$ mediates formation of transformed foci downstream of dopamine (D2S) receptor to mediate cellular transformation. Furthermore, Gαi3 couples to TNFAIP8 in Balb-D2S cells to mediate transformation [170]. In addition, overexpression of Gαo inhibited dopamine-induced transformation, whereas Gαi1 induced abnormal cell growth independent of receptor activation. This evidence indicates a strong G protein subunit specificity in a variety of cellular processes [171]. However, the mechanisms which confer selectively among these closely related subtypes of G proteins remains unclear.

1.10 Effectors and concepts relevant to this thesis

1.10.1 RGS domain-containing RhoGEF and regulation by the $G\alpha_{12/13}$-family

p115-RhoGEF/Lsc, leukemia-associated RhoGEF (LARG), postsynaptic density 95, disk large, zona occludens-1 (PDZ)-RhoGEF also called glutamate transporter EAAT4 associated protein (GTRAP48), and A-kinase anchoring proteins (AKAP)- lymphoid blast crisis (Lbc) (AKAP-Lbc) are members of the mammalian RhoGEF family that contain RGS domains. p115-RhoGEF, PDZ-RhoGEF (PRG) and LARG contain an N-terminal RGS homology (RH) domain, whereas Lbc-RhoGEF has a C terminal RH domain and shares ~40% sequence identity to the consensus RGS domain [80]. They share two common domains, Dbl-homology (DH) and pleckstrin-homology (PH), characteristic of GEFs for Rho family GTPases [172]. The DH domain binds and stabilizes nucleotide and Mg^{2+}-free Rho transition states, enhancing GTP binding, and the PH domain is necessary for the full GEF activity and regulates localization [75, 173]. PRG and LARG also contain an N-terminal PDZ domain, which facilitates interaction with cell surface receptors such as plexins, insulin-like growth factor receptors, or GPCRs [174, 175].

$G\alpha_{12}$ and $G\alpha_{13}$ are ubiquitously expressed and regulate p115RhoGEF, LARG, PDZ-RhoGEF, and AKAP-Lbc [75, 80, 176-179]. Rho regulates cytoskeleton reorganization, and active $G\alpha_{12}$ and $G\alpha_{13}$ induce actin stress fiber formation in a Rho-dependent manner [180-182]. p115-RhoGEF directly binds to $G\alpha_{12}$ and $G\alpha_{13}$ via the RGS domain *in vitro*, but only active $G\alpha_{13}$ stimulates GEF activity of p115-RhoGEF towards Rho, which links Lysophosphatidic acid (LPA) or thrombin receptors to RhoA [81, 176, 183-186]. Following this discovery, PRG and LARG regulation by the G12 family was shown [187, 188]. LARG is known to be activated by $G\alpha_{12}$ and requires phosphorylation of the RhoGEF by Tec tyrosine kinase [189]. Active $G\alpha_{12}$ has been shown to activate AKAP-Lbc [78, 190]. However, it has not yet been shown to bind or to be activated by $G\alpha_{12/13}$ subunits using purified proteins *in vitro*. p115RhoGEF and LARG have been shown to act as specific GAPs for $G\alpha_{12}$ and $G\alpha_{13}$, while the RGS domain of PRG lacks detectable GAP activity for these G protein subunits [81, 189, 191, 192]. RH-RhoGEFs directly link the activation of GPCRs by extracellular ligands to the regulation of Rho activity in cells, resulting in serum response element (SRE)-mediated gene transcription and cellular transformation [193, 194]. Oligomerization of p115-RhoGEF, LARG and PDZ-RhoGEF negatively regulates its catalytic activity and may prevent interaction with RhoA [175].

1.10.2 PDZ-RhoGEF

PDZ-RhoGEF (PRG) is a GEF for Rho GTPases that plays a critical role in signaling [187, 195]. PRG is a 1522 amino acid protein with ~200 residue DH domain, followed by ~100 residue PH domain, a pattern found in all RhoGEFs (Fig. 1.10). In addition to the tandem DH-PH domains [172]. The DH domain binds to and stabilizes nucleotide and Mg^{2+}-free transition states of RhoA to enhance its nucleotide exchange. PRG contains an N-terminal PDZ domain of ~80 residues and

proline-rich domains followed by a ~200 residues RH domain, which bear distant homology to canonical RGS domains [196]. In addition, it contains an acidic autoinhibitory motif [197], a proline-rich essential for PM localization, cortical actin reorganization and cell rounding [198], and a 25-amino acid, actin cytoskeleton binding motif [199].

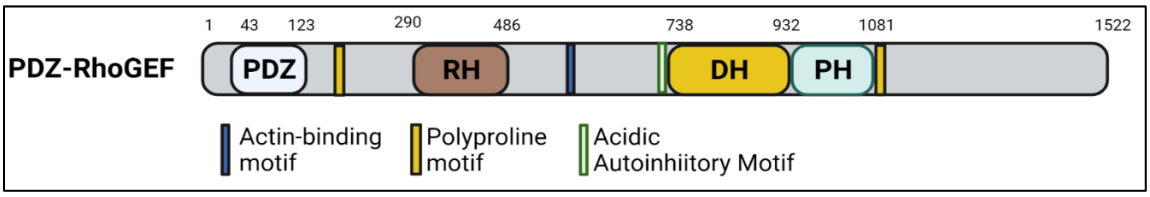

Figure 1.10: Domain organization of PRG.
PDZ- Postsynaptic density 95, disk large, zona occludens-1, DH- Dbl-homology, PH- Pleckstrin-homology, RH- RGS homology domain

PRG regulates a wide range of biological processes. It binds to class B plexins via PDZ domains and regulates axon guidance [200, 201] and is involved in neurotrophin-induced neurite outgrowth [202]. PRG and LARG bind to plexin B via the PDZ domain and regulate growth cone morphology [201, 203]. PRG enhances insulin/IGF-1 signaling by ROCK (Rho-kinase)-dependent phosphorylation of the insulin receptor substrate-1 (IRS-1) in adipose tissue to control mammalian metabolism and obesity [204]. It also regulates the activity of the neuronal glutamate transporter EAAT4 [205]. Through focal adhesion kinase (FAK), PRG regulates Rho/ROCKII-dependent focal adhesion movement and trailing-edge retraction in response to LPA [206]. PRG activation downstream of the FPR receptor has been proposed to mediate activation of $G\alpha_{12/13}$-RhoA-dependent backness, important for migration [207]. It has been shown to interact with microtubule-associated light chain 2 (MLC2) to govern microtubule integrity and actin cytoskeleton reorganization [208]. It also interacts with Pyk2 and TROY to regulate Rho mediated glioblastoma cell invasion and survival [209].

PRG binds to $G\alpha_{12/13}$ proteins via its RH domain [187] to regulate RhoA, and $G\alpha_s$ via its DH/PH domain to regulate Cdc42 and induce filopodia-like cell protrusions [210]. However, PRG activity toward RhoA doesn't increase when combined with $G\alpha_{13}$ *in vitro* [191].

1.10.3 Small GTPase Rho

Rho GTPases are a family of small GTPases within the Ras-related small GTPase superfamily. RhoA, RhoB and RhoC are closely related and ubiquitously expressed isoforms of Rho. RhoA plays a key role in regulating actin cytoskeleton, cell adhesion, migration, growth, vesicle trafficking, cell cycle, neurite extension/retraction, membrane transport pathways, gene transcription, etc [211]. Clostridium botulinum C3 exoenzyme (C3 toxin) ADP-ribosylates an arginine residue of RhoA, leading to Rho inactivation. It is widely utilized to examine the functional involvement of Rho proteins in cell biological processes [212-214].

The best characterized Rho effectors, ROCK1/2, are ubiquitously expressed serine/threonine kinases, which translocate from the cytosol to the PM and bind to RhoA-GTP [215]. ROCK phosphorylates multiple proteins, including FAK, Jun N-terminal kinase (JNK), myosin phosphatase (MYPT1), LIM kinase (LIMK), and Diaphanous (mDia). FAK phosphorylation has been shown to induce focal adhesions and stress fiber formation. Stress fiber polymerization ultimately leads to activation of serum response factor (SRF). SRF binding to the serum response element (SRE) sequences in the promoter of specific genes leads to the regulation of transcription of multiple genes. SRF requires a co-activator, MAL, which translocates from the cytoplasm to the nucleus in response to Rho activation [216]. p115-RhoGEF, PDZ-RhoGEF and LARG activation were demonstrated to be involved in focal adhesion formation and movement [217]. MLC phosphatase (MLCP) phosphorylation by ROCK inhibits its catalytic activity

preventing dephosphorylation of myosin light chain II (MLCII) and increased levels of the phosphorylated regulatory light chain MLC20 of myosin II, which enhances actomyosin cross-bridge formation and cell contraction. ROCK can also directly phosphorylate myosin light chain [215, 218, 219]. Rho is also known to activate mDia (mammalian homolog of Drosophila diaphanous), which catalyzes actin nucleation, polymerization and produces long, straight actin filaments [220]. Cooperation of mDia and ROCK is required for the assembly of stress fibers [221], both of which are regulated by Rho.

1.10.4 Small G proteins Ras and RasGAPs

Ras, the founding member of the small GTPases, was originally identified as a viral oncogene. The Ras superfamily is divided into five major subfamilies, Ras, Rho, Rab, Ran and Arf (ADP ribosylation factor) based on sequence and functional similarity [222]. These proteins function as binary switches; in their "on" state, the protein binds GTP and subsequently interacts with target proteins, and in their "off" state, they bind to GDP. In cells, GDP-bound Rho is bound to Rho-guanine nucleotide dissociation inhibitors (GDI), which masks the geranylgeranyl residue responsible for membrane association, stabilizes the complex in the cytoplasm and inhibits the exchange of GDP for GTP [223].

Small G proteins have weak intrinsic GTPase activity, and binding of GAPs increases the hydrolysis rate by up to 10^5, leading to an increased GDP-bound state of these GTPases [224]. GEFs stabilize the transition state to allow dissociation of GDP, facilitating GTP binding [225, 226].

RasGAPs are multidomain proteins with structurally diverse domains (e.g., SH2, SH3, PH, RBD domains) in addition to their catalytic GAP domains [227, 228]. RasGAPs are classified into

four major families: RASA1, NF1, GAP1, and SynGAP [229, 230]. RASA1 (Ras p21 protein activator 1)/p120GAP was the first RasGAP to be identified, and its overexpression leads to reversion of the transformed phenotype of c-ras transformed NIH 3T3 cells [231-233]. Subsequently, Neurofibromin (NF1) was identified, and its germline mutations are associated with Neurofibromatosis Type 1 disorder [234]. The GAP1 family includes RASA2 (Ras p21 protein activator-2)/GAP1m, RASA3 (Ras p21 protein activator 3)/GAPIP4BP, RASA4 (Ras p21 protein activator-4)/CAPRI, and RASAL1 (Ras protein activator like-1). GAP1 members are GAPs for both Ras and Rap1. The SynGAP family members include SynGAP (synaptic Ras GTPase-Activating Protein-1), DAB2IP (Dab2 interacting protein), RASAL2 (Ras protein activator like-2), and RASAL3 (Ras protein activator like-3) (Fig. 1.11). All the members of the family have a conserved GAP domain and additional accessory domains specific for that class of RasGAP.

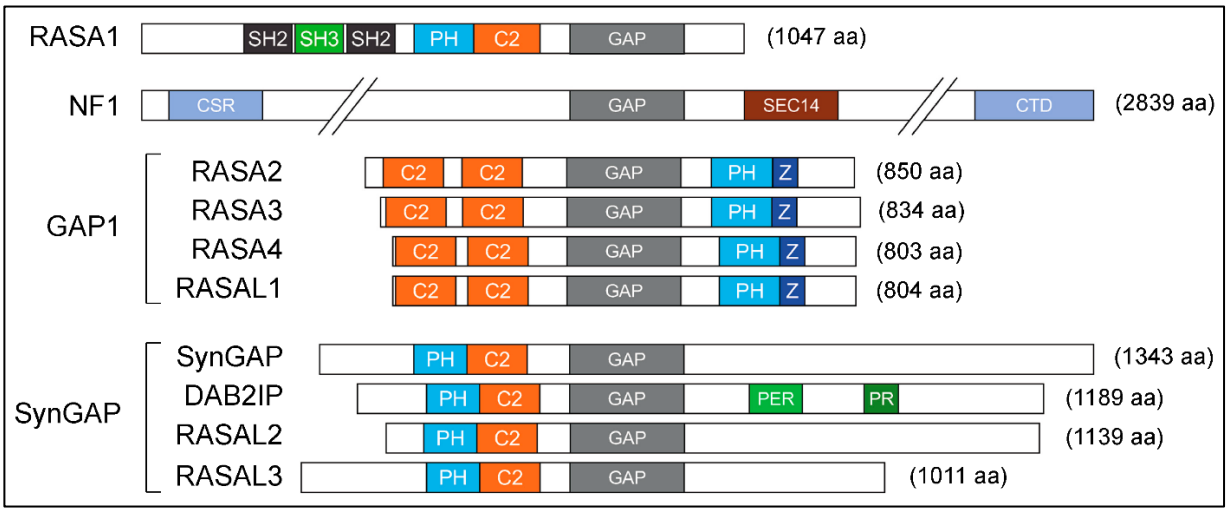

Figure 1.11: Domain organization of RasGAPs.
SH2-Src homology 2 domain; SH3-Src homology 3 domain; PH-pleckstrin homology domain; C2-calcium-dependent phospholipid-binding motif; CSR-Cys/Ser-rich region; SEC14-CRAL-TRIO lipid-binding domain; CTD-C-terminal domain; Z-Btk-type zinc finger motif; PER- period-like domain; PR-proline-rich region. Note that domains are not drawn to scale. Adapted from [230].

RasGAPs show differential tissue distribution depending on the isoform [230]. Loss of RasGAP activity either by inactivating mutations or epigenetic modifications result in the

accumulation of GTP-bound Ras and therefore increased signaling through Ras-regulated pathways.

1.10.5 Adenylate cyclase

Adenylate cyclase (AC) is an integral membrane protein consisting of twelve transmembrane and two cytoplasmic catalytic domains [235-238]. The catalytic region binds to the G proteins. A soluble form of AC has recently been characterized, which is activated by bicarbonate and calcium ions [239, 240]. AC synthesizes cAMP from ATP, and activation by G proteins leads to increase intracellular levels of cAMP. cAMP, a second messenger, binds to intracellular effectors such as PKA and EPAC and activates them. There are at least nine isoforms of AC, and all are stimulated by exposure of cells to the diterpene forskolin, except AC IX [241]. Different isoforms are differentially expressed among tissues and have distinct patterns of regulation [242-245]. $G\alpha_s$ stimulates all transmembrane AC isoforms, whereas $G\alpha_i$ directly inhibits AC I, III, V, VI, VIII, and IX [246-248]. Regulation of AC by $G\beta\gamma$ subunit is AC isoform-specific [137, 240, 249]. $G\beta\gamma$ potentiates Gs-mediated activation of AC II, IV, VI, VII and IX, and can inhibit AC I, III, V and VIII [242, 250, 251]. Five of the ACs are regulated by calcium [252]. Three of these are stimulated by calcium, and two are inhibited [253]. $G\alpha_q$ can indirectly stimulate AC I, II, III, V and VII via PKC activation [254].

1.10.6 Neutrophil chemotaxis

Chemotaxis is the directed movement of a cell driven by a gradient of diffusible chemotactic stimulus. Chemotaxis is involved in multiple processes, including tissue formation, wound healing, cancer cell invasion and metastasis. Neutrophils are a type of white blood cell and

are the fastest moving cells in higher animals. They migrate toward chemoattractants derived from invading microbes and/or produced by infected hosts to arrive correctly at sites of infection for pathogen killing. They are the first cells to reach sites of infection or inflammation [255]. Chemoattracts that bind to the receptors on the neutrophils include fMLP, C5a, platelet-activating factor (PAF), interleukin (IL)-8, etc. Upon chemoattractant binding, GPCRs transduce an activation signal leading to biochemical responses and physiological defense against bacterial infection and tissue damage [256]. Dysregulation of chemokine signaling leads to diseases ranging from allergy, inflammation, autoimmunity, and cardiovascular disorders [257, 258].

1.10.7 FPR receptor

Formyl-peptide receptors (FPRs) are Gi-coupled GPCRs involved in chemotaxis. They bind to N-formyl peptides produced by the degradation of either bacteria or host-derived formylated peptides from host mitochondria [256, 259, 260]. FPR receptors are expressed in phagocytic leukocytes and govern host defense and inflammation resolution. FPR family constitutes FPR1, FPR2/ALX (lipoxin receptor), and FPR3. Amino acid identity among these receptors is: FPR1 and FPR2 share 69%, FPR1 and FPR3 share 56%, whereas FPR2 and FPR3 share 83% identity [261]. Formyl-methyl-leucine-phenylalanine (fMLF or fMLP) is a classical FPR1 receptor ligand. FPR2 is a highly promiscuous receptor, and in addition to fMLP, it binds to lipids, peptides, and proteins [262, 263]. FPR3 is expressed on eosinophils, monocytes, macrophages, and dendritic cells but not human neutrophils. It is relatively insensitive to formylated peptides [264]. FPR receptors couple mainly to the $G\alpha_i$ family of G proteins [265], but some indirect evidence suggests that it can couple to the $G\alpha_{12/13}$ family of G proteins as well [266].

1.11 Understanding protein-protein interactions and interactome

Proteins are fundamental biomolecules made up of amino acid building blocks. They are dominant players in the cell, representing about ~55% of the total dry mass [267]. There are about 25,000-30,000 protein-coding genes in the human genome. However, the proteome of an organism is much greater, consisting of about 1-2 million proteins [268]. This is primarily due to alternative splicing of transcripts from 92-94% of multi-exon human genes, which increases the complexity of the transcriptome, and a myriad of post-translational modifications (PTMs) exponentially increases the complexity of the proteome (Fig. 1.12) [269, 270].

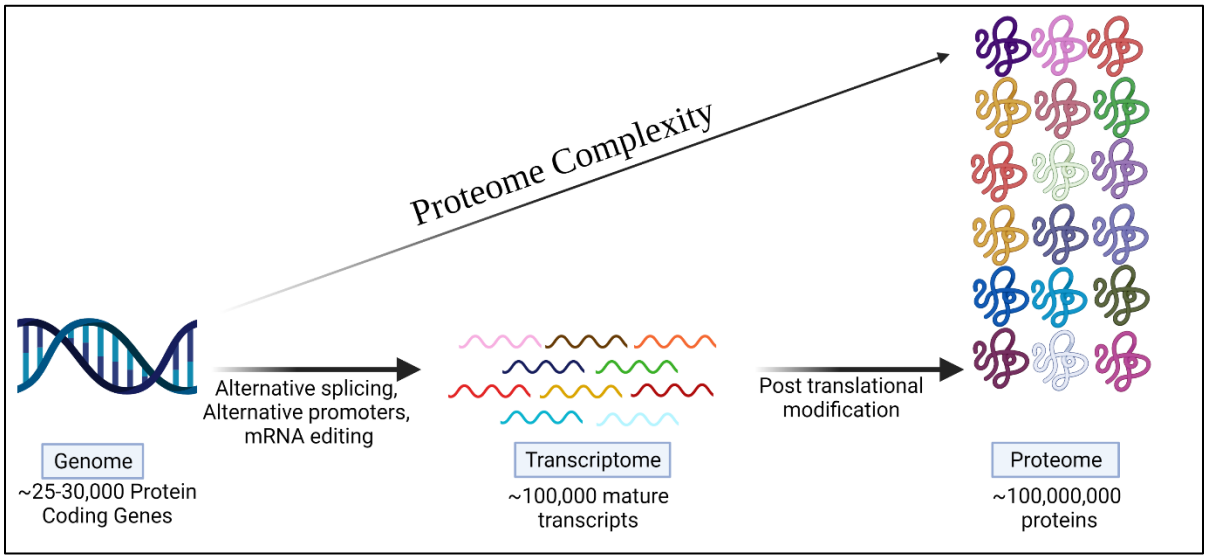

Figure 1.12: Schematic representation of the increase in complexity of the proteome from the genome.
From genome to proteome, multiple processes, including alternate splicing, post-translational modifications, contribute to complex proteome. Adapted from www.thermofisher.com

Proteins and their functional interactions are the backbones of the molecular machinery of the cell. A protein may modulate other proteins' activities by changing conformations, leading to activation, inactivation, stabilization, degradation, or post-translational modification etc. Protein-protein interactions (PPIs) are fundamental for mediating complex molecular relationships in living systems. PPIs regulate a gamut of cellular processes, including gene expression, signal transduction, cell cycle, metabolism, immune responses etc. [268]. The complete network of PPIs

that can take place within a cell is called the interactome [271]. Therefore, unraveling the interactome of a particular cell can provide opportunities to understand biology, disease pathophysiology and allow manipulation or modulation of signaling pathways at different nodes allowing the design of novel medicines with unique capabilities.

PPIs are context-dependent, meaning not all possible interactions necessarily occur in any cell and at any given time. Interactions between proteins can depend on the developmental stage of the cell, cell type, cell-cycle phase, protein modifications, presence of cofactors or other interacting partners, and factors in the environmental milieu [272]. PPIs can be intracellular or extracellular: Extracellular PPIs involve membrane-anchored proteins or secreted factors, whereas intracellular PPIs involve intracellular or membrane-anchored proteins.

PPIs are specific physical contacts established between two or more proteins by selective molecular docking as a result of biochemical events [272]. Meaning, the contact should be a consequence of biomolecular forces and not just the proteins bumping into each other by chance, and the interaction surface should be evolved for a specific purpose distinct from housekeeping functions such as protein production and degradation [273]. Some complexes assemble transiently, and some form stable interactions involved in the formation of multimeric protein complexes, such as proteosomes, ribosomes, RNA polymerase, ATPase pumps, etc. Other stable interactions involve covalent interactions such as disulfide bonds. During transient interactions, proteins interact briefly and reversibly with other proteins, depending on the cellular factors, to execute a transient action. Such interactions occur during signal transduction events such as binding of the ligands to the receptor, binding the G proteins to the receptor or activation of gene expression by transcription factor [272]. Non-covalent, transient interactions involve hydrogen bonds, hydrophobic and ionic interactions.

For centuries, the proteins and their biological functions have been studied by highly focused, reductionist approaches, which have produced a wealth of information on the functional and molecular properties of individual proteins and their interactions. However, for a comprehensive understanding of the biology of a cell, studying the interactome as an integrated network and understanding the individual components is important. In recent years, high throughput experimental and computational approaches have been developed to obtain comprehensive data sets of all the potential binary and complexes in an unbiased way [274, 275]. Comprehensive network maps, illustrated as nodes (eg. proteins, DNAs, RNAs) linked by edges corresponding to molecular interactions (eg. protein-protein, protein-DNA), are generated by such studies. Following the network map, a systematic study by perturbation of individual nodes and edges helps in understanding networks at a molecular level, and ultimately, reliable biological models can be generated.

In addition to physical interactions, an interactome consists of proteins that have functional contact. For instance, proteins as a part of multicomplex machinery, part of the same signaling/metabolic cascade, or involved in the same biomolecular process would have functional connections but may not interact physically [272, 276].

A plethora of methods is developed, ranging from biophysical to in vivo approaches enabling unbiased discovery of PPIs. Two of the most widely used high throughput methods to study PPIs are yeast two-hybrid (Y2H), and affinity purification coupled to mass spectrometry (AP-MS). Y2H is a binary method that investigates direct, physical interactions between protein pairs, whereas AP-MS is a co-complex method that identifies components of stable complexes without pairwise determination of protein partners. In addition, the former method is non-MS based, whereas the later is MS-based. Each of the approaches has its strengths and drawbacks,

especially with regard to sensitivity and specificity. In the following section, the details of both the methods and the pros, cons are described. After that, a relatively new method, proximity-based labeling (PBL) coupled to mass MS and its advantages and variations are described.

1.12 Methods to investigate PPI

1.12.1 Yeast Two-Hybrid (Y2H)

Principle

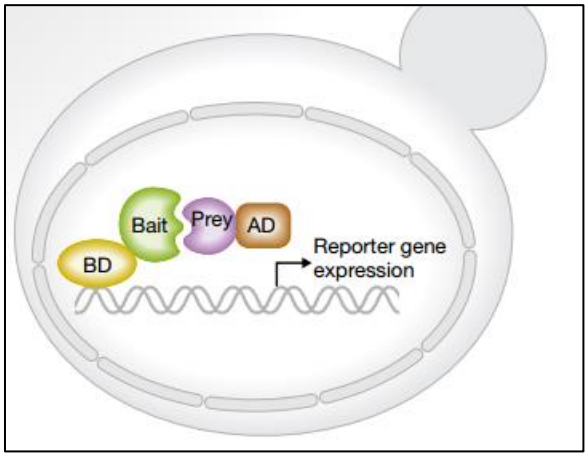

Figure 1.13: Schematic representation of Y2H method.
AD- Activation domain, BD- DNA-binding domain. Adapted from [277].

Y2H was first described in the yeast, *Saccharomyces cerevisiae* as a biological model and is one of the oldest PPI technologies [278]. Y2H is the conceptual pioneer binary technology based on the functional reconstitution of the two halves of a transcription factor (eg. Gal4 for yeast, lexA for bacteria) that are bound to bait and prey proteins and subsequent activation of the selective reporter (eg. His3). Two domains of the transcription factor, activation domain (AD) and DNA-binding domain (BD), are fused to potential interaction partners (the prey) and the protein of interest (called the bait), respectively (Fig. 1.13). When co-expressed in the nucleus of a yeast cell, physical interaction between the bait and prey reconstitutes functional transcription machinery that activates the expression of a reporter gene(s) and results in a measurable output. The output can

be the activation of one or several reporter genes expressing enzymes that allow the yeast to synthesize essential amino acids or nucleotides and allow growth under selective conditions or yield a color signal (β-galactosidase assay). In high throughput screens, the prey is usually a collection of unknown proteins from a cDNA or genomic library, screening of which against a specific bait could lead to the discovery of novel interaction partners.

Pros and Cons of Y2H

Y2H is simple, rapid, easy to set up, low-cost, and scalable for use in both low and high-throughput formats. The lack of a cumbersome purification step also increases the proficiency of the method. In addition, the PPI screen is carried out *in vivo*, which is essential for understanding their functions in the cellular context. This method can also detect weak and transient interactions as brief activation of the reporter genes may be sufficient to generate a signal [279].

Though Y2H is one of the widely used PPI identification methods, a serious challenge related to the high throughput screen is the frequent occurrence of false-positive and negative interactions.

False negatives are true interactions that go undetected during the screening procedure. As Y2H takes place in the nucleus, it has several disadvantages for proteins in their non-native compartment. For instance, as proteins are removed from their natural biological context, interactions that require specific post-translational modifications might be missed. For example, the interaction between phosphotyrosine proteins and SH2-domain-containing proteins might not be detected when the machinery for a specific post-translational modification is lacking in yeast cells. Interactions that require cofactors may also be precluded from binding if the cofactors are not present in the yeast cell nucleus or in yeast altogether. Failure in the nuclear localization

because of the stronger localization sequence for other locations can also preclude interaction from happening. This method is limited to the analysis of soluble full length or domains of proteins or soluble domains of membrane proteins. Improper folding of the proteins, especially integral membrane proteins, could lead to false negatives. Occasionally, some proteins might require a special environment, such as proteins of secretory compartments which require oxidative conditions, may not interact when present in the nuclear environment [280]. Y2H will also miss interacting pairs when bait or prey proteins that are toxic to the cell or prey proteins fail to express. As the proteins are genetically tagged with AD or BD, the tag could occlude the natural interaction domain or cause steric hindrance, ultimately preventing the PPI.

On the contrary, false positives are interactions that occur only in the context of the YTH and may not normally occur under physiological conditions and, therefore, may not have any biological relevance. Approximately 25 to 45% false positives are estimated from large-scale YTH approaches [281, 282]. The fusion proteins used in this method are also often overexpressed or present at a different level than their natural concentration in the cell, which can lead to nonspecific interactions. Forced targeting of non-nuclear proteins could lead to nonspecific interaction; for instance, a membrane protein in the absence of membrane might be misfolded in the nucleus, exposing hydrophobic surfaces that can non-specifically interact with other proteins. If bait or prey proteins bind and activate the reporter gene directly, it can lead to autoactivation of the reporter gene and thus false-positive transcriptional activity. Bait or prey proteins that overcome nutritional selection or nonspecific interaction of bait protein with the AD or, occasionally, spontaneous mutations in bait, prey or even the yeast strain could cause constitutive reporter gene expression. Y2H data are regarded as proof of binary interaction, but yeast proteins may act as a bridge for the interaction in certain cases.

To address limitations associated with Y2H, several new approaches such as membrane yeast two-hybrid (MYTH), mammalian membrane two-hybrid (MaMTH) system [283] assay for membrane protein interactions [284, 285], and cytosolic yeast two-hybrid system (cytoYTH) have been developed [286]. MYTH method has been successfully employed for 48 full-length GPCRs [287].

1.12.2 Affinity purification coupled to mass spectrometry (AP-MS)

Principle

Affinity purification coupled to mass spectrometry (AP-MS) is the conceptual predecessor of co-complex methods, which can identify both direct and indirect stable interactions among proteins *in vivo*. In AP-MS, the protein of interest immobilized on an affinity capture matrix (agarose or magnetic beads) is a bait. This can be achieved either using an endogenous protein with a specific antibody raised against it or expression of the protein fused with an in-frame epitope tag (eg. FLAG, V5, HA, His, c-myc). Usually, fusion baits are expressed at their endogenous expression levels. Cell or tissue lysates are then passed through the bait-matrix to pulldown the endogenous prey proteins that interact with the bait. Proteins that don't interact pass through the matrix and are washed off. To achieve a lower background binding, the bait is often fused with a tandem affinity purification (TAP) tag to perform two subsequent affinity purification steps (Fig. 1.14). Once the complex of proteins is co-purified, it is usually digested with trypsin to generate peptides that are separated using high-pressure liquid chromatography (HPLC), ionized, and then detected by MS.

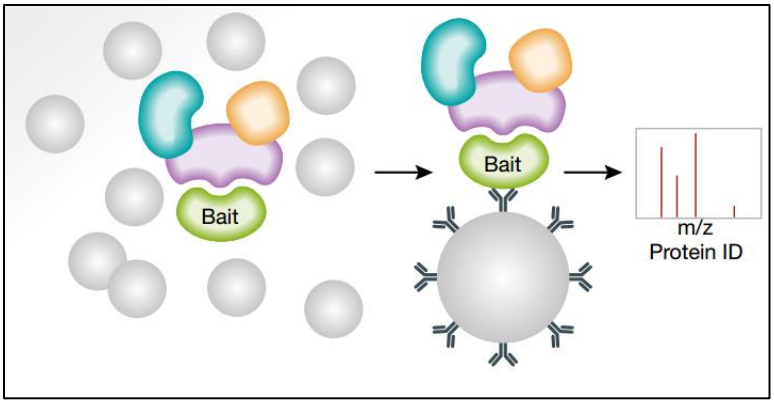

Figure 1.14: Schematic representation of AP-MS method.
Adapted from [277].

Pros and Cons of AP-MS

Unlike binary technologies, AP-MS methods don't require library preparation. It opens the door to identify novel protein interactions and, therefore, novel functions of the protein. In addition, PPIs can be identified under normal and pathological conditions, allowing the determination of novel cellular functions and their dysfunction in disease using normal or pathological cell or tissue lysates. This allows the determination of novel protein functions and pathogenic mechanisms. Preys are present in their native cellar environment, at the endogenous expression levels eliminating the issues related to protein tagging, steric hindrance, and (over) expression. Using antibodies against natural form of the bait proteins, multiple isoforms of the bait can be screened for the prey simultaneously. Epitope tagging allows the flexibility to add the tag to a position that doesn't hinder the protein's ability to interact with the interaction partners and allow purification of the proteins for which the antibodies aren't available. MS can detect protein concentrations at sub picomolar concentration, and protein interactions present at a very low abundance can also be identified.

Inherent to AP-MS, which require interactions to survive cell lysis and stringent washes, proteins are solubilized and purified with the bait protein, which may lead to both false-positive

and false-negatives. It can be challenging to achieve effective extraction of the protein complexes from poorly soluble subcellular locations like membranes, cytoskeleton, and nuclear lamina. In addition to effective extraction, retaining the integrity of the protein complexes, especially the ones mediated by transient or weak interactions, might be difficult as those interactions can be disrupted by detergent or buffer conditions during lysis, subsequent purification, and critical stringent washing steps. In addition, with cell lysis, the protein concentrations dramatically decrease, and as a result, the binding equilibrium will be altered, leading to false negatives. Therefore, many biologically important, transient, and weak interactions might go undetected following rigorous washing steps during AP.

Identification of spurious interactions as a result of lysis is another challenge, as proteins from different subcellular compartments encounter one another in the unnatural environment of a cellular lysate which might not normally occur in vivo. Another major limitation is nonspecific binding and enrichment of abundant contaminant proteins, leading to difficulty in identifying a bona fide interacting protein from the nonspecific background binding [288]. In some cases, epitope-tagged protein expression may lead to protein mis localization or improper folding. AP/MS can identify interactions between multiple proteins. However, unlike Y2H, the data can’t be used to assign the direct interactions between two proteins.

1.12.3 Proximity-based labeling-coupled-MS (PBL-MS)

Principle

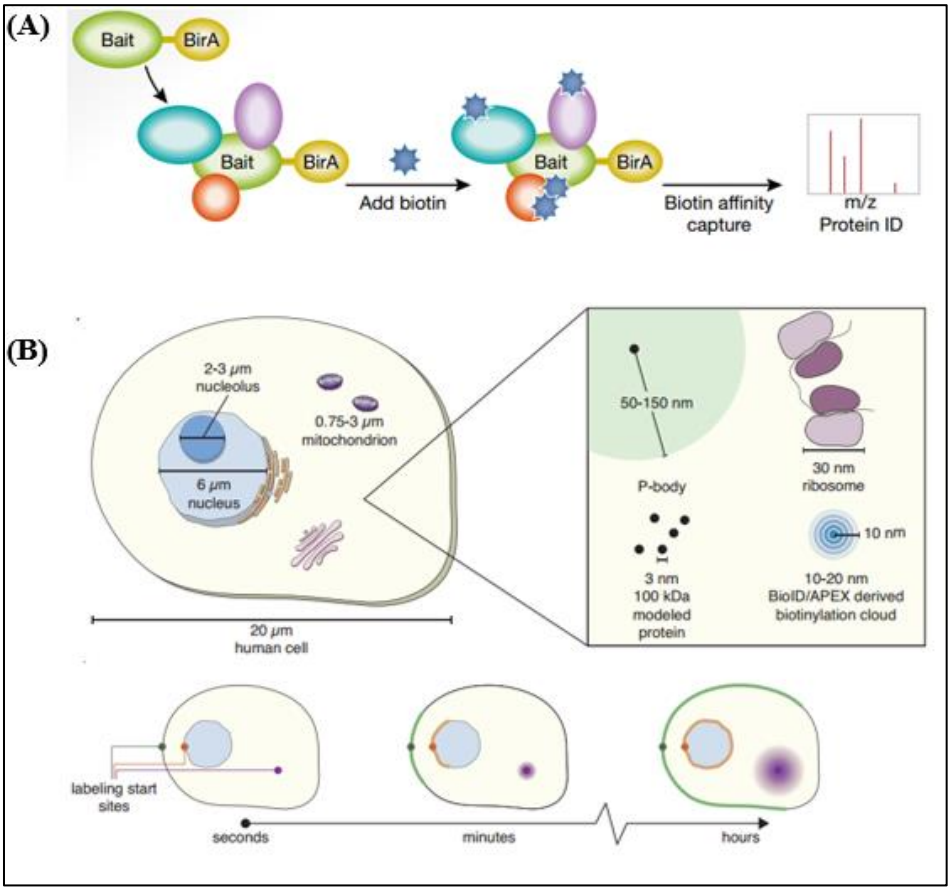

Figure 1.15: (A) Schematic representation of PBL-MS method. (B) size and time considerations in PDB–MS experiments.
Top panel- Relative diameters of different subcellular structures in relation to the estimated labeling radii of BioID and APEX. Adapted from [277]. Bottom panel- Consideration of bait and biotinylated prey protein dynamics as a function of time in PBL-MS experiments. Adapted from [289].

Proximity-based labeling (PBL) methods identify possible PPIs by covalently modifying proteins that are in proximity, typically within a 10-20 nm radius in the intact cell (Figure 1.15). Generally, the bait is fused with an enzyme that uses biotin or a phenolic biotin derivative. Expression of this fusion protein in the presence of biotin leads to biotinylation of nearby proteins. After biotin labeling, cells are lysed, proteins are extracted, followed by selective enrichment by affinity capture using streptavidin linked to a matrix and subsequently identified by MS. Since the

PPIs have been "marked" prior to cell lysis, many of the issues with cell lysis and stringent washing associated with AP-mass spec discussed above are avoided.

There are two main classes of enzymes utilized for this study: biotin ligases and peroxidases.

Biotin ligases

Biotin ligase based methods are based on the properties of the naturally occurring *Escherichia coli* enzyme BirA, a biotin protein ligase, which catalyzes endogenous biotinylation of a specific lysine residue on acetyl-CoA carboxylase [290]. BirA activates biotin to the highly reactive and unstable biotinoyl-5'-AMP (bio-AMP) intermediate, which is normally held in the active site until it is transferred to its target protein. BirA binds its substrate and transfers biotin to the lysine residues within a short acceptor peptide sequence on the substrate. A mutant BirA called BirA* prematurely releases bio-AMP in the medium, which reacts with amine groups on lysine residues in proximate proteins [291, 292]. BioID, BioID2, TuroID, BASU, and miniTurbo enzymes are engineered from BirA. BioID and BioID2 require labeling for 18-24 hr to have enough labeling for the identification by MS and generates static interaction maps. BioID2 is significantly smaller than BioID, which decreases the chances of target protein mislocalization and structure disruption [293]. TurboID, which carries 15-point mutations and miniTurbo with 13 mutations and an N-terminal deletion in BirA, can efficiently label proximal proteins in 10-30 min [294].

Peroxidases

Another class of proximity enzymes were engineered from a peroxidase enzyme that catalyzes the redox reactions. In the presence of peroxidases, phenolic compounds such as tyramine or phenolic aryl azide derivatives react with hydrogen peroxide (H_2O_2) to generate a short-lived free radical. Radicals generated from tyramine can covalently label side chains of aromatic amino acids, including tyrosine and tryptophan [295]. Horseradish peroxidase (HRP) is the best-studied peroxidase but exhibits poor labeling efficiency in reducing environments. Engineered ascorbic acid peroxidase (APEX), when incubated with biotin-phenol and H_2O_2 generates biotin-phenoxy radicals that covalently react with aromatic amino acids in minutes [296]. The APEX enzyme retains activity in reducing environments, allowing PPI detection in most subcellular environments. The labeling time for the APEX is in seconds, and therefore, dynamic interaction maps can be generated.

As tyramine-based reagents can label side chains of aromatic amino acids, including tyrosine and tryptophan, the labeling is relatively infrequent compared to biotin ligase-based methods, which modify lysine residues, which tend to be abundant and more solvent-exposed compared with aromatic amino acids [297].

Pros and Cons of proximity labeling

Similar to AP-MS, PBL-MS is a library-independent method. PPIs are detected in their natural cellular environment at endogenous protein expression levels since labeling occurs in the cell prior to lysis. Since biotin gets covalently attached to the protein, harsh conditions for membrane solubilization and efficient protein extraction don't prevent PPI detection. The biotin

mark remains on the protein even after the interaction has ceased or the protein has moved out of the vicinity and is thus well suited for identifying weak or transient interactions.

In addition, a relatively large quantity of the protein interactors can be labelled over time and subsequently enriched and detected by MS as compared to AP-MS, which detects the proteins which are statically binding at that time. Therefore, it is also more effective at detecting low abundance proteins as compared to AP-MS [298]. However, because the labeling radius of BioID or APEX results in detecting proteins close to the bait, fundamentally, these approaches readout proximity and not direct or indirect interactions, and the PPI is inferred.

Labeling of colocalized proteins simply because of the abundance or diffusion can lead to a higher background and complicate the analysis. Critical to this approach is judicious consideration of appropriate protein control; for example, targeting the ligase to the same cellular compartment as the bait protein can help distinguish interacting proteins from background compartment labeling. Another important consideration is that BioID and APEX are relatively bulky tags and may affect the normal functioning of the bait proteins. Interacting proteins farther from the enzyme tagged bait protein location may fall outside the labeling cloud and might not be detected. Due to its slow reaction time, BioID requires 18-24 hr labeling time to get sufficient protein for MS, leading to high background. In contrast, APEX acts in the minute range well-suited to investigate studies that require temporal resolution to generate dynamic interaction maps, such as characterization of G-protein-coupled receptor signaling [296]. Since the half-life of bio-AMP is minutes in water as opposed to biotin-phenoxyl radical, which is <1 ms, BioID is expected to have a larger labeling radius than APEX [299].

As described above, there are several false positive and negative interactions identified with each method; careful follow-up analysis to identify true interactions is required. Usually, a

combination of methods is recommended to confirm and validate PPIs. Taken together, identification of protein interaction networks allows a deeper understanding of biochemical cascades and molecular etiology of disease, as well as the discovery of putative protein targets of therapeutic interest.

1.13 Proteomics using Mass Spectrometry (MS)

The term "proteomics" was first coined in 1996 and defined as "PROTein complement of a genOME" [300]. The functional information of the genome is characterized by proteome. The proteome is dynamic and changes depending on the stimulation, cell type, and so on. To understand a biological function, proteomics studies are more relevant than analysis of mRNA. mRNA is not a direct reflection of the protein content in the cell, and studies have shown a poor correlation between mRNA and protein expression levels.

One of the analytical methods to study proteomics is mass spectrometry (MS), which measures the molecular weight of ions based on their mass-to-charge (m/z) ratios. Before MS, the first step in the proteomics experiment is the separation of proteins based on their physicochemical properties.

1.13.1 Sample preparation

To identify PPIs, protein complexes are purified from non-binders prior to their analysis by MS. This can be done by biochemical fractionation methods, namely 1- and 2-dimensional sodium dodecyl sulfate-polyacrylamide gel electrophoresis (SDS-PAGE) and stained using silver or Coomassie brilliant blue (CBB) stain [301, 302]. Then the separated complexes are extracted

from the gel, enzymatically digested (usually trypsin), fractionated by HPLC, and analyzed by MS (Fig. 1.16).

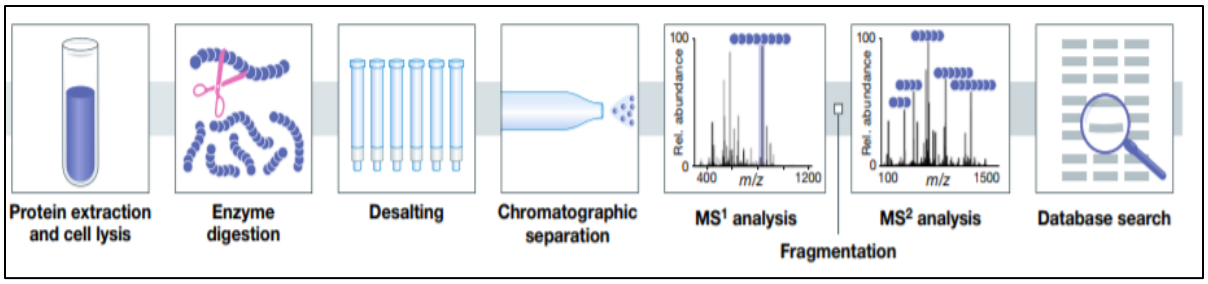

Figure 1.16: Workflow of a general proteomic experiment.
Adapted from [303].

Gel extraction and digestion are tedious and inefficient processes that may result in the loss of low abundance proteins. More recently, methods have been developed where isolated protein complexes are digested in-solution without biochemical fractionation [304]. Compared to proteins eluted from the gel, in-solution digested proteins can be of high abundance and complexity. As MS can identify only a limited number of peptides at a time, proteins are fractionated before running on the MS machine.

1.13.2 Components of mass spectrometry (MS)

There are three principal components of MS: an ionization source, which converts molecule from solid or liquid phase to an ionized aerosol, a mass analyzer in which the ions are separated by their mass/charge (m/z) values via a magnetic or electric field, and a detector which detects separated ions and their abundance, and a plot of ion abundance versus m/z can be obtained.

Ionization

The samples which need to be analyzed by MS must be charged and dry. The ionization source is the component of MS in which target materials are ionized. Commonly used soft ionization methods are matrix-assisted laser desorption ionization (MALDI) and electrospray ionization (ESI) which generates ions without significant loss of sample integrity [305].

In MALDI, the sample is embedded with matrix molecules and then subjected to laser mediated irradiation leading to vaporization of the matrix and formation of molecular ions [306] (Fig. 1.17). In ESI, a liquid sample flows from a microcapillary tube in which high voltage is applied, causing dispersion of the sample solution into aerosols. Evaporation of the solvent by a drying gas (usually nitrogen) results in the formation of desolvated ions [307].

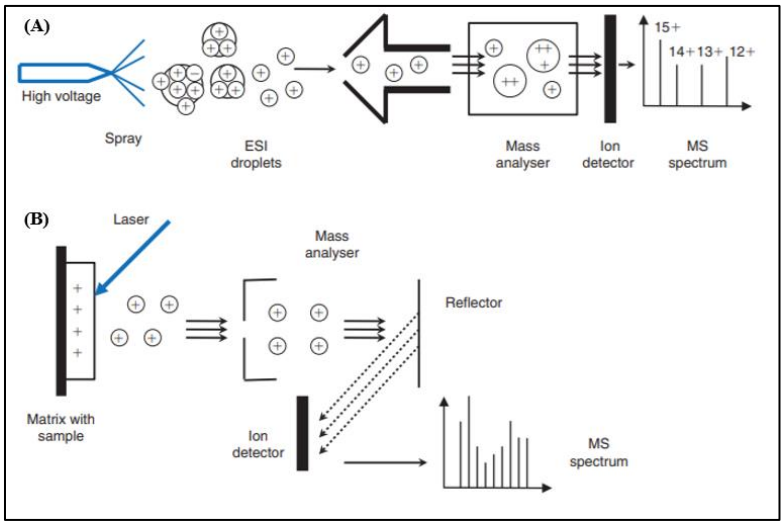

Figure 1.17: Principle of ESI and MALDI.
(A) ESI- Electrospray ionization **(B)** MALDI- Matrix-assisted laser desorption ionization. Adapted from [308].

Mass analyzer

After ionization, ionized molecules are resolved in mass analyzers based on their m/z ratio in a vacuum. Commonly used mass analyzers are quadrupole, ion trap and time-of-flight. Quadrupole mass analyzer uses an electric field generated between four axial rods through which direct current (DC) and radio frequency (RF) is passed. Any ion in the electric field will have its

trajectory deflected by the electric field based on its m/z ratio. Only a specific m/z value will resonate with the field and show a stable trajectory, at a given DC and RF combination. It, therefore, will be able to navigate to the end of the quadrupole and get detected. Ions with other m/z values with unstable trajectories collide with the quadrupoles, lose their charge and not be detected [309]. Ion traps "trap" ions in the electric field, which is then sequentially ejected for separation based on m/z resonance frequency. In contrast to a quadrupole mass analyzer, in an ion trap mass analyzer, the ions are stored and then selectively ejected from the ion trap instead of discarding them. TOF uses an electric field to accelerate ionized molecules in an ion-accelerating region and a flight tube. The flight time needed by the ions with a particular m/z is accelerated by a potential voltage to reach the detector [310].

Detector

Mass spectrometers can have a stand-alone ionization source and an analyzer or have a combination with two or more analyzers within one instrument. The names of the instruments are derived from the name of their ionization source and the mass analyzer.

1.13.3 Quantitative proteomics

The quantity of proteins can be measured by two methods, label-free quantification based on spectral counting or stable isotope labeling (Fig. 1.18). The spectral counts are the total numbers of spectra assigned for a protein, which is directly correlated with the protein abundance or area under the curve of the precursor ions' chromatographic peaks when liquid chromatography is coupled with MS/MS [311]. As samples are run separately in a label-free experiment, any variation in sample preparation or analysis reduces the reproducibility affecting quantitation [312, 313]. In

addition, it works well with the highly abundant proteins, but the reliability decreases dramatically for proteins with low abundance [314].

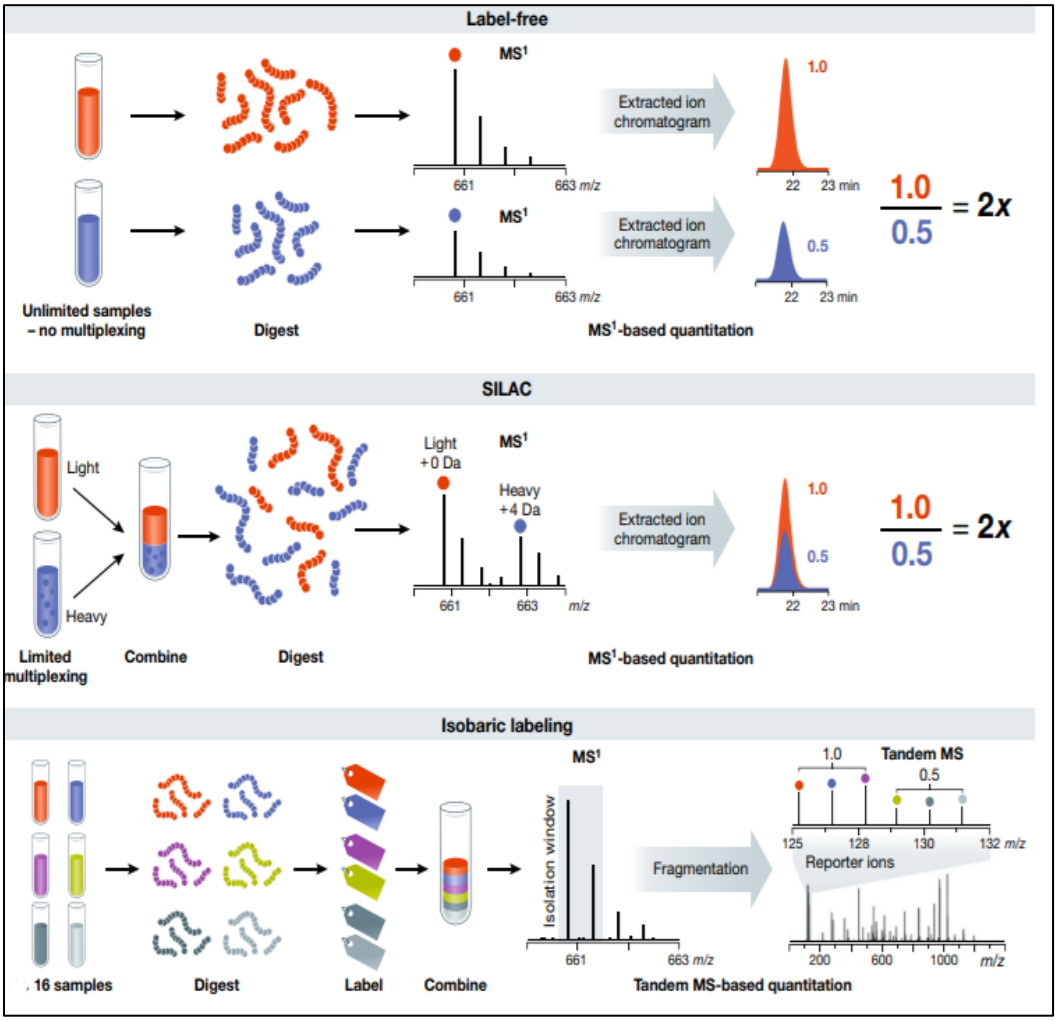

Figure 1.18: Schematic of three major quantitative methods used in MS.
Adapted from [303]

To overcome the disadvantages associated with label-free methods, stable isotope-labeled peptides are used. Most used quantitative proteomic methods include stable isotope labeling with amino acids in cell culture (SILAC), isotope-coded affinity tag (ICAT), and isobaric tag for relative and absolute quantitation (iTRAQ) or tandem mass tags (TMT) [315-317]. SILAC depends on labeling of select amino acids (usually arginine or lysine) in cell culture with “light” or “heavy”, which can be differentiated through MS. In ICAT, cysteine residues of proteins get

covalently attached to the ICAT reagent, which comprises an affinity tag, isotopically coded linker, and a reactive group. With this tag, two conditions or proteomes can be compared simultaneously. For more than two samples, iTRAQ/TMT reagents are used, which differentially label the amine group at the N-termini and lysine residues of peptides after protein digestion. Each iTRAQ/TMT reagent contains a mass reporter region (M), a cleavable linker region (F), a mass normalization region (N) and a protein reactive group (R). As whole M-F-N-R regions of the tags have the same total molecular weights and structure, isobaric tag labelled proteins are indistinguishable in mass. Therefore, their peptides appear as single peaks in MS1 spectra. Isotope-encoded reporter ions from the tags result in quantitative information in the MS/MS spectra after peptide fragmentation which gives rise to the mass reporter ions.

1.14 Thesis Overview

A major focus of this thesis is to identify novel effectors of $G\alpha_i$ and $G\alpha_q$ to understand their interactome to understand biology better. In chapter 1, I have detailed GPCR and G protein signaling, their classical effectors and regulators. Besides, detailed information on the role of Gi in chemotaxis and previous findings from our group, which has laid the foundation for this study, is described. Furthermore, traditional and relatively new methods to identify and characterize PPIs and their pros and cons are discussed in detail. In chapter 2, optimization of an intact cell proximity labeling method to identify novel interactors of $G\alpha_i$ and $G\alpha_q$ using two promiscuous biotin ligase enzymes, BioID2 and TurboID, respectively, is described. Our validation approach for the MS data, and previously unappreciated concept of interaction of G proteins with “a network of interactors”, are introduced. In chapter 3, a detailed characterization of one of the potential effectors, PRG, with active $G\alpha_i$ and differential regulation by multiple $G\alpha_i$ isoforms is described.

Preliminary findings on the interaction of different RasGAPs is also detailed. Finally, in chapter 4, the overall implications of our high throughput mass spec screens, current effectors and future directions are described.

Chapter-2

A Network of G Protein $G\alpha_i$ and $G\alpha_q$ Signaling Interactors is Revealed by Proximity Labeling Proteomics

Part of this chapter is published in bioRxiv (Chandan NR., 2021) [318].

2.1 Abstract

Gi proteins are the most abundant of all the G proteins family members, and Gi-coupled G-protein-coupled receptors (Gi-GPCRs) are the most ubiquitously expressed receptors. A vast majority of the functions attributed to Gi-GPCRs are known to be mediated by Gβγ subunits, and the $G\alpha_i$ is classically associated with inhibition of adenylate cyclase (AC). Our recent work discovered novel roles of $G\alpha_i$ in cell polarization and adhesion, however, the molecular details remained to be studied. To identify novel molecular targets of $G\alpha_i$ involved in these roles and to address the idea that possibly multiple targets of G_i-coupled receptors remain to be identified, we adopted an intact cell proximity-based labeling approach. We used BioID2, a promiscuous biotin ligase enzyme, coupled to tandem mass tag (TMT)-based quantitative proteomic mass spectrometry (MS). To identify true targets engaged by active $G\alpha_i$, we quantitatively compared proteomic data from proximity-labeling experiments with BioID2 fused to inactive $G\alpha_{i1}$ ($G\alpha_{i1}$) with BioID2 fused to constitutively active $G\alpha_{i1}$-Q204L ($G\alpha_{i1}$-QL). BioID2-with a PM targeting sequence, CaaX, was used as a membrane-targeted control. Known binding partners for Gα subunits including, GPCRs, Gβ, Gγ, AC, and Ric8A, were identified by mass spectrometry (MS) validating the method. We validated multiple families of protein candidates for selective biotinylation by a constitutively active BioID2-tagged $G\alpha_{i1}$ mutant not previously linked to Gi

signaling. Gene ontology analysis identified proteins involved in different cellular processes, suggesting a previously unappreciated network of interactions for activated $G\alpha_i$ proteins in intact cells.

Using this study as a method blueprint, we utilized TurboID-based proximity labeling coupled MS to identify novel interactors of $G\alpha_q$. Known binding partners of active $G\alpha_q$-Q209L ($G\alpha_q$-QL) including PLCβ, Trio, p63RhoGEF, GRK2 were identified, further supporting the validity of this approach. Identification of a set of new interacting proteins provides the potential for revealing new signaling pathways for GPCRs and consequently new potential targets for therapeutic intervention. In addition, the data suggest that protein-protein interactions (PPI) don't occur in isolation and calls for more global analysis of PPI identification and characterization to reveal networks of G protein regulated pathways. These data present a new paradigm for G protein-coupled signaling and will significantly impact our understanding of the biology regulated by these pharmacologically important receptors.

2.2 Introduction

G protein-coupled receptors (GPCRs) are a major class of cell surface receptors that regulate multiple physiological and pathophysiological processes in response to various ligands. Activated GPCRs bind to heterotrimeric G proteins consisting of Gα subunits and Gβγ constitutive heterodimers and catalyze the exchange of GTP for GDP on the Gα subunits. Subsequent conformational changes in the Gα subunit cause it to dissociate from the receptor and Gβγ subunits. Both Gα and Gβγ subunits then transduce signals from receptors to downstream effector proteins, including second messenger generating enzymes and ion channels [319-322].

The α-subunits that define the basic properties of heterotrimeric G proteins are divided into four families, $G\alpha_s$, $G\alpha_{i/o}$, $G\alpha_{q/11}$, and $G\alpha_{12/13}$ [319]. The $G\alpha_{i/o}$ family is an abundant and ubiquitous class of G protein subunits consisting of various isoforms including $G\alpha_{i1}$, $G\alpha_{i2}$, $G\alpha_{i3}$, and $G\alpha_o$ [38]. $G\alpha_{i/o}$ coupled GPCRs comprise nearly one hundred receptors for a wide variety of ligands including, opioids, cannabinoids, prostaglandins, histamine, somatostatins, chemokines, and neurotransmitters such as acetylcholine, adrenaline, serotonin, and dopamine [38]. $G\alpha_{i/o}$ subunit activity is classically associated with AC inhibition [323].

$G\alpha_{i/o}$-coupled chemokine and chemoattractant GPCRs regulate directional cell migration and adhesion involved in tissue formation, wound healing, immune response, and also in cancer cell invasion and metastasis [257, 324, 325]. Gβγ subunits released from Gi heterotrimers are central mediators of chemokine driven chemotaxis, whereas $G\alpha_i$ has been proposed to function passively through the GDP-GTP exchange-dependent cycling of free and bound Gβγ subunits [154]. Identification of signaling mechanisms specifically downstream of $G\alpha_i$ subunits has been hampered by the fact that perturbations that inhibit $G\alpha_i$ signaling also inactivate Gβγ signaling. For example, modification of $G\alpha_i$ by pertussis toxin (PTX) blocks interactions between the $G\alpha_i$-βγ heterotrimer and GPCRs, thereby inhibiting both Gα and Gβγ signaling [121]. Similarly, knockout (KO) of specific G protein α subunits, either in mice or with specific short inhibitory RNAs in cell culture, prevents signaling by both Gα and its associated Gβγ subunits [326]. Using a small-molecule Gβγ activator developed in our laboratory, we identified a role for active $G\alpha_i$ ($G\alpha_i$-GTP) in regulating neutrophil and HT1080 fibrosarcoma cell migration [160, 161]. In these studies, we showed that Gβγ promotes cell adhesion and $G\alpha_i$-GTP promotes de-adhesion, processes that must be coordinated for cells to move [161]. $G\alpha_i$-GTP regulation of adhesion is independent of 3',5'-

cyclic adenosine monophosphate (cAMP) signaling [160]; however, a direct effector responsible for this, that is regulated by $G\alpha_i$ was not identified.

Previous reports show that active-$G\alpha_{i2}$ regulates Ras, c-Jun N-terminal kinase (JNK) and extracellular signal-regulated kinase (ERK), causing oncogenic transformation of Rat-1 fibroblast cells [327]. Active $G\alpha_{i2}$ has also been reported to increase cell proliferation and anchorage-independent growth in NIH3T3 cells [328]. However, a decrease in cAMP is not sufficient to explain the underlying mechanism of cellular proliferation. Thus, it is likely that other cAMP-independent processes regulated by $G\alpha_i$ signaling have yet to be identified.

Methods previously used to identify new effectors of $G\alpha_i$ beyond AC include the yeast-two hybrid (Y2H) system and immunoprecipitation (IP) followed by MS [162, 329, 330]. While these methods have successfully identified interacting proteins, they have limitations. IP-MS methods recover only strong interaction partners that survive cell lysis and repeated detergent washes. GPCR-dependent signal transduction processes often involve transient PPI that is lost after cell disruption. The Y2H systems lack appropriate cellular context, and only fragments of proteins are used to identify binding interactions. Cell context is critical for optimizing interactions between signal transduction components through compartmentalization and interactions with membrane surfaces. Thus, it is likely that multiple G protein interactions may have been missed by these traditional approaches.

To circumvent these challenges, we adopted a proximity-based labeling approach using BioID2, a promiscuous biotin ligase enzyme, coupled to MS [293, 331]. Our goal was to capture $G\alpha_i$ subunit interactions with potential signal transduction partners and complexes in intact cells of interest. Using this approach, we identified multiple known binding partners of $G\alpha_i$, including $G\beta\gamma$ subunits and AC. Multiple classes of proteins involved in diverse cellular processes, including

cell migration and amino acid transport, were identified as potential interaction partners of active $G\alpha_{i1}$. We characterized one such protein, PDZ-RhoGEF (PRG), and validated it to be a novel effector of active $G\alpha_i$ downstream of Gi-coupled chemoattractant receptors, described in chapter 3.

Following the success of BioID2-$G\alpha_i$ screen, we performed proximity-based labeling coupled MS screen for another G proteins subtype, $G\alpha_q$. This was done using an improved enzyme with faster labeling kinetics, TurboID. Classically, $G\alpha_q$ signals via the activation of phospholipase C β (PLCβ) which catalyzes the hydrolysis of phosphatidylinositol 4,5-bisphosphate (PIP2) into diacylglycerol (DAG) and 1,4,5- inositol trisphosphate (IP3), resulting in subsequent activation of protein kinase C (PKC) and calcium efflux from the endoplasmic reticulum [73]. In addition, $G\alpha_q$ activates with RhoGEF; Trio, Kalirin, and p63RhoGEF, which leads to RhoA activation [332-334]. It is estimated that $G\alpha_q$ molecules expressed in a cell significantly outnumbers those of PLCβ, supporting the concept that PLCβ cannot account for all of the $G\alpha_q$-mediated cellular functions, suggesting the existence of alternative $G\alpha_q$ effectors responsible for PLCβ-independent $G\alpha_q$ functions [335].

In vitro studies have revealed the ability of $G\alpha_q$ to simultaneously bind to both PLCβ and phosphatidylinositol 3-kinase (PI3K) and can form stable and coexisting signaling complexes in the same cell. However, larger complexes containing G proteins with both PLCβ and phosphatidylinositol 3-kinase (PI3K) do not exist [335]. This suggests that separate pools of G protein and different effectors likely exist.

For many years, proteins and their biological functions have been studied using highly focused, biochemical reductionist approaches, which has produced a wealth of information on the functional and molecular properties of individual proteins and their interactions. However, for a

comprehensive understanding of the biology of a cell as a whole, a global interactome study of the proteins is called for. Investigation of the G protein interactome on a global scale and identification of a novel signaling pathway regulated by G_i and G_q-coupled GPCRs will have a significant impact on our understanding of the biology regulated by these ubiquitous and pharmacologically important receptors.

2.3 Material and methods

2.3.1 Plasmid cDNA constructs

BioID2 fused N-terminally with c-myc tag and C-terminally with mVenus followed by CaaX plasma membrane (PM) targeting motif (KKKKKKSKTKCVIM, derived from the C terminus of KRas), was a gift from Dr. Sundeep Malik, University of Rochester. TurboID fused N-terminally with V5 and C-terminally with mVenus followed by CaaX PM targeting motif, TurboID-Gα_q and TurboID-Gα_q-QL was a gift from Dr. Mathew Brody, University of Michigan. The following plasmids were obtained from Addgene: MCS-BioID2-HA (Kyle Roux, Plasmid #74224) [293], V5-TurboID-NES-pCDNA3 (Alice Ting, Plasmid # 107169) [294], pCDNA3-HA PSPC1(Yuh-Shan Jou, Plasmid #101764) [336], FLAG-p54 (Benjamin Blencowe, Plasmid #35379) [337], pEGFP-ATF6-(S1P-) (Ron Prywes, Plasmid #32956) [338], GFP-nArgBP2 (Guoping Feng, Plasmid #74514) [339], GFP-Golgin-84-TEV (Ayano Satoh, #42108), mEmerald-Parvin-C-14 (Michael Davidson, Plasmid #54214), EGFP-Vimentin-7 (Michael Davidson, Plasmid #56439), pGFP-Cortactin (Kenneth Yamada, Plasmid #50728). Gα clones in pcDNA3.1+ were obtained from the cDNA Resource Center. The sequences of the clones are available upon request.

2.3.2 Design and cloning of cDNA constructs

BioID2-HA was inserted between Ala^{121} and Glu^{122} of human $G\alpha_{i1}$-WT and $G\alpha_{i1}$-QL with the linker sequence SGGGGS flanking BioID2-HA on either side. The final clone was organized as follows: $G\alpha_{i1}$(1-121)-Linker-BioID2-HA-Linker-$G\alpha_{i1}$(122-355). V5-TurboID was inserted between F^{124} and E^{125} of human $G\alpha_q$-WT and $G\alpha_q$-QL with the linker sequence SGGGGS flanking V5-TurboID on either side. The final clone was organized as follows: $G\alpha_q$(1-124)-Linker-V5-TurboID-Linker-$G\alpha_q$(125-359).

2.3.3 Cell culture

A293 and HT1080 cells were obtained from American Type Culture Collection (ATCC). A293, A293-FPR1, and HT1080 cells were grown in DMEM (10013CV, Corning) supplemented with 10% fetal bovine serum (FBS) (10437028, Gibco) and 100 units of penicillin/streptomycin (P/S) (15140122, Gibco) at 37 °C with 5% CO_2. Media was supplemented with 100 µg/mL Geneticin (G418) (G8168, Sigma) to select A293-FPR1 cells. Trypsin-EDTA (25200056, Gibco) was used for cell passaging.

2.3.4 Reagents

The following primary and secondary antibodies were utilized: $G\alpha_{i1/2}$ (anti-sera) [340], HA (3724, Cell Signaling), FLAG (F1804, Sigma), c-myc (13-2500, Invitrogen), Streptavidin-IRDye800 (925-32230, LI-COR, V5 (R960-25, Invitrogen). Primary antibodies were made in 3% BSA and 0.1% sodium azide and the blots were incubated in primary antibody overnight at 4 °C except 1 hr incubation at RT for streptavidin-IRDye800. Secondary antibody goat anti-rabbit

DyLight^{TM} 800 (SA535571, Invitrogen), goat anti-mouse IRDye 800CW (926-32210, LICOR) at 1:10,000 dilution and goat anti-rabbit Alexa Fluor 488 (A11034, Invitrogen) at 1:1000 dilution.

2.3.5 Proximity labeling using BioID2 and TurboID followed by western blotting

A293 cells were plated in a 6-well plate at a density of 0.35×10^6 cells per well in DMEM media. 24 hr after plating, media was replaced with 2 mL DMEM supplemented with 50 µM and 500 µM Biotin for BioID2 and TurboID screen, respectively (B4501, Sigma) (prepared as previously described) [341] and 10% FBS. The cells were then transfected with 1 µg of BioID2 clone (BioID2-G$\alpha_{i1,}$ BioID2-Gα_{i1}-QL or BioID2-CaaX) or TurboID clone (TurboID-G$\alpha_{q,}$ TurboID-Gα_{q}-QL or TurboID-CaaX) and 100 ng of yellow fluorescent protein (YFP) cDNAs in each well using 1:3 DNA: Lipofectamine 2000 (11668019, Invitrogen) ratio. 24 hr after concurrent transfection and biotin labeling for BioID2 clones or after 24 hr transfection followed by 1 hr labeling for TurboID clones, 300 µL 1× Laemmli buffer was added per well, and the lysates were collected, boiled for 10 min at 95 °C, 40 µL of was resolved on 4-20% Mini-protean TGX^{TM} Gel (4561094, Bio-Rad) and detected by western blot. Anti-HA (1:2000), anti-PDZ-RhoGEF (1:1000), anti-c-myc (1:2000), anti-V5 (1:2000), Streptavidin-IRDye800 (1:3000) were utilized.

2.3.6 Proximity labeling using BioID2 followed by streptavidin pulldown and western blotting

A293 cells were plated in a 10 cm dish at a density of 2.0×10^6 cells per dish. The next day, the media was replaced with 10 mL DMEM supplemented with 50 µM Biotin and 10% FBS. Thereafter, the cells were transfected with 3 µg of BioID2-Gα_{i1}, BioID2-Gα_{i1}-QL, or BioID2-CaaX and 3 µg of protein of interest (HA-PSPC1, FLAG-p54-HA, GFP-ATF6, GFP-ArgBP2,

Golgin A5-GFP, Parvin-GFP, Vimentin-GFP, Cortactin-GFP) in each dish using 1:3 DNA: Lipofectamine 2000 ratio. 24 hr after transfection and labeling, the cells were harvested by centrifugation at 4000× g for 10 min and lysed in 500 µL ice-cold lysis buffer (modRIPA buffer: 50 mM Tris, 150 mM NaCl, 0.1% SDS, 0.5% Sodium deoxycholate, 1% Triton X-100, final pH 7.5) supplemented with 1× protease inhibitor (PI) cocktail (P8849, Sigma), 1 mM Phenylmethylsulfonyl fluoride (PMSF) (786-055, G-Biosciences) for 10 min on ice. The lysates were further incubated with 125 units of Benzonase (E1014-25KU, Sigma) in an end-over-end rotator at 4 °C for 20 min. 0.3% SDS was added to lysates and incubated for an additional 10 min at 4 °C. Lysates were centrifuged at 15000× g for 10 min, and the supernatant was transferred to fresh tubes, and total protein concentration was equalized using Pierce 660-nm protein assay reagent (22660, Thermo Fisher Scientific). 5% of equalized lysates were taken out before pulldown to analyze the biotinylation of inputs by western blot analyses. The remaining lysates were incubated with 100 µL Pierce™ streptavidin magnetic beads slurry (88817, Thermo Fisher Scientific) per sample in an end-over-end rotator at 4 °C for 18 hr to capture biotinylated proteins. Following streptavidin pulldown, beads were washed twice with ice-cold modRIPA, and once with ice-cold 1× PBS. 30 µL 1× Laemmli buffer was added to the beads, boiled for 10 min at 95 °C, and the supernatant was loaded on the SDS-PAGE followed by western blot analyses. Antibody dilutions were anti-HA (1:2000) and anti-c-myc (1:2000).

2.3.7 Proximity labeling using BioID2 and TurboID for mass spectrometry-based proteomic analysis

Low passage HT1080 cells (passage number up to 15) were used for proximity labeling experiments. HT1080 cells were plated into 175 cm^2 flasks at a density of 5.5×10^6 cells per flask.

The next day, the media was replaced with 35 mL DMEM containing 50 µM biotin and 10% FBS. Subsequently, the cells were transfected with 8 µg of BioID2 and 4 µg of YFP cDNAs in each flask. 0.6 µL of Viromer® Red (VR-01LB-00, Lipocalyx, Germany) reagent was used per 2 µg of cDNA for transfection, resulting in ~80-85% transfection efficiency. 24 hr after labeling and transfection, the labeling medium was decanted, cells were washed twice with 1×PBS, and harvested at 4000× g for 10 min. This step was repeated twice using 1×PBS to recover the maximum number of cells. The supernatant was aspirated, and pellets were snap-frozen and stored at -80°C until further use.

The method for TurboID-$G\alpha_q$ mass spec sample prep was the same as for BioID2-$G\alpha_{i1}$ except for a few variations: Low passage A293 cells were used for the experiment, and the cells were transfected using Lipofectamine 2000. The labeling period was 1 hr as opposed to 24 hr for BioID2 clones.

All stock solutions used for streptavidin pulldown were freshly prepared, except lysis buffer. Low protein binding tubes (022431081, Eppendorf) were used for sample preparation. Frozen pellets were lysed in 1 mL of ice-cold lysis solution (composition described above) for 10 min on ice, incubated with 125 units of Benzonase with end-over-end rotation at 4 °C for 20 min. 0.3% SDS was added to lysates and incubated for another 10 min at 4 °C. Lysates were centrifuged at 15,000× g for 15 min, the supernatant was transferred to fresh tubes, and total protein concentration was equalized using Pierce 660-nm protein assay reagent. 5% of equalized lysates were saved before pulldown to analyze the biotinylation of inputs by western blot analysis. The remaining equalized lysates were incubated with 500 µL Pierce™ streptavidin magnetic beads slurry per sample, in an end-over-end overnight 4°C for 18 hr. Subsequently, the beads were washed twice with modRIPA, once with four different solutions: 1 M KCl, 0.1 M Na_2CO_3, 2%

SDS (made in 50 mM Tris pH 7.5), and 2 M Urea (made in 10 mM Tris pH 8.0). Finally, the beads were washed twice with 1× PBS and were snap-frozen and stored at -80 °C until further processing for mass spectrometry.

2.3.8 Protein digestion and TMT labeling

On-bead digestion followed by LC-MS/MS analysis was performed at the mass spectrometry-based Proteomics Resource Facility of the Department of Pathology at the University of Michigan. Samples were reduced (10 mM DTT in 0.1 M TEAB at 45°C for 30 min), alkylated (55 mM 2-chloroacetamide at room temperature (RT) for 30 min in the dark, and subsequently digested using 1:25 trypsin (V5113, Promega): protein at 37° C with constant mixing using a thermomixer. 0.2% TFA was added to stop the proteolysis, and peptides were desalted using a Sep-Pak C18 cartridge (WAT036945, Waters Corp). The desalted peptides were dried in a Vacufuge and reconstituted in 100 µL of 0.1 M TEAB. A TMT10plex^{TM} isobaric labeling kit (0090110, Thermo Fisher Scientific) was used to label each sample per manufacturer's protocol. The samples were labeled with TMT 10-plex reagents at RT for 1 hr. The reaction was quenched by adding 8 µL of 5% hydroxylamine for 15 min, combined, and subsequently dried. An offline fractionation of the combined sample into 8 fractions was performed using a high pH reversed-phase peptide fractionation kit, as per the manufacturer's protocol (84868, Pierce). Fractions were dried and reconstituted in 12 µL of 0.1% formic acid/2% acetonitrile for LC-MS/MS analysis. Sample-to-TMT channel information is provided below:

Table 2-1: Sample-to-TMT channel information

Replicate number	Sample ID	TMT Channel	Replicate number	Sample ID	TMT Channel
1	BioID2-$G\alpha_{i1}$	126	1	TurboID-$G\alpha_q$	126
1	BioID2-$G\alpha_{i1}$ -QL	127N	1	TurboID-$G\alpha_q$-QL	127N
1	BioID2-CaaX	128N	1	TurboID-CaaX	129N
2	BioID2-$G\alpha_{i1}$	128C	2	TurboID-$G\alpha_q$	130N
2	BioID2-$G\alpha_{i1}$ -QL	129N	2	TurboID-$G\alpha_q$-QL	131N
2	BioID2-CaaX	129C	2	TurboID-CaaX	127C
3	BioID2-$G\alpha_{i1}$	130N	3	TurboID-$G\alpha_q$	128C
3	BioID2-$G\alpha_{i1}$ -QL	130C	3	TurboID-$G\alpha_q$-QL	129C
3	BioID2-CaaX	131	3	TurboID-CaaX	131C

2.3.9 Liquid chromatography-mass spectrometry analysis

An Orbitrap Fusion (Thermo Fisher Scientific) and RSLC Ultimate 3000 nano-UPLC (Dionex) was used to acquire the data. To achieve superior quantitative accuracy, we employed multinotch-MS3 [342]. 2 µL of each fraction was resolved on a nano-capillary reverse phase column (PepMap RSLC C18 column, 75 µm i.d. × 50 cm; Thermo Scientific) at the flowrate of 300 nL/min using 0.1% formic acid/acetonitrile gradient system (2-22% acetonitrile in 110 min;22-40% acetonitrile in 25 min; 6 min wash at 90% followed by 25 min re-equilibration) and directly sprayed onto the Orbitrap Fusion using EasySpray source (Thermo Fisher Scientific). Mass spectrometer was set to collect one MS1 scan (Orbitrap; 120K resolution; AGC target $2x10^5$; max IT 50 ms) followed by data-dependent, "Top Speed" (3 seconds) MS2 scans (collision-induced dissociation; ion trap; NCD 35; AGC $5x10^3$; max IT 100 ms). For multinotch-MS3, the top 10 precursors from each MS2 were fragmented by HCD followed by Orbitrap analysis (NCE 55; 60K resolution; AGC $5x10^4$; max IT 120 ms, 100-500 m/z scan range).

Proteome Discoverer (v2.4; Thermo Fisher) was used for data analysis. Tandem MS spectra were searched against SwissProt human protein database using the following search parameters: MS1 and MS2 tolerance were set to 10 ppm and 0.6 Da, respectively;

carbamidomethylation of cysteines (57.02146 Da) and TMT labeling of lysine and N-termini of peptides (229.16293 Da) were considered static modifications; oxidation of methionine (15.9949 Da) and deamidation of asparagine and glutamine (0.98401 Da) were considered variable. Proteins and peptides that passed ≤1% false discovery rate threshold were retrained for subsequent analysis. Quantitation was performed using TMT reporter ion in MS3 spectra with an average signal-to-noise ratio of 10 and <50% isolation interference.

2.3.10 Normalization and sorting criteria

Only a small fraction of all the proteins labeled by BioID2-$G\alpha_{i1}$ are expected to have increased enrichment in BioID2-$G\alpha_{i1}$-QL samples relative to the BioID2-$G\alpha_{i1}$ samples. Most of the proteins are expected to be equally enriched across samples as the majority of the labeling is based on proximity rather than $G\alpha_{i1}$-QL-specific interactions. Therefore, to quantitatively compare the samples across groups, we summed the total TMT signal for each sample to obtain a normalization factor used to normalize the values for each protein across experimental groups. Normalized abundance ratio and p-values were used for the subsequent analysis. Proteins constituting the active $G\alpha_{i1}$ interactome fulfilled all the following criteria: PSM>5, Abundance ratio BioID2-$G\alpha_{i1}$/BioID2-CaaX ≥ 0.8 and BioID2-$G\alpha_{i1}$-QL/ BioID2-$G\alpha_{i1}$ ≥ 1.3, Abundance ratio P-value BioID2-$G\alpha_{i1}$-QL/BioID2-CaaX <0.05.

For the TurboID-$G\alpha_q$ screen, the following criteria were used to filter proteins constituting the active $G\alpha_q$ interactome: PSM ≥5, Abundance ratio TurboID-$G\alpha_q$/TurboID-CaaX ≥ 0.6 and TurboID-$G\alpha_q$-QL/ TurboID-$G\alpha_q$ ≥ 1.3, Abundance ratio P-value BioID2-$G\alpha_{i1}$-QL/BioID2-CaaX <0.05.

2.3.11 Gene ontology analysis.

Gene ontology (Go) analysis was performed using the DAVID Bioinformatics resource at https://david.ncifcrf.gov. Proteins selected based on the criteria in Figure 2.4 C were submitted based on gene identifiers to the analysis server and analyzed by functional annotation clustering.

2.3.12 Immunofluorescence staining

A293 cells (2×10^4 cells/well) were plated on a poly-D-lysine coated 8-well chamber µ-slide (80826, Ibidi) and transfected with BioID2 clones (200 ng cDNA/well) the following day using 1:3 DNA: Lipofectamine 2000 ratio. 24 hr post-transfection, cells were fixed with 4% (w/v) paraformaldehyde (PFA) (15710, Electron microscopy sciences) for 10 min at RT and washed with phosphate-buffered saline (PBS, BP3994, Fisher). Subsequently, cells were blocked and permeabilized with 10% normal goat serum in 1× PBS containing 0.1% (v/v) Triton X100 (1× PBS-T) for 1 hr at RT. Primary anti-HA antibody HA (3724, Cell Signaling) was used at 1:500 dilution in 2% goat serum in 1×PBS-T overnight at 4°C. The next day, cells were washed three times with 1× PBS-T and incubated with secondary antibody (goat anti-rabbit Alexa Fluor 488) at a dilution of 1:1000 in 1× PBS-T for 1 hr at RT. The nuclei were stained with DAPI for 15 min and washed once with 1× PBS-T and 1× PBS. Cells were imaged on a LEICA DMi8 microscope in confocal mode with a 63× oil lens using 405 nm excitation for DAPI and 488 nm for Alexa Fluor 488 secondary antibody. Acquisition parameters were kept constant for all the conditions of an experiment.

2.3.13 Glosensor cAMP reporter assay

A293 cells (4×10^4 cells/well) were plated per well in a 96-well plate (655983, Greiner). The following amounts of DNA were used per well: 50 ng of pGloSensor™-20F cAMP plasmid (E1171, Promega), 125 ng of untagged $G\alpha_{i1}$-WT, $G\alpha_{i1}$-QL or BioID2 fused $G\alpha_i$ clones or empty vector (control, pCDNA3.1+). Reverse transfection was performed using 1:3 DNA: Lipofectamine 2000 ratio. 24 hr after transfection, cells were washed once with 1× PBS, and 75 µL of 2 mM D-luciferin (LUCK-1G, Goldbio) in Leibovitz's L-15 medium (21083-027, Gibco) was added for 2 hr at 37 °C, 5% CO_2 incubator. Cells were treated with vehicle or 1 µM forskolin (Fsk) (11018, Cayman Chemicals), and luminescence was measured using a Varioskan™ LUX multimode microplate reader for 30 min.

2.3.14 Western blotting

Samples were resolved on 4-20% Mini-protean TGX™ Gels (4561094, Bio-Rad), were transferred to a nitrocellulose membrane (66485, Pall Corporation), and stained with Ponceau S (141194, Sigma). Membranes were blocked with 5% non-fat milk powder in TBST (0.1% Tween-20 in Tris-buffered saline) at RT for 1 hr with constant shaking. Membranes were probed with primary antibodies for 1 or 2 hr at RT or overnight at 4 °C. The membranes were washed with TBST, incubating with secondary antibody for 1 hr at RT, washed with TBST, and imaged using an Odyssey Infrared Imaging System (Li-Cor Biosciences).

2.3.15 Statistical analysis

All the experiments were performed at least three times, except Figure 2.4E, which was repeated twice. Data shown are expressed as mean ± SD or as a representative experiment of three

independent experiments. Statistical significance between various conditions was assessed by determining P values using the Student's t-test, one-way or two-way ANOVA with Tukey's multiple comparisons test. (**P < 0.01, *** < 0.001, ****<0.0001). Western blot images were scanned using Licor and quantified using Image Studio Lite (Version 5.2). All data were analyzed using GraphPad Prism 7.0 (GraphPad; La Jolla, CA), and schematic representations of the figures were created with BioRender.com and Adobe illustrator.

2.3.16 Data and materials availability

The mass spectrometry proteomics data have been deposited to the ProteomeXchange Consortium via the PRIDE partner repository with the dataset identifier PXD027905 [343].

2.4 Results

Identification of novel interacting partners of Gαi

2.4.1 Rational design of BioID2 fused Gαi1

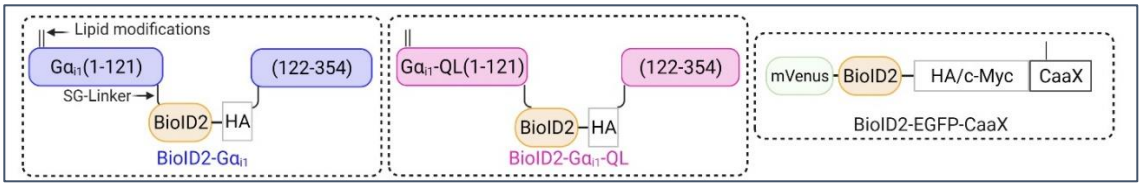

Figure 2.1: Schematic of BioID2 fusion constructs.
BioID2 was inserted between residues A121-E122 in the αb-αc loop (the first loop of the helical domain) of human Gαi1, flanked by SG-linkers. Palmitoylation and myristylation sites on the Gαi1 subunit and the farnesylation sites on CaaX moiety are labeled as lipid modifications.

To identify proteins that selectively interact with the active form of Gαi1 using proximity labeling, we fused the promiscuous biotin ligase, BioID2 [293] to Gαi1 (BioID2-Gαi1) and constitutively active Gαi1-Q204L (BioID2-Gαi1-QL). We inserted BioID2 as an internal tag in the

αb-αc loop of $G\alpha_{i1}$, which has been shown to tolerate GFP insertion, allowing the N and C termini to interact with membranes and receptors [344] (Fig. 2.1).

In the absence of receptor-dependent activation in cells, $G\alpha_{i1}$ is primarily GDP-bound and inactive (referred to as $G\alpha_{i1}$), whereas a Q204L mutation in $G\alpha_{i1}$ renders it GTPase-deficient, and therefore constitutively GTP-bound and active (referred to as $G\alpha_{i1}$-QL) [345]. Comparison of active to inactive $G\alpha_{i1}$ allowed us to search for targets that interact selectively with the activated $G\alpha_{i1}$. As a control for general promiscuous labeling of proteins because of abundance or simply due to co-residence at the PM, a PM-targeted BioID2 fused to the C-terminal PM targeting motif of KRas (BioID2-CaaX) was used. Thus, three experimental groups, BioID2-$G\alpha_{i1}$, BioID2-$G\alpha_{i1}$-QL, and BioID2-CaaX, were used to screen for potential targets that selectively interact with $G\alpha_{i1}$-GTP (Fig. 2.1A).

2.4.2 BioID2 fused $G\alpha_{i1}$ localizes predominantly to the PM and biotinylates endogenous proteins

To characterize the functionality of BioID2 fused $G\alpha_{i1}$ proteins, we examined their localization in A293 cells. All three proteins, BioID2-$G\alpha_{i1}$, BioID2-$G\alpha_{i1}$-QL, and BioID2-CaaX, localized predominantly to the PM (Fig. 2.2 A). Subsequently, we tested the biotin labeling efficiency of BioID2 fused $G\alpha_{i1}$ proteins in A293 cells. Cells transiently transfected with the indicated cDNA clones were incubated with biotin, and lysates were probed with fluorescently tagged streptavidin. Multiple proteins were biotinylated in BioID2-$G\alpha_{i1}$, BioID2-$G\alpha_{i1}$-QL, and BioID2-CaaX samples, and biotinylation was dependent on BioID2 and biotin (Fig. 2.2 B). There were differences in the total biotinylation pattern amongst the three experimental groups, suggesting that the three fusion proteins labeled endogenous proteins differentially.

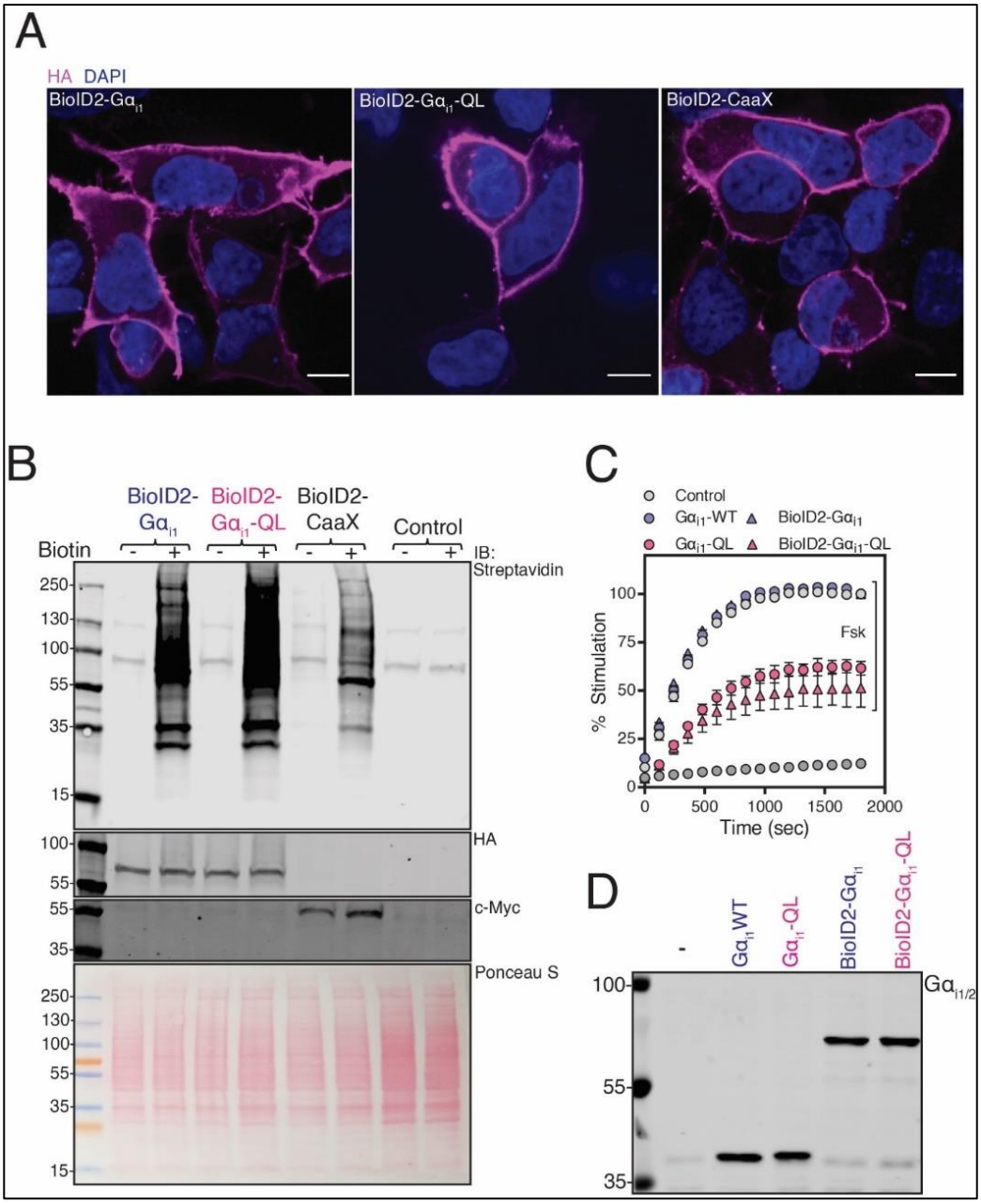

Figure 2.2: Characterization of BioID2 fused Gα$_{i1}$ and Gα$_{i1}$-QL.
(A) Following the transfection of HA-tagged BioID2 fused constructs into A293 cells for 48 hr, cells were immunostained with an HA antibody. Nuclei were stained with DAPI. Representative images from three randomly selected fields of view are shown. Scale bar, 10 µm. **(B)** Transfected BioID2 fused constructs biotinylate multiple proteins in cells. A293 cells were transfected with indicated constructs and labeled in the presence of biotin for 24 hr. Top panel: Biotinylated proteins present in the whole-cell lysates after 24 hr of labeling were detected on a streptavidin western blot. The two bands at 130 and ~90 kDa correspond to endogenously biotinylated proteins in control lanes. Middle panels: Expression of the BioID2-Gα$_{i1}$ and QL was tested with HA antisera, and BioID2-CaaX was tested using an anti-c-Myc antibody on western blots. Bottom Panel: Ponceau S-stained blot showing total protein loading. Western blots represent one of three independent experiments that yielded similar results. **(C)** Cells were transfected with cAMP Glosensor^{TM} along with BioID2 tagged and untagged Gα$_{i1}$ constructs for 24 hr. Luminescence as a measure of cAMP accumulation was monitored for 30 min (x-axis) after Forskolin (Fsk) stimulation and represented as % stimulation (y-axis) relative to the maximum signal in the respective WT group with 1 µM Fsk treatment. **(D)** Western blot showing the expression of various constructs. Data represent one of three independent experiments that yielded similar results.

2.4.3 BioID2 fused $G\alpha_{i1}$-QL inhibits cAMP accumulation

We evaluated the ability of $G\alpha_{i1}$-QL to inhibit AC by measuring inhibition of forskolin (Fsk)-stimulated cAMP production using a cAMP biosensor (cAMP-Glo^{TM}). As expected, both untagged and BioID2 tagged $G\alpha_{i1}$-QL reduced the rate and extent of cAMP generated upon Fsk addition (Fig. 2.2 C). Conversely, the $G\alpha_{i1}$-GDP counterparts did not affect Fsk stimulated cAMP accumulation. Western blot confirmed a similar abundance of these proteins (Fig. 2.2 D). These experiments established that $G\alpha_{i1}$-QL fused with BioID2 can localize to the PM, inhibit AC, and thus behave similarly to the untagged counterpart.

2.4.4 Proximity labeling-coupled MS in HT1080 fibrosarcoma cells

Our goal was to identify proteins regulated by $G\alpha_i$ that could be involved in cell migration downstream of chemokine or chemoattractant receptors. HT1080 fibrosarcoma cells express FPR1 receptors, adhere and migrate on fibronectin-coated surfaces, and are comparatively easy to grow and transfect relative to neutrophil-like cells. Roles for $G\alpha_{i1}$ and $G\beta\gamma$ in cell adhesion and migration have been previously established in these cells [161, 346]. For these reasons, we chose HT1080 cells for the proximity labeling experiments to increase the probability of identifying effectors of $G\alpha_{i1}$ relevant to cell migration.

In HT1080 cells transfected with BioID2-$G\alpha_{i1}$, BioID2-$G\alpha_{i1}$-QL, or BioID2-CaaX, BioID2 fused $G\alpha_{i1}$ subunits were expressed at levels similar to endogenous $G\alpha_i$ (Fig. 2.3 C). To perform quantitative comparison of biotinylated proteins after purification with streptavidin beads, each sample was labeled with a unique isobaric tandem mass tag (TMT). This allowed triplicate samples from each group to be pooled and analyzed in a single MS run to compare relative protein abundance (Fig. 2.3 B).

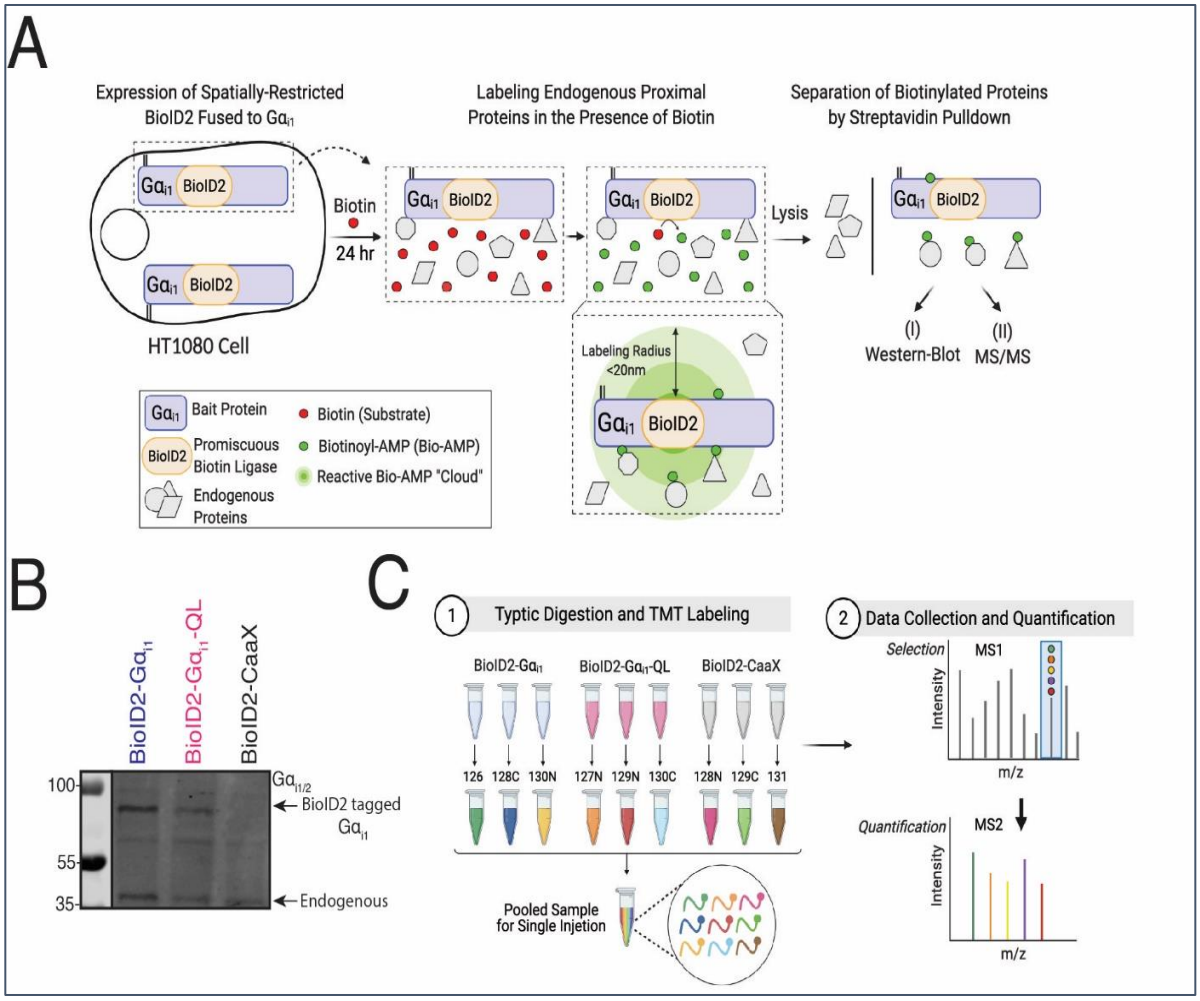

Figure 2.3: Principle and experimental workflow of proximity labeling of Gαi1 interactome.
(A) Schematic of principle and experimental workflow of proximity-based labeling using BioID2. HT1080 cells were used for mass spectrometry experiments and A293 cells were used for pulldown western blot. Cells were transfected with the indicated constructs and labeled for 24 hr in the presence of biotin. Gαi1 fused BioID2 biotinylates proteins in proximity (< 20 nm) in an unbiased manner to identify candidate interacting proteins of Gαi1. **(B)** Schematic of sample processing and mass spectrometry analysis. Samples pulled down using streptavidin beads were digested with trypsin and labelled with a TMT tag. Triplicate samples of BioID2-Gαi1 and BioID2-Gαi1-QL and BioID2-CaaX were pooled and resolved by LC-MS, and the data was analyzed using proteome discover. **(C)** Western blot for BioID2-Gαi1 constructs and endogenous Gαi1 protein in HT1080 cells that were used for proximity labeling experiments. Data represent one of three independent experiments that yielded similar results.

2.4.5 MS data analysis identifies multiple known and candidate interacting proteins

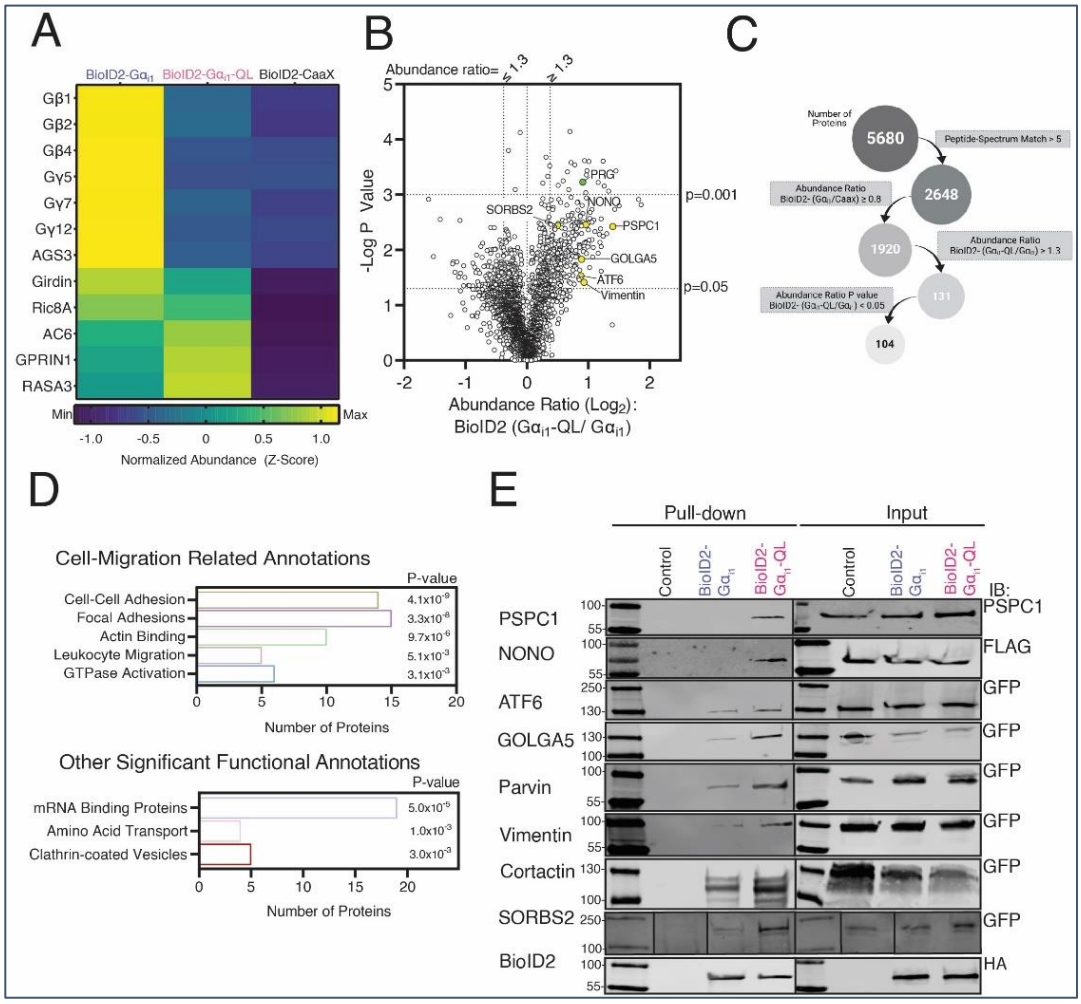

Figure 2.4: Proximity labeling proteomics results of BioID2-Gαi screen.
(A) Heat map showing the relative changes in abundance of known binding partners of Gαi that were identified in the mass spectrometry analysis. **(B)** Volcano plot of all high confidence proteins identified where the BioID2-Gαi1/BioID2-CaaX ratio was greater than 0.8. PRG is highlighted in green, and the candidate proteins investigated in 2E are labeled in yellow. **(C)** Schematic showing filtering criteria for selection of proteins enriched in BioID2-Gαi1-QL samples relative to BioID2-Gαi1. **(D)** Representative classes from GO analysis of proteins from B that met the final criteria in C. P values was generated with the DAVID software. **(E)** Validation of candidate proteins for their proximity and enrichment with BioID2-Gαi1-QL. cDNA clones encoding indicated epitope or GFP tagged proteins were co-transfected with BioID2-Gαi1 or BioID2-Gαi1-QL, labeled with biotin for 24 hr, followed by streptavidin pulldown and western blotting. Western blots are representative of experiments performed twice, yielding qualitatively comparable data.

We detected several proteins known to interact with Gαi including, Gβ and γ subunit isoforms, which were selectively enriched in the BioID2-Gαi1 samples relative to BioID2-Gαi1-QL, as expected (Fig. 2.4 A). Several isoforms of AC were detected, but there was no statistically significant difference between the BioID2-Gαi1-QL and BioID2-Gαi1 samples. Ric8A was also

equally labeled by BioID2-Gα_{i1}-QL and BioID2-Gα_{i1}. Gα_i-GTP effectors, GPRIN1 and RASA3 [162, 347], were highly enriched in BioID2-Gα_{i1}-QL samples relative to BioID2-Gα_{i1} samples (Fig. 2.4 A). Multiple receptors were also identified, but most were not significantly enriched in either the BioID2-Gα_{i1}-QL or BioID2-Gα_{i1} samples.

Overall, ~5000 proteins were isolated and identified (Fig. 2.4 B). We selected proteins with a minimum of 5 peptides assigned to each protein to ensure the robustness of the data. We also filtered the data to include only proteins for which the ratio of normalized abundance for the BioID2-Gα_{i1} and BioID2-CaaX roughly equivalent or greater (BioID2-Gα_{i1}/ BioID2-CaaX > 0.8). The rationale behind this criterion was that because BioID2-CaaX labels proteins at the PM based on proximity within the compartment, proteins labeled to a similar extent by BioID2-CaaX and BioID2-Gα_{i1} are likely colocalized with BioID2-Gα_{i1} at the PM. Proteins labeled to a greater extent by BioID2-Gα_{i1} than BioID2-CaaX could be PM resident proteins that selectively interact with Gα_{i1} in its inactive GDP-bound state but could also be proteins labeled by BioID2-Gα_{i1} in other compartments or cytosolic proteins that interact with Gα_{i1} at the PM.

To identify proteins that selectively interact with Gα_{i1}-QL, we further filtered the data and included only those proteins with BioID2-Gα_{i1}-QL/BioID2-Gα_{i1} normalized abundance ratio $\geq$1.3 and a P-value < 0.05 (Fig. 2.4 C). This resulted in a list of 104 candidate proteins (Fig. 2.4 C, D, Table 2-2). These 104 Gα_{i1}-QL enriched proteins were analyzed using DAVID gene ontology software to identify classes of proteins involved in different cellular processes [348]. Several enriched targets regulate various aspects of cell migration (Fig. 2.4 E top). These data suggest that active Gα_i may regulate cell migration through a protein interaction network rather than just a single target. Other classes of proteins identified with high confidence were mRNA binding

proteins, amino acid transporters, and proteins involved in clathrin-mediated endocytosis (Fig. 2.4 E bottom).

Most of these proteins have not been previously identified as targets of $G\alpha_i$. To further validate selective enrichment of potential $G\alpha_i$ binding proteins with BioID2-$G\alpha_{i1}$-QL, we tested a subset of enriched proteins based on the availability of epitope or fluorescent protein (FP)-tagged cDNA clones in a proximity labeling-coupled biotinylation Western blot assay. These proteins included PSPC1 (paraspeckle component 1), p54 (nuclear RNA-binding protein, 54-kD or NONO), ATF6 (Activating Transcription Factor 6), SORBS (Sorbin and SH3 domain-containing protein 2 or ArgBP2), GOLGA5 (Golgin A5) and Vimentin (Fig. 2.4 B, highlighted in yellow). We also included two proteins of interest that did not quite reach statistical significance, parvin, and cortactin.

Each protein-coding cDNA was individually co-transfected with BioID2-$G\alpha_{i1}$-QL, BioID2-$G\alpha_{i1}$, or control plasmid in A293 cells. Cells were treated with biotin and subjected to streptavidin pulldown. Of the 12 proteins tested, 8 showed enriched labeling by BioID2-$G\alpha_{i1}$-QL relative to BioID2-$G\alpha_{i1}$ (Fig. 2.4 E), confirming preferential interaction between the active form of $G\alpha_{i1}$ and the candidate proteins. Co-transfection of these cDNAs with BioID2 tagged $G\alpha_{i1}$ cDNAs did not increase the expression of the proteins, suggesting that increased biotin labeling was not due to an increase in expression. These data support the idea that many of the other proteins among the 104 proteins enriched in the BioID2-$G\alpha_{i1}$-QL samples were in close proximity to the active form of $G\alpha_{i1}$. Overall, the data suggest that $G\alpha_i$ regulates multiple classes of cellular processes through mechanisms that involve coordinated network interactions with a variety of protein targets.

Identification of novel interacting partners of $G\alpha_q$

2.4.6 Rational design of TurboID fused $G\alpha_q$

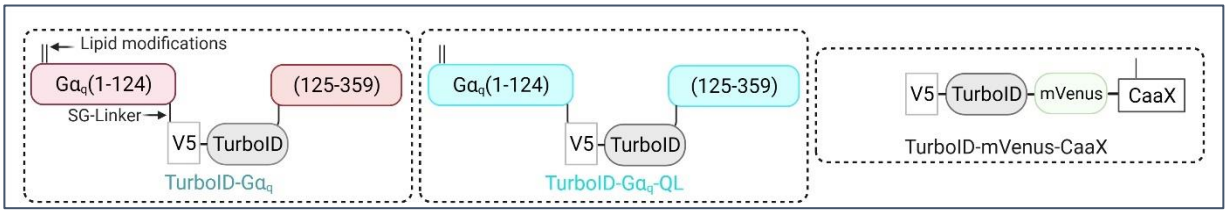

Figure 2.5: Schematic of TurboID fusion constructs.
TurboID was inserted between residues F124-E125 of the helical domain of human $G\alpha_q$, flanked by SG-linkers. Palmitoylation sites on the $G\alpha_{i1}$ subunit and the farnesylation site on CaaX moiety are labeled as lipid modifications.

With the success of BioID2-$G\alpha_i$ screen, in addition to the identification of novel $G\alpha_q$ interactors, our goal was to understand the PPIs of $G\alpha_q$ on a global level. To identify proteins that selectively interact with the active form of $G\alpha_q$ using proximity labeling, we quantitatively compared samples expressing TurboID fused to $G\alpha_q$ (TurboID-$G\alpha_q$) and TurboID fused to constitutively active $G\alpha_q$-Q209L (TurboID-$G\alpha_q$-QL). We inserted TurboID as an internal tag in α-helical domain (between F124 and E125), the same location where introduced BioID2 into $G\alpha_{i1}$ (Fig. 2.5). GDP bound $G\alpha_q$ is inactive (referred to as $G\alpha_q$), whereas a Q209L mutation in $G\alpha_q$ renders it constitutively GTP-bound and active (referred to as $G\alpha_q$-QL) [345]. As a control for general promiscuous labeling of proteins because of abundance or simply due to co-residence at the PM, a PM-targeted TurboID fused to the PM targeting CaaX motif was used. Thus, three experimental groups, TurboID-$G\alpha_q$, TurboID-$G\alpha_q$-QL, and TurboID-CaaX, were used to screen for potential targets that selectively interact with $G\alpha_q$-GTP (Fig. 2.5).

2.4.7 TurboID fused with $G\alpha_q$ biotinylates endogenous proteins

We tested the biotin labeling efficiency of TurboID fused $G\alpha_q$ proteins in A293 cells. Cells transiently transfected with the indicated cDNA clones were incubated with biotin, and lysates

were probed with fluorescently tagged streptavidin. Multiple proteins were biotinylated in TurboID-Gα_q, TurboID-Gα_q-QL, and TurboID-CaaX samples (Fig. 2.6). There were differences in the total biotinylation pattern amongst the three experimental groups, suggesting that the three fusion proteins labeled the endogenous proteins differentially.

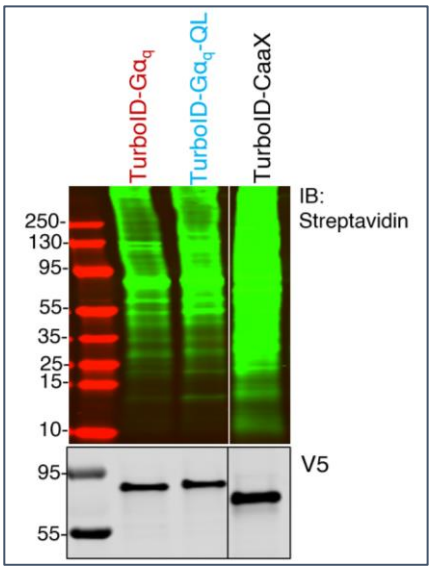

Figure 2.6: Characterization of TurboID fused Gα_q and Gα_q-QL.
Transfected TurboID fused constructs biotinylate multiple proteins in cells. A293 cells were transfected with indicated constructs for 24 hr and labeled in the presence of biotin for 1 hr. Top panel: Biotinylated proteins present in the whole-cell lysates after 1 hr of labeling were detected on a streptavidin western blot. Bottom panel: Expression of the TurboID-CaaX, TurboID-Gα_q and QL were tested with V5 antibody on western blots. Western blot represents one of three independent experiments that yielded similar results.

2.4.8 MS data analysis identifies multiple known and candidate interacting proteins

Unlike Gα_i, multiple *bona fide* interactors of active Gα_q are known, and many of them were identified by MS (Fig. 2.7). We used A293 cells due to their ease of manipulation and high transfection efficiency. We detected several proteins known to interact with Gα_q including, PLCβ isoforms 1,3 and 4, RhoGEF; Trio, Kalirin, and p63RhoGEF, which were selectively enriched in the TurboID-Gα_q-QL samples relative to TurboID-Gα_q, as expected (Fig. 2.7 A). Ric8A was also equally labeled by TurboID-Gα_q-QL and TurboID-Gα_q.

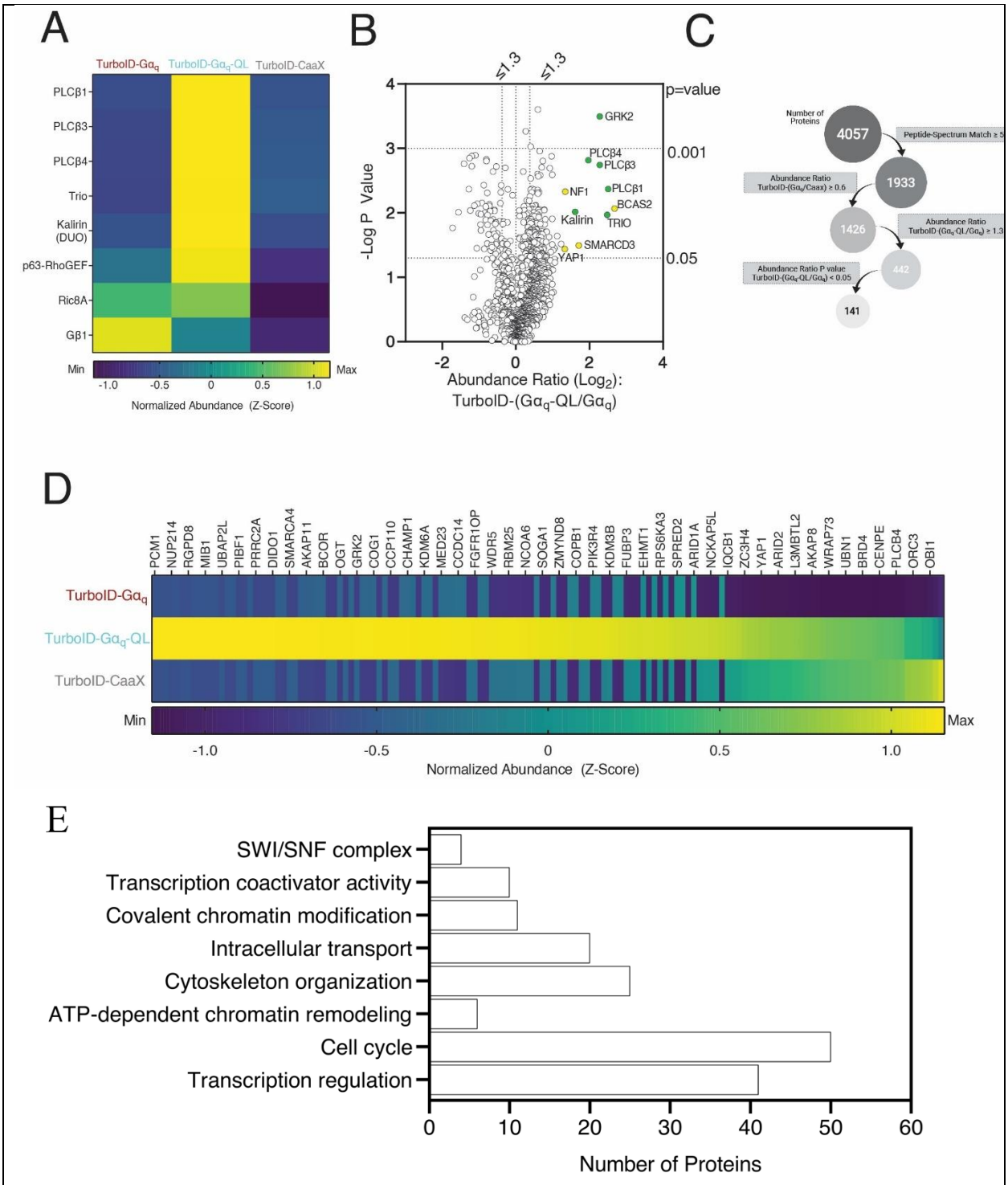

Figure 2.7: TurboID-Gα$_q$ proximity labeling proteomics results.
(A) Heat map showing the relative changes in abundance of known binding partners of Gα$_q$ that were identified in the mass spectrometry analysis. **(B)** Volcano plot of all high confidence proteins identified where the TurboID-Gα$_q$/TurboID-CaaX ratio was greater than or equal to 0.6. Known interactors are highlighted in green, and the candidate proteins investigated we are currently investigating are labeled in yellow. **(C)** Schematic showing filtering criteria for selection of proteins enriched in TurboID-Gα$_q$-QL samples relative to TurboID-Gα$_q$. **(D)** Heat Map of Proteins Identified as Enriched in TurboID-QL Samples Based on the criteria in Fig. 2.7 C **(E)** Representative classes from GO analysis of proteins from B that met the final criteria in C.

Overall, ~4000 proteins were isolated and identified (Fig. 2.7 B, C). We selected proteins with a minimum of 5 peptides assigned to each protein to ensure the robustness of the data. We also filtered the data to include only proteins for which the ratio of normalized abundance for the TurboID-Gα_q and TurboID-CaaX normalized abundance ratio ≥ 0.6.

To identify proteins that selectively interact with Gα_q-QL, we further filtered the data and included only those proteins with TurboID-Gα_q-QL/TurboID-Gα_q normalized abundance ratio $\geq$ 1.3 and a P-value < 0.05 (Fig. 2.7 C). This resulted in a list of 141 candidate proteins (Fig. 2.7 C, D). These 141 Gα_q-QL enriched proteins were analyzed using DAVID gene ontology software to identify classes of proteins involved in different cellular processes [348]. Several enriched targets were classified in the functional groups involved in the regulation of various aspects of chromatin remodeling and transcription (Fig. 2.7 E). These data suggest that active Gα_q may regulate cell migration through a protein interaction network rather than just a single target. Further validation of these proteins can open doors to explore new biology downstream of Gα_q-coupled receptors.

2.5 Discussion

In this study, we used an unbiased approach to identify novel effectors of Gα_i and Gα_q. The proximity labeling method used in this study has advantages over previously used methods [162, 329, 330], including allowing the detection of transient complex formation in the context of an intact cell. One potential drawback is that apart from detecting direct or indirect interactions, proximity-based methods can also identify the proteins that do not interact but are located within 10-20 nm, perhaps in the same cellular compartment. However, the ratiometric enrichment strategy

employed here comparing constitutively active $G\alpha_i$ to inactive $G\alpha_i$ largely circumvented this issue. GTP binding to Gα subunits leads to conformational changes that drive new PPIs.

In principle, selective enrichment in the GTP-bound state could result from a few processes: (i) GTP-selective PPI causing an increase in proximity, (ii) GTP driven changes in Gα subunit compartmentalization within the membrane or cell, or (iii) Gα-GTP driven changes in selective protein expression. There is some evidence that Gα activation leads to changes in compartmentalization within the PM but not for larger-scale changes in subcellular distribution [349]. There is overwhelming evidence that G protein α subunit activation results in conformational changes that drive new protein interactions [321]. G protein targets may not be easily identified by traditional methods due to their often-low abundance, cell context specificity, and often transient interactions. Thus, proximity labeling with proper controls is a viable approach for investigating $G\alpha_i$ subunit interactions in intact cells and may represent a general approach for the identification of signaling partners and networks downstream of G proteins.

Multiple known $G\alpha_i$ binding partners were identified in the proximity labeling MS experiments. Gβ subunits, Gγ subunits, and GPSM1 (AGS3) [56] were enriched in inactive $G\alpha_{i1}$ samples, whereas GPRIN1 [347], Rasa3 [162], and GIV [350] were enriched in $G\alpha_{i1}$-QL samples. Many AC isoforms were identified but somewhat surprisingly were equally enriched in both $G\alpha_{i1}$ and $G\alpha_{i1}$-QL samples. It has been suggested that $G\alpha_i$-AC complexes can be formed regardless of the activation state of Gi and that AC activation results from conformational rearrangement of the prebound G protein heterotrimer [351-353]. GPCRs were detected by MS, but the overall labeling efficiency was low for many of them, leading to lower confidence in identification for some of the receptors, and most were not significantly enriched with either $G\alpha_{i1}$ or $G\alpha_{i1}$-QL. This finding could be because of their low abundance or lack of preference of the inactive receptors for $G\alpha_{i1}$ or $G\alpha_{i1}$-

QL. Overall, many *bona fide* $G\alpha_i$ targets were identified in the MS screen, validating the method, suggesting that additional $G\alpha_i$ effectors are likely to be identified.

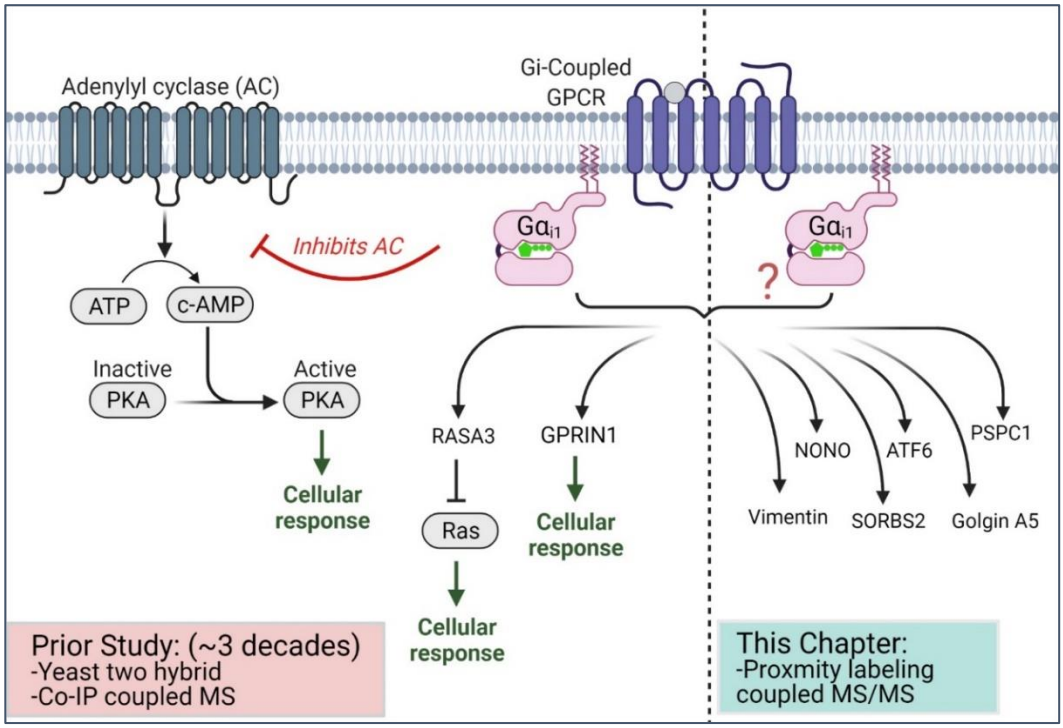

Figure 2.8: Schematic diagram summarizing major findings of this study

The identification of multiple proteins suggests that the role of $G\alpha_i$ in cell migration may involve a network of PPI similar to the role of $G\beta\gamma$ in cell migration. These potential interactions remain to be independently investigated, but many are likely "true" interaction partners. Indeed, the biotinylation validation assays with a subset of BioID2-$G\alpha_{i1}$-QL enriched proteins selected based on the availability of the cDNA clones in DNA repositories (Fig. 2.4 F), support the idea that many of these proteins selectively interact with activated $G\alpha_i$. Thus, in a complex process such as chemoattractant-dependent cell migration, $G\alpha_i$ is likely to play more than one role.

In addition, in the TurboID-$G\alpha_q$ screen, as expected, multiple binding partners were identified in the proximity labeling MS experiments. Gβ1 subunit was enriched in inactive $G\alpha_q$ samples whereas multiple PLCβ isoforms PLCβ1, PLCβ3, PLCβ4; multiple RhoGEFs: Trio,

Kalirin, and p63RhoGEF which were selectively enriched in $G\alpha_q$-QL. Overall, canonical and noncanonical interactors were identified in the MS screen, further validating the method, suggesting that additional $G\alpha_q$ effectors are likely to be identified.

Our study sets a paradigm to use in cell proximity labeling method for any signaling protein molecule, validated for two proteins $G\alpha_i$ and $G\alpha_q$, to identify novel signaling partners. In addition, validation of multiple potential effectors of $G\alpha_i$ suggests a previously unappreciated network of interactions for activated $G\alpha_i$ and perhaps all the G proteins in intact cells.

Table 2-2: List of 104 proteins identified by MS and selected using the criteria

Filter criteria descried in Fig. 2.4 C.

1	Accession	Description	# PSMs	Abundance Ratio			Abundance Ratio P-Value			Abundances (Normalized)								
2				(QL) / (CaaX)	(WT) / (CaaX)	(QL) / (WT)	(QL) / (CaaX)	(WT) / (CaaX)	(QL) / (WT)	CaaX, A	CaaX, B	CaaX, C	QL, A	QL, B	QL, C	WT, A	WT, B	WT, C
3	Q9H2P0	Activity-dependent neuroprotector homeobox protein OS=Homo sapiens OX=9606 GN=ADNP PE=1 SV=1	83	3.56	0.932	3.623	0.00179854	0.234136219	0.00152355	3045.3	3042.1	3031.6	9841.8	10829	11805	2716.6	3061.4	2826.6
4	P51610	Host cell factor 1 OS=Homo sapiens OX=9606 GN=HCFC1 PE=1 SV=2	151	2.515	0.988	2.69	0.0016698	0.585708724	0.00183723	6082.8	5993.1	6021.2	14648	15072	16519	5446	6226.1	5949.8
5	Q8WXF1	Paraspeckle component 1 OS=Homo sapiens OX=9606 GN=PSPC1 PE=1 SV=1	38	2.472	0.963	2.639	0.00266887	0.350343622	0.00378392	1427	1279.6	1160.7	3192.7	3352.8	2869.4	1017.4	1270.2	1118
6	Q15283	Ras GTPase-activating protein 2 OS=Homo sapiens OX=9606 GN=RASA2 PE=1 SV=3	41	5.823	2.465	2.363	0.00378356	0.017370597	0.00024828	724	642.6	560	3431.3	4422.3	3261.2	1443.3	1941.7	1380.4
7	Q6ZU65	Ubinuclein-2 OS=Homo sapiens OX=9606 GN=UBN2 PE=1 SV=2	19	1.813	0.881	2.015	0.02690057	0.460373234	0.00668978	894.2	734.5	809.1	1372.3	1596.1	1467.1	787.6	792.3	705.5
8	Q6NZI2	Caveolae-associated protein 1 OS=Homo sapiens OX=9606 GN=CAVIN1 PE=1 SV=1	34	2.78	1.349	2.001	0.01170158	0.081168018	0.00786233	1061.8	1203.7	800.2	2578.9	3346	2886.8	1432.8	1499.9	1442.8
9	Q7Z589	BRCA2-interacting transcriptional repressor EMSY OS=Homo sapiens OX=9606 GN=EMSY PE=1 SV=2	25	1.758	0.883	1.991	0.00460029	0.045626089	0.00882898	1261.7	1205.6	1323.8	2013.8	2120	2382	1180.4	1065	1136.3
10	P21359	Neurofibromin OS=Homo sapiens OX=9606 GN=NF1 PE=1 SV=2	140	3.691	1.925	1.952	0.00110907	0.005182364	0.00721564	3628.9	4077.1	3431.2	12715	15050	13971	6514.5	8636.1	6605.6
11	Q7Z417	Nuclear fragile X mental retardation-interacting protein 2 OS=Homo sapiens OX=9606 GN=NUFIP2 PE=	50	1.851	1.037	1.951	0.00361352	0.674169732	0.00754508	3146.2	3408.8	2796.6	6381.2	6308.1	4988.2	3261.8	3233.5	3000.5
12	Q15233	Non-POU domain-containing octamer-binding protein OS=Homo sapiens OX=9606 GN=NONO PE=1 SV=	136	1.998	1.042	1.948	0.00427139	0.909999494	0.00347846	5930.6	6125.3	5107	10909	12241	10986	4990.4	6385.6	5640
13	P08670	Vimentin OS=Homo sapiens OX=9606 GN=VIM PE=1 SV=4	404	2.599	1.285	1.911	0.00599187	0.18868592	0.0386264	9603.2	11880	16077	24960	33151	35234	13058	11872	20660
14	O15085	Rho guanine nucleotide exchange factor 11 OS=Homo sapiens OX=9606 GN=ARHGEF11 PE=1 SV=1	17	2.288	1.183	1.876	0.00119126	0.034630749	0.0005915	436.5	443.7	396.4	998.8	1086.3	879.6	513	587.8	468.8
15	Q8TBA6	Golgin subfamily A member 5 OS=Homo sapiens OX=9606 GN=GOLGA5 PE=1 SV=3	39	2.86	1.494	1.852	0.02317238	0.045449759	0.01483612	1465.4	1927.4	1290.1	4190.6	3785.6	4166.3	2189	2471.5	2249.8
16	P18850	Cyclic AMP-dependent transcription factor ATF-6 alpha OS=Homo sapiens OX=9606 GN=ATF6 PE=1 SV=	12	2.184	1.21	1.836	0.00022934	0.10451648	0.02951156	334.2	303.4	353.4	713	674.2	771.9	502.1	367.2	401.1
17	P82094	TATA element modulatory factor OS=Homo sapiens OX=9606 GN=TMF1 PE=1 SV=2	79	2.441	1.387	1.816	0.00395689	0.00295316	0.00896952	2745.2	2986.6	2713.9	6700.2	6445.1	7066	3690.5	4143.7	3880.5
18	Q92733	Proline-rich protein PRCC OS=Homo sapiens OX=9606 GN=PRCC PE=1 SV=1	6	1.712	0.962	1.806	0.00936035	0.350591677	0.00333619	457.8	406.8	294	698.3	696.4	532.2	350	391.3	294.6
19	Q9H0G5	Nuclear speckle splicing regulatory protein 1 OS=Homo sapiens OX=9606 GN=NSRP1 PE=1 SV=1	10	1.747	0.913	1.805	0.03267701	0.116671656	0.0348068	603.1	529.7	328.4	880.8	925.5	686.3	550.5	512.8	282.2
20	Q01650	Large neutral amino acids transporter small subunit 1 OS=Homo sapiens OX=9606 GN=SLC7A5 PE=1 S	19	1.742	0.967	1.799	0.10726762	0.840371214	0.00797575	934.4	1784.7	963	1627.6	2121.9	2134.1	903.2	1363.1	1186.5
21	Q9HCK8	Chromodomain-helicase-DNA-binding protein 8 OS=Homo sapiens OX=9606 GN=CHD8 PE=1 SV=5	35	1.446	0.813	1.778	0.07733457	0.085158949	0.00190821	2730.7	1882.1	1570.2	3103.7	2871.8	2271.1	1745.8	1529.5	1320
22	P48634	Protein PRRC2A OS=Homo sapiens OX=9606 GN=PRRC2A PE=1 SV=3	70	1.905	1.044	1.749	0.00781235	0.190497593	0.00410344	2875.1	2744.2	2787.6	5476.1	5259.5	4545.3	3001.2	3006.3	2808.9
23	Q9BWU0	Kanadaptin OS=Homo sapiens OX=9606 GN=SLC4A1AP PE=1 SV=1	8	1.492	0.918	1.728	0.03656752	0.536016613	0.01828253	422.5	274.9	325.4	630.4	537.5	473.1	304	311.1	298.6
24	P16070	CD44 antigen OS=Homo sapiens OX=9606 GN=CD44 PE=1 SV=3	87	1.735	1.012	1.714	0.09573101	0.702358176	0.00028811	5670.6	8830.8	5419.1	9838.1	10466	10935	5739.3	6190.2	6266.4
25	Q8N163	Cell cycle and apoptosis regulator protein 2 OS=Homo sapiens OX=9606 GN=CCAR2 PE=1 SV=2	39	1.259	0.854	1.713	0.12464505	0.180701835	0.01945232	3951.6	1939.5	2367.6	4301.2	2927.8	2980.1	2261.7	1709	2022.3
26	Q6MZP7	Protein lin-54 homolog OS=Homo sapiens OX=9606 GN=LIN54 PE=1 SV=3	19	2.088	1.592	1.708	0.03127086	0.208714314	0.04204213	911.1	698.3	389.2	1600.7	1458.2	1110	885.7	1111.6	650
27	P08195	4F2 cell-surface antigen heavy chain OS=Homo sapiens OX=9606 GN=SLC3A2 PE=1 SV=3	164	1.456	0.862	1.688	0.11012972	0.25944831	0.00275045	6598.5	11622	7911.5	9605.9	13002	13539	5687.2	8328.3	8019.1
28	P27816	Microtubule-associated protein 4 OS=Homo sapiens OX=9606 GN=MAP4 PE=1 SV=3	91	1.535	0.859	1.684	0.01806887	0.289915185	0.02921186	7394.7	5161.3	3872.2	11352	8912.2	5440.2	4962.6	5292.9	3325
29	O14867	Transcription regulator protein BACH1 OS=Homo sapiens OX=9606 GN=BACH1 PE=1 SV=2	15	1.515	0.937	1.643	0.05281121	0.27445605	0.00237849	690.4	752.1	811.5	1062.3	1139.1	969.9	646.7	725.6	568.3
30	Q9UPY5	Cystine/glutamate transporter OS=Homo sapiens OX=9606 GN=SLC7A11 PE=1 SV=1	20	1.605	0.978	1.642	0.09428359	0.596425382	0.0011248	1052.2	2276.8	1457	1689.2	2617.1	2576	1028.6	1582.5	1640.5
31	Q05682	Caldesmon OS=Homo sapiens OX=9606 GN=CALD1 PE=1 SV=3	28	1.533	0.959	1.625	0.02649652	0.309875735	0.00901621	2055.4	1689.8	1029.2	2638.3	2589.7	1603.3	1415.2	1630.9	986.6
32	Q7Z406	Myosin-14 OS=Homo sapiens OX=9606 GN=MYH14 PE=1 SV=2	39	2.521	1.253	1.619	0.04406322	0.15731837	0.03821805	160.3	116.4	158.3	404.1	383.8	269.6	200.9	237.1	190.6
33	Q9Y2D5	A-kinase anchor protein 2 OS=Homo sapiens OX=9606 GN=AKAP2 PE=1 SV=3	66	1.891	1.111	1.618	0.00394045	0.239869649	0.01012397	3064.9	2771.8	2091.4	5796.1	5730.3	3758.8	3079.2	3600.1	2322.6
34	Q15637	Splicing factor 1 OS=Homo sapiens OX=9606 GN=SF1 PE=1 SV=4	14	1.321	0.917	1.612	0.04642006	0.098404882	0.02854077	763.2	604.9	814	1008.2	955.1	1014.7	625.3	554.6	758.2
35	Q13029	PR domain zinc finger protein 2 OS=Homo sapiens OX=9606 GN=PRDM2 PE=1 SV=3	7	1.516	0.846	1.607	0.06589934	0.304870444	0.00843035	230.6	245	325.5	372.1	371.4	384.2	242.2	207.2	239.1
36	P15622	Zinc finger protein 250 OS=Homo sapiens OX=9606 GN=ZNF250 PE=1 SV=3	6	1.805	1.144	1.6	0.00165968	0.038463011	0.0008093	250	265.5	244.9	451.2	476.3	474.8	274.7	303.7	296.8
37	Q4KMQ2	Anoctamin-6 OS=Homo sapiens OX=9606 GN=ANO6 PE=1 SV=2	24	2.411	1.508	1.598	0.01007346	0.021000041	0.00495097	926	1188.1	1098.3	2232.7	2298.6	2788.3	1396.8	1529.6	1655.9
38	P35749	Myosin-11 OS=Homo sapiens OX=9606 GN=MYH11 PE=1 SV=3	89	2.293	1.33	1.573	0.02893955	0.127393772	0.01574166	207	131.6	146	474.6	441.7	288.5	260.1	280.9	194.2
39	Q9Y618	Nuclear receptor corepressor 2 OS=Homo sapiens OX=9606 GN=NCOR2 PE=1 SV=3	46	1.269	0.808	1.57	0.10583913	0.081906717	0.00154085	3911.4	2267.2	2189.3	4136	2964.6	2778.9	2506.1	1905	1769.7
40	Q9NR09	Baculoviral IAP repeat-containing protein 6 OS=Homo sapiens OX=9606 GN=BIRC6 PE=1 SV=2	56	1.323	0.953	1.567	0.0751939	0.726781399	0.02000988	1995	2227.2	1794.3	3519.9	2947.7	2263.6	2242.8	1881.1	1710.1
41	Q9ULV4	Coronin-1C OS=Homo sapiens OX=9606 GN=CORO1C PE=1 SV=1	53	2.106	1.301	1.543	0.02672821	0.052580232	0.01938354	2254.3	2313.2	3883.6	4747.2	5168.2	6063.6	2932.3	3349.3	4526.9
42	O15265	Ataxin-7 OS=Homo sapiens OX=9606 GN=ATXN7 PE=1 SV=1	9	1.177	0.909	1.537	0.10945065	0.166056568	0.03057785	137.6	144.5	143.2	161.9	170.1	222.3	105.4	131.4	135.6
43	Q15836	Vesicle-associated membrane protein 3 OS=Homo sapiens OX=9606 GN=VAMP3 PE=1 SV=3	6	2.37	1.368	1.535	0.0426335	0.219647649	0.01355127	133.3	190.8	103.5	315.9	289.8	255.3	182.4	188.8	176.4
44	Q96JQ2	Calmin OS=Homo sapiens OX=9606 GN=CLMN PE=1 SV=1	12	1.273	0.833	1.529	0.04565978	0.014383508	0.00530922	571.5	532.8	442.2	727.7	612.5	607.3	475.9	429.3	384.2
45	Q4KMP7	TBC1 domain family member 10B OS=Homo sapiens OX=9606 GN=TBC1D10B PE=1 SV=3	19	1.762	1.2	1.527	0.00090983	0.047112063	0.01698891	648.2	728.5	592.4	1132.5	1346.3	1043.7	741.5	874.3	790.3
46	Q86SJ2	Amphoterin-induced protein 2 OS=Homo sapiens OX=9606 GN=AMIGO2 PE=1 SV=1	52	2.986	2.043	1.526	0.01474245	0.016828067	0.01457049	1503.5	2486.4	1148.1	4489.2	7110.6	5253.8	2942.3	5079	3135.7
47	Q96Q45	Transmembrane protein 237 OS=Homo sapiens OX=9606 GN=TMEM237 PE=1 SV=2	27	1.911	1.261	1.515	0.03713009	0.061726496	0.02703283	929.7	1275.6	838.8	1776.3	1912.6	1936	1172.2	1421.4	1128.8
48	Q9HD26	Golgi-associated PDZ and coiled-coil motif-containing protein OS=Homo sapiens OX=9606 GN=GOPC	15	1.855	1.338	1.512	0.01982392	0.146017491	0.00718463	696.4	580.9	590.7	1083.9	1214.4	1096	716.7	784.4	790.2
49	Q14677	Clathrin interactor 1 OS=Homo sapiens OX=9606 GN=CLINT1 PE=1 SV=1	38	1.648	1.114	1.506	0.05324794	0.501863257	0.00056293	2056.5	2024.8	1205.2	2764	3337.8	2463.7	1835.5	2256.3	1610.4
50	P14209	CD99 antigen OS=Homo sapiens OX=9606 GN=CD99 PE=1 SV=1	10	1.851	1.262	1.484	0.03801579	0.273199188	0.00362905	308.6	500.2	326.5	571	706.9	674.9	389.3	476.2	424.6
51	Q63HQ0	AP-1 complex-associated regulatory protein OS=Homo sapiens OX=9606 GN=AP1AR PE=1 SV=1	7	2.11	1.448	1.478	0.0008838	0.002843246	0.01122497	282.1	349.9	298	595.2	697.2	637.5	394.2	523.5	431.4
52	P46060	Ran GTPase-activating protein 1 OS=Homo sapiens OX=9606 GN=RANGAP1 PE=1 SV=1	85	1.378	0.886	1.476	0.34903264	0.257889175	0.00675183	4680.1	4193.5	9354.9	6447.8	6010.5	8294.2	4148	4071.3	5960.1
53	O15126	Secretory carrier-associated membrane protein 1 OS=Homo sapiens OX=9606 GN=SCAMP1 PE=1 SV=2	30	2.04	1.367	1.473	0.02337259	0.035201393	0.024156	1359.2	1791.9	1092.6	2772.6	2994.3	2672.2	1858.3	2372.8	1814.2
54	O14776	Transcription elongation regulator 1 OS=Homo sapiens OX=9606 GN=TCERG1 PE=1 SV=2	13	1.218	0.867	1.472	0.25936427	0.25980328	0.03797551	620.9	471	377.3	598.9	601	459.4	376	408.2	368.1
55	Q15418	Ribosomal protein S6 kinase alpha-1 OS=Homo sapiens OX=9606 GN=RPS6KA1 PE=1 SV=2	44	3.69	2.512	1.469	0.00502923	0.019584258	0.00963003	1510.6	1298.1	1301.7	4491	5220.5	4803.4	2897.2	3830.3	3269.9
56	P29317	Ephrin type-A receptor 2 OS=Homo sapiens OX=9606 GN=EPHA2 PE=1 SV=2	243	1.606	1.096	1.465	0.07645119	0.341351509	0.00926734	10456	15636	10853	16794	21332	25422	11464	15257	15956
57	O75054	Immunoglobulin superfamily member 3 OS=Homo sapiens OX=9606 GN=IGSF3 PE=2 SV=3	25	1.685	1.152	1.463	0.03980292	0.103403829	0.02139125	754.1	950.6	804.8	1270.9	1354.9	1680.9	868.7	1061.7	1115
58	Q6NYC8	Phostensin OS=Homo sapiens OX=9606 GN=PPP1R18 PE=1 SV=1	18	1.3	0.917	1.457	0.05915519	0.451880004	0.00673286	1063.9	840.3	868.8	1292.8	1321.4	1129.3	818.6	907.3	796.8
59	Q07157	Tight junction protein ZO-1 OS=Homo sapiens OX=9606 GN=TJP1 PE=1 SV=3	108	1.776	1.178	1.456	0.03079967	0.174789663	0.01365175	5629.1	6657.6	4510.5	9996.8	10796	10716	6203.8	7844.5	7357
60	Q96B97	SH3 domain-containing kinase-binding protein 1 OS=Homo sapiens OX=9606 GN=SH3KBP1 PE=1 SV=2	9	1.408	0.894	1.453	0.16719307	0.446198051	0.03022997	619	466.3	669.8	871.6	735.3	686.7	553.1	505.9	541.3
61	Q14644	Ras GTPase-activating protein 3 OS=Homo sapiens OX=9606 GN=RASA3 PE=1 SV=3	62	3.466	2.71	1.449	0.03038417	0.033909671	0.04070622	1425.5	1642.3	1091.8	4229.3	5692.5	7370.2	2919.2	4451.3	4388.3
62	P98082	Disabled homolog 2 OS=Homo sapiens OX=9606 GN=DAB2 PE=1 SV=3	8	1.525	1.053	1.448	0.00232873	0.061091734	0.00964753	274.3	338.7	260.8	396.8	522.5	397.7	299.1	351	274.6
63	O14523	Phospholipid transfer protein C2CD2L OS=Homo sapiens OX=9606 GN=C2CD2L PE=1 SV=3	25	1.847	1.29	1.446	0.01802567	0.02528196	0.01733896	997.8	1195.5	923.7	1842.8	2007.7	2093.6	1274.5	1542.2	1370.2
64	Q8NDV7	Trinucleotide repeat-containing gene 6A protein OS=Homo sapiens OX=9606 GN=TNRC6A PE=1 SV=2	19	1.646	1.142	1.441	0.03018978	0.699520803	0.00968527	1037.8	831.5	772.7	1379.5	1420.1	1271.9	868.8	1016	882.5
65	Q8NG31	Kinetochore scaffold 1 OS=Homo sapiens OX=9606 GN=KNL1 PE=1 SV=3	15	1.33	0.926	1.437	0.02915833	0.35563847	0.0012266	735.4	585.1	657.3	978.3	886.8	829.8	680.9	604.3	590.9
66	Q9NV06	DDB1- and CUL4-associated factor 13 OS=Homo sapiens OX=9606 GN=DCAF13 PE=1 SV=2	9	1.235	0.893	1.436	0.02133169	0.161581102	0.01652127	205.7	225.4	200.9	254	289.4	232.6	200.3	201.2	162
67	Q8N9T8	Protein KRI1 homolog OS=Homo sapiens OX=9606 GN=KRI1 PE=1 SV=3	18	1.165	0.813	1.433	0.13258319	0.311737457	0.04087912	808.7	893.3	824.6	1103.5	1040.8	880.9	860.2	726.3	524
68	Q8WWI1	LIM domain only protein 7 OS=Homo sapiens OX=9606 GN=LMO7 PE=1 SV=3	100	1.243	0.879	1.429	0.04245629	0.174798005	0.01441079	5566.9	5190.4	4259.9	6193.5	6539.2	5295	4334.5	4561.5	4156.2
69	Q9H2G9	Golgin-45 OS=Homo sapiens OX=9606 GN=BLZF1 PE=1 SV=2	17	3.695	2.364	1.429	0.00061516	0.001294164	0.00807508	445.4	574.5	395.8	1650.8	1933.3	1462.5	1041.1	1358	1023.4
70	Q9BY89	Uncharacterized protein KIAA1671 OS=Homo sapiens OX=9606 GN=KIAA1671 PE=1 SV=2	77	1.978	1.403	1.424	0.00871404	0.021273678	0.0304025	2979.5	2853.9	2435.6	5434.7	5643.6	5568.7	3816.7	4342.6	3418.1
71	P43121	Cell surface glycoprotein MUC18 OS=Homo sapiens OX=9606 GN=MCAM PE=1 SV=2	57	1.183	0.831	1.424	0.71697335	0.18181568	0.003867	3696.4	5527.1	3061.6	4371.9	4286	4108.3	3071	3070.7	2727.8
72	P23229	Integrin alpha-6 OS=Homo sapiens OX=9606 GN=ITGA6 PE=1 SV=5	88	1.641	1.072	1.423	0.11482307	0.597135689	0.01655029	5136.2	6347.2	4397.7	8429.2	7211.6	8619.2	5505.6	5513.2	6058.7
73	Q96A33	Coiled-coil domain-containing protein 47 OS=Homo sapiens OX=9606 GN=CCDC47 PE=1 SV=1	15	1.542	1.091	1.419	0.02634863	0.653997471	0.00759228	741.5	704	866.1	1148.5	1085.3	1111.8	809.2	825.9	770.2
74	Q658P3	Metalloreductase STEAP3 OS=Homo sapiens OX=9606 GN=STEAP3 PE=1 SV=2	31	1.681	1.175	1.416	0.07991711	0.265922359	0.01159778	1668.8	2175.1	1250.7	2806.1	2771.9	2722	1960.7	2159.2	1921.8
75	O00571	ATP-dependent RNA helicase DDX3X OS=Homo sapiens OX=9606 GN=DDX3X PE=1 SV=3	122	1.479	1.074	1.415	0.04426611	0.154345279	0.02724345	5499.8	4466.8	5218.9	8131.5	8449.9	7147.4	5746.1	5414.9	5602.8
76	Q9Y4J8	Dystrobrevin alpha OS=Homo sapiens OX=9606 GN=DTNA PE=1 SV=2	11	1.88	1.527	1.415	0.0250001	0.069094775	0.0262533	202.8	239.7	226.3	381.2	429	587	309.6	295.6	414.9
77	Q13425	Beta-2-syntrophin OS=Homo sapiens OX=9606 GN=SNTB2 PE=1 SV=1	47	2.305	1.632	1.413	0.0106603	0.0103643	0.01117839	1284.1	1464.8	1463.6	2959.7	3199.9	4334	2095.1	2337.1	2779
78	P41440	Folate transporter 1 OS=Homo sapiens OX=9606 GN=SLC19A1 PE=1 SV=3	7	1.796	1.465	1.412	0.04685651	0.280151559	0.0349266	381.5	599.6	573.3	685.3	832.1	1223.5	558.7	550.4	866.7
79	O94875	Sorbin and SH3 domain-containing protein 2 OS=Homo sapiens OX=9606 GN=SORBS2 PE=1 SV=3	10	2.561	1.817	1.41	0.00230368	0.011760921	0.00363458	328.5	359.5	260.5	932.8	920.8	632.5	666.6	653.1	421.9
80	P19634	Sodium/hydrogen exchanger 1 OS=Homo sapiens OX=9606 GN=SLC9A1 PE=1 SV=2	22	1.886	1.354	1.393	0.03384165	0.048728554	0.02634668	1109.3	1712.3	1139.6	2091.9	2731.2	2801.3	1501.8	2230.7	1943.8
81	Q8IWB9	Testis-expressed protein 2 OS=Homo sapiens OX=9606 GN=TEX2 PE=1 SV=2	14	1.525	1.132	1.391	0.03525614	0.199701764	0.007074	854.3	727.4	578.9	1204.1	1109.5	1104.8	865.8	823.1	743.1
82	O15047	Histone-lysine N-methyltransferase SETD1A OS=Homo sapiens OX=9606 GN=SETD1A PE=1 SV=3	9	1.157	0.84	1.391	0.0384368	0.014789688	0.01340149	365.4	374.3	350.9	422.6	405.4	415	288	314.6	298.4
83	O95425	Supervillin OS=Homo sapiens OX=9606 GN=SVIL PE=1 SV=2	42	1.519	1.136	1.375	0.00071249	0.037252658	0.00393693	1591.6	1527.1	1492.5	2392.8	2319.8	2330.6	1707.7	1767.6	1694.9
84	O75962	Triple functional domain protein OS=Homo sapiens OX=9606 GN=TRIO PE=1 SV=2	124	1.561	1.165	1.373	0.03180698	0.541876205	0.02828469	6969.3	5311.4	4188.1	9725.4	9943.7	6537.8	5937.3	7241	4878
85	Q08378	Golgin subfamily A member 3 OS=Homo sapiens OX=9606 GN=GOLGA3 PE=1 SV=2	44	1.14	0.833	1.373	0.07393176	0.135900394	0.01345178	2273.9	2180.6	1617.4	2517.5	2486.5	2086.5	1619.8	1816.6	1519.8
86	Q86YS7	C2 domain-containing protein 5 OS=Homo sapiens OX=9606 GN=C2CD5 PE=1 SV=1	21	1.626	1.283	1.365	0.0149011	0.061944897	0.01737918	1002	1122.1	877	1628.9	1788.6	1724.8	1150.7	1440.1	1264
87	Q15643	Thyroid receptor-interacting protein 11 OS=Homo sapiens OX=9606 GN=TRIP11 PE=1 SV=3	68	1.356	1.023	1.364	0.02835534	0.571466593	0.00420726	3512	3340.1	2691.3	4763.2	4363.5	4266.3	3593	3199.7	2999.1
88	O15020	Spectrin beta chain, non-erythrocytic 2 OS=Homo sapiens OX=9606 GN=SPTBN2 PE=1 SV=3	121	1.338	1.007	1.363	0.07868995	0.489659816	0.00788977	4354.5	5236.3	3229	5827.8	5904	4794.3	4386.6	4331.6	3274.9
89	Q96PY5	Formin-like protein 2 OS=Homo sapiens OX=9606 GN=FMNL2 PE=1 SV=3	47	2.536	2.089	1.353	0.00422011	0.008136429	0.04742782	695	816.7	605.4	1762.5	1983.1	1809.6	1240.5	1706.5	1337.3
90	P21675	Transcription initiation factor TFIID subunit 1 OS=Homo sapiens OX=9606 GN=TAF1 PE=1 SV=2	7	1.34	1	1.351	0.00566806	0.662813585	0.04259435	310.4	297.4	342.7	415.8	401.9	433.4	336.1	297.4	277.2
91	Q9C004	Protein sprouty homolog 4 OS=Homo sapiens OX=9606 GN=SPRY4 PE=1 SV=2	10	1.424	1.047	1.35	0.09329507	0.881685143	0.01597037	572.5	755.1	607.7	814.9	841.5	940	632.7	623.5	636.4
92	P53365	Arfaptin-2 OS=Homo sapiens OX=9606 GN=ARFIP2 PE=1 SV=1	9	1.632	1.214	1.344	0.0009238	0.009228877	0.0145707	212	233.7	190.7	346.1	388.1	301.2	257.5	278.2	242.6
93	Q9Y5X1	Sorting nexin-9 OS=Homo sapiens OX=9606 GN=SNX9 PE=1 SV=1	9	1.118	0.845	1.34	0.18526076	0.064890439	0.00736341	280	303.3	286.3	280.2	347.9	319.9	209.2	256.2	254.5
94	Q8NDT2	Putative RNA-binding protein 15B OS=Homo sapiens OX=9606 GN=RBM15B PE=1 SV=3	7	0.991	0.82	1.337	0.89739484	0.141603427	0.0239983	167.1	133.5	220.2	165.5	162.4	172.9	137	116.3	129.4
95	Q12959	Disks large homolog 1 OS=Homo sapiens OX=9606 GN=DLG1 PE=1 SV=2	21	1.558	1.167	1.335	0.01736865	0.072055431	0.00186216	688.7	895.7	740.6	1072.8	1292.6	1320.4	803.4	1001	984
96	Q99666	RANBP2-like and GRIP domain-containing protein 5/6 OS=Homo sapiens OX=9606 GN=RGPD5 PE=1 SV	98	1.377	1.034	1.332	0.00305984	0.667968258	0.04940975	386.3	377.6	442.4	538.9	519.9	583.1	412.8	390.3	344.9
97	Q9Y426	C2 domain-containing protein 2 OS=Homo sapiens OX=9606 GN=C2CD2 PE=1 SV=2	22	1.855	1.388	1.331	0.00265341	0.009047368	0.02841712	1069.1	1245.3	1167.7	1992.9	2114	2166.6	1497.3	1728	1492.5
98	Q6PJF5	Inactive rhomboid protein 2 OS=Homo sapiens OX=9606 GN=RHBDF2 PE=1 SV=2	14	1.341	1.014	1.328	0.07259512	0.639641502	0.00552534	797.8	939.6	667.2	1011.7	1260.3	1189.6	713.3	953	896.1
99	O43688	Phospholipid phosphatase 2 OS=Homo sapiens OX=9606 GN=PLPP2 PE=1 SV=1	9	1.434	1.126	1.325	0.08924047	0.328820331	0.00636362	307.9	364.2	411.5	441.4	492.4	911.5	346.5	357.5	688.1
100	Q96QD8	Sodium-coupled neutral amino acid transporter 2 OS=Homo sapiens OX=9606 GN=SLC38A2 PE=1 SV=2	19	1.387	1.127	1.322	0.14227829	0.991131535	0.01046886	953.2	1432.4	1232.4	1321.7	1496.9	1847.2	1074.5	1115.9	1396.9
101	Q13439	Golgin subfamily A member 4 OS=Homo sapiens OX=9606 GN=GOLGA4 PE=1 SV=1	52	1.469	1.115	1.317	0.01063396	0.09002361	0.0012384	2644.3	2459.8	2132.5	3563.5	3612.8	3277.5	2736.2	2743.5	2433.9
102	P46939	Utrophin OS=Homo sapiens OX=9606 GN=UTRN PE=1 SV=2	226	2.607	2.09	1.316	0.00220301	0.006800214	0.03416395	7065.7	7287.3	6671.2	17028	18995	18792	12937	16338	13946
103	Q8IVF7	Formin-like protein 3 OS=Homo sapiens OX=9606 GN=FMNL3 PE=1 SV=3	46	2.053	1.731	1.315	0.00659563	0.037872709	0.03595352	1318.9	1440.4	1377.2	2461	2956.7	3152.8	1737	2492.7	2397.8
104	P55011	Solute carrier family 12 member 2 OS=Homo sapiens OX=9606 GN=SLC12A2 PE=1 SV=1	44	1.504	1.112	1.314	0.08458435	0.440264745	0.00345388	2183.9	3285	2378	3285.2	3856.1	4175	2429.4	3015.3	3177.2
105	O15554	Intermediate conductance calcium-activated potassium channel protein 4 OS=Homo sapiens OX=9606	6	1.058	0.867	1.311	0.47035738	0.231683084	0.02713722	360.2	482.2	449.4	381	447.7	638.4	312.2	341.4	445.3

Chapter-3

Identification and Characterization of PDZ-RhoGEF and RasGAPs as Novel Targets of $G\alpha_i$ Signaling

Part of this chapter is published in bioRxiv (Chandan NR., 2021) [318].

3.1 Abstract

G protein-coupled receptors (GPCRs) that couple to the Gi family of G proteins are key regulators of cell and tissue physiology. One of the processes that the $G\alpha_{i/o}$ coupled chemoattractant GPCRs regulate is cell migration and cell adhesion. Our recent work discovered novel, cAMP signaling independent, roles for $G\alpha_i$ in neutrophils and fibrosarcoma cell migration downstream of chemoattractant receptors. However, the molecular target(s) of $G\alpha_i$ in these processes remain to be identified. While $G\alpha_i$ canonically signals via direct inhibition of adenylate cyclase (AC), studies from our lab and reports from others suggest that $G\alpha_i$ may regulate cell functions through non-canonical mechanisms. We adopted an intact cell proximity-based labeling approach using BioID2 coupled to tandem mass tag (TMT)-based quantitative proteomics to identify proteins that selectively interact with the GTP-bound form of $G\alpha_{i1}$ as described in chapter 2. Extensive characterization of one candidate protein, PDZ-RhoGEF (PRG), revealed that active-$G\alpha_{i1}$ strongly activates PRG. Strikingly, large differences in the ability of $G\alpha_{i1,}$ $G\alpha_{i2,}$ and $G\alpha_{i3}$ isoforms to activate PRG were observed despite over 85% sequence identity. We also demonstrated the functional relevance of the interaction between active $G\alpha_i$ and PRG *ex vivo* in primary human neutrophils. This is the first study that shows the RhoA regulation downstream of the Gi-coupled receptor. In addition, preliminary experiments validated the $G\alpha_i$ regulation of Ras

via a group of Ras-GTPase activating proteins (GAPs) subtypes. Overall, identification of the relatively ubiquitously expressed PRG and a group of RASA proteins as new $G\alpha_i$-GTP targets will have broad implications for regulation of downstream signaling by Gi-coupled GPCRs in multiple biological systems and in the development of novel therapeutic approaches.

3.2 Introduction

GPCRs are seven-transmembrane receptors that bind to guanine nucleotide-binding proteins (G proteins), Gα and Gβγ. In the inactive form, Gα is bound to GDP and Gβγ. Receptor activation triggers the exchange of GDP for GTP on Gα, leading to its dissociation from the receptor and the Gβγ complex. [324]. Cell migration and adhesion are fundamental biological processes regulated by chemokine G-protein-coupled receptors (GPCRs) [324]. Chemokine receptors couple to the PTX-sensitive $G_{i/o}$ family of Gα ($G\alpha_i$) proteins [324]. Dysregulation of chemokine signaling leads to diseases ranging from allergy, inflammation, autoimmunity and cardiovascular disorders [257, 258] and cancer cell invasion and metastasis [257, 325, 354]. Thus, studying chemokine receptor signaling is fundamental to understanding the basis of various diseases and is important for therapeutic targeting.

The role of Gβγ in chemokine signaling has been well characterized and is thought to be a major transducer of these processes [101], whereas only a few targets of $G\alpha_i$ are definitively identified [151-153]. Recent work from our lab revealed a novel role for $G\alpha_i$ signaling in neutrophil adhesion and migration; however, the direct effectors of active $G\alpha_i$-GTP involved in these processes aren't identified yet [161]. Therefore, to find novel targets that have the potential to interact with activated $G\alpha_{i1}$, we screened for targets selectively enriched by activated $G\alpha_{i1}$ ($G\alpha_{i1}$-

Q204L-BioID2) relative to inactive $G\alpha_{i1}$ ($G\alpha_i$-BioID2) in HT1080 cells using proximity-based labeling approach.

One such protein was the RH family RhoGEF, PDZ-RhoGEF (PRG), also known as ARHGEF11. The role of PRG in regulating cell migration downstream of Gi-coupled chemoattractant receptors is well characterized, but it is thought to be mediated primarily by coupling to $G\alpha_{12/13}$ subunits [207, 266]. We demonstrated that PRG was an effector of active $G\alpha_{i1}$ and $G\alpha_{i3}$ but was poorly activated by $G\alpha_{i2}$, a highly homologous (~85% identical) $G\alpha_i$ family member. In addition, we demonstrated that PRG was activated downstream of Gi-coupled receptors and showed the involvement of Gi in the regulation of PRG in human neutrophils. PRG is relatively ubiquitously expressed [187]; thus, its identification as a new Gαi-GTP target has implications for the regulation of Rho in various tissues and cell types by Gi-coupled GPCRs.

In addition to Rho, it is involved in multiple processes, including cell cytoskeleton reorganization and thus cell adhesion and migration. A previous study has reported RASA1 regulation downstream of chemotactic peptide, N-formylmethionine-leucyl-phenylalanine (fMLF) receptor, FPR [355]. Activation of FPR has been shown to activate Ras via inhibition of RASA1 in human neutrophils. Gi-coupled dopamine D2S (short isoform) receptor-mediated activation of RASA3 has been shown to inhibit Gq-coupled, thyrotropin-releasing hormone (TRH) receptor-stimulated Ras/ ERK1/2 activation in rat pituitary cells [162]. These data indicate that active $G\alpha_{i1}$ may regulate multiple RasGAP proteins; however, whether RASA is activated or inhibited may depend on the RASA member. Our MS data identified $G\alpha_{i1}$-GTP-dependent enrichment of multiple RasGAP family members in HT1080 cells, leading us to hypothesize that $G\alpha_i$ may regulate a network of RasGAP proteins and that there are more prominent roles for $G\alpha_i$ regulation of Ras signaling downstream of multiple Gi-coupled receptors. Our preliminary co-

immunoprecipitation studies show that all four RasGAPs (RASA1, RASA2, RASA3 and NF1) preferentially interact with active compared to inactive $G\alpha_{i1}$. Detailed characterization of subtype-specific regulation is required.

Identification and characterization of new targets regulated by $G\alpha_i$ both individually and in networks provide insights that will aid in the investigation of the functional roles of Gi-coupled GPCRs in multiple biological processes.

3.3 Material and methods

3.3.1 Plasmid cDNA constructs

C-terminally c-myc tagged full-length PRG cDNA in a mammalian expression vector was a gift from Dr. John Tesmer, Purdue University. A293-FPR1 stable cell lines were generated by Dr. Jesi To, University of Michigan, and A293-$G\alpha_{12/13}$ CRISPR cells were a gift from Dr. Graeme Milligan, University of Glasgow, UK. All Gα clones in pcDNA3.1+ were obtained from the cDNA Resource Center. $G\alpha_{i1}$-FLAG-APEX2, $G\alpha_{i1}$-QL-FLAG-APEX2, Lyn-FLAG-APEX2, and EGFP-BioID2-HA-CaaX were synthesized by GenScript. The sequences of the clones are available upon request. The following plasmids were obtained from Addgene and were a gift from Dominic Esposito R777-E227 Hs.RASA1 (Plasmid # 70511), R777-E229 Hs.RASA2 (Plasmid # 70513), R777-E231 Hs.RASA3 (Plasmid # 70515), R777-E139 Hs.NF1 (Plasmid # 70423) and were cloned into pEZYflag destination vector (Yu-Zhu Zhang, Plasmid # 18700) [356].

3.3.2 Design and cloning of cDNA constructs

GFP-PRG was generated from PRG amplification from FL-c-myc-PRG and insertion into the pEGFP-N1 vector.

3.3.3 Cell culture

A293 and HT1080 cells were obtained from American Type Culture Collection (ATCC). A293, A293-FPR1, and HT1080 cells were grown in DMEM (10013CV, Corning) supplemented with 10% fetal bovine serum (FBS) (10437028, Gibco) and 100 units of penicillin/streptomycin (P/S) (15140122, Gibco) at 37 °C with 5% CO_2. Media was supplemented with 100 µg/mL Geneticin (G418) (G8168, Sigma) to select A293-FPR1 cells. Trypsin-EDTA (25200056, Gibco) was used for cell passaging.

3.3.4 Reagents

The following primary and secondary antibodies were utilized: $G\alpha_{i1/2}$ (anti-sera) [340], PDZ-RhoGEF (ab110059, abcam), HA (3724, Cell Signaling), FLAG (F1804, Sigma), P-MLC (3671, Cell Signaling), c-myc (13-2500, Invitrogen), GFP (A11122, Invitrogen). Primary antibodies were made in 3% BSA and 0.1% Sodium azide and the blots were incubated in primary antibody overnight at 4 °C except 1 hr incubation at RT for streptavidin-IRDye800. Secondary antibody goat anti-rabbit DyLight™ 800 (SA535571, Invitrogen), goat anti-mouse IRDye 800CW (926-32210, LICOR) at 1:10,000 dilution and goat anti-rabbit Alexa Fluor 488 (A11034, Invitrogen) at 1:1000 dilution.

3.3.5 Proximity ligation assay (PLA)

In situ PLAs were performed using Duolink™ Kit (DUO92101, Sigma) as per manufacturer's protocol with some modifications. 2×10^4 cells were plated on 14 mm coverslips in a 35 mm dish (D11030H, Matsunami) and the following day, 100 ng of $G\alpha_{i1}$-FLAG-APEX2, $G\alpha_{i1}$-QL-FLAG-APEX2 or Lyn-FLAG-APEX2 with 25 ng EGFP-PRG were transfected and the

cDNAs were allowed to express for 48 hr with media change after 24 hr. The cells were then washed twice with 1× PBS and fixed with 4% PFA and 4% sucrose made in 1× PBS for 10 min in the dark at RT. The cells were permeabilized and blocked using freshly prepared 5% goat serum, 1% BSA, 0.2% Triton X100 in TBS. Subsequently, rabbit anti-GFP (1:750) (A11122, Invitrogen) and mouse anti-FLAG- (1:750) (F1804, Sigma) antibodies were diluted in Duolink® antibody diluent and incubated overnight at 4 °C in a humidified chamber. A total 40 µL reaction mixture including PLA probe binding, ligation, amplification steps in a humidified chamber. The dilution factors for all the reagents were kept used as per manufacturer's instructions. 2 mL of either buffer-A or B were used per wash as directed in the manual. After final washes, all the aqueous media was removed, 80 µL of mounting media was added to the cells. Random fields were imaged on the LEICA DMi8 microscope in confocal mode with a 63× oil lens, using 405 nm excitation for DAPI, 488 nm for GFP-PRG and 568 nm for PLA dots. Acquisition parameters were kept constant for all the conditions of an experiment. The intensity of PLA dots and GFP-PRG was measured for ≥ 100 cells per condition, using ImageJ, and are represented on the X and Y-axis, respectively.

3.3.6 Luciferase reporter assay

A293 cells were plated, 4×10^4 cells per well, in a 96-well plate (655983, Greiner). The following amounts of DNA were used per well: 25 ng of SRE luciferase reporter (E134A, Promega), 2.5 ng of c-myc-PRG and 125 ng of each Gα or Gα-QL subunit. For the assay to determine the concentration dependence for activation, 0.75, 2.5, 7.5, 25, 75, 125 ng $G\alpha_{i1}$ or $G\alpha_{i1}$-QL. pcDNA3.1 were used. Empty vector was used to keep the total amount of DNA constant in each well. Transfection was performed using 1:3 DNA: Lipofectamine 2000 (Invitrogen) ratio. Reverse transfection was performed, meaning cells were plated and transfected at the same time.

12 hr after transfection, media was replaced with 75 µL of serum-free media for another 12 hr, and 75 µL (1:1 volume) of One-Glo^{TM} reagent (E6110, Promega) was added to each well, incubated for 10 min at RT. The luminescence signal was measured using Varioskan^{TM}LUX multimode microplate reader (Thermo Scientific^{TM}). A293-FPR1 cells were transfected and treated with 100 ng/mL PTX (P7208, Sigma) for 12 hr and subsequently, fMLF (0.01, 0.1, 1, 10 µM) was added in serum-free media with or without PTX, for the next 12 hr.

3.3.7 Rhotekin pulldown assay

Active RhoA levels were measured using the RhoA pulldown activation assay biochem kit (BK036-S, Cytoskeleton Inc.) using GST Rhotekin beads. The levels of the GTP-RhoA associated with GST-Rhotekin-RBD were quantified by western blot analysis. Briefly, A293 cells were plated in a 6-well plate at a density of 3.5 x 10^5 cells per well and transfected with 1 µg $G\alpha_{i1}$, 100 ng c-myc-PRG and, 250 ng RhoA-HA per well using 1:3 DNA: Lipofectamine 2000 ratio. 20 hr after transfection, cells were cultured in serum-free media for 4 hr. Cells in each well were then lysed with 300 µL of RhoA lysis buffer with 1×PI (included with the kit), and lysates were equalized for total protein amount. Samples from two wells were pooled for each experimental group (total 600 µL, ~600 µg protein per experimental group). The lysates were incubated with 50 µg of GST-Rhotekin bound beads in an end-over-end rotator for 1 hr at 4 °C. Beads were washed twice with wash buffer (included with the kit), eluted in 40 µL 1× Laemmli sample buffer, and analyzed by western blot using an anti-HA (1:2000), anti-c-myc antibody (1:2000) and anti-$G\alpha_{i1/2}$ antisera (1:3000). Band intensities were quantified using Image Studio Lite (version 5.2).

3.3.8 FPR1-A293 cell protrusions assay

FPR-1-A293 cells (2×10^4 /well) were plated in an 8-well chamber slide coated with poly-D-lysine. The following plasmids were transfected per well: 100 ng YFP, 4 ng PRG, 125 ng $G\alpha_{i1}$ or empty vector have equal amount of cDNAs per well in all wells. Plasmids were transfected using 1:3 DNA: Lipofectamine 2000 ratio. 24 hr after transfection, the media was changed to fresh media, with or without PTX (100ng/mL) (P7208, Sigma) for 24 hr more. Subsequently, the cells were washed once with 1× PBS and placed in HBSS + HEPES (10mM) pH 7.3. The cells were imaged every 20 seconds for 40 min, and formyl-methionyl-leucyl-phenylalanine fMLF (F3506, Sigma) or vehicle was added 5 min after the video initiation. The videos were taken at 10× magnification on the LEICA DMi8 microscope using a 488 nm excitation filter. To quantify the % cells with protrusions, the total number of cells in the first frame of a video were counted in ImageJ by 'analyze particles' option, and cells with the protrusions were manually counted from the videos in a blinded manner.

3.3.9 Human neutrophil isolation

Human peripheral blood was obtained from the Platelet Pharmacology and Physiology Core at the University of Michigan. The core maintains a blanket IRB for basic science studies, which does not require HIPAA information, and enrolls healthy subjects that follow the protection of human subject standards. De-identified samples were used in the study. Neutrophils were isolated from human peripheral blood as described previously [357]. Freshly isolated blood was carefully layered on top of 1-step polymorphs (AN221725, Accurate chemicals and scientific corporation) (1:1 Blood and Polymorphs) and centrifuged at 1000× g for 45 min and buffy coat was transferred to fresh tubes. Red blood cells were lysed using 0.1× PBS hypotonic solution for

45 sec, and immediately 4× PBS was added. The tubes were centrifuged at 400× g for 10 min, and pelleted cells were resuspended in modified Hanks' balanced salt solution (mHBSS). Neutrophil preparations were at least 95% pure, as confirmed by nuclear morphology.

3.3.10 Immunostaining of human neutrophils

Each well of an 8-well chamber µ-slide was coated with 5 µg of fibronectin (F1141, Sigma) overnight at 4°C. Freshly isolated human neutrophils were preincubated with either vehicle or 500 ng/mL PTX for 2 hr at 37 °C with gentle rotation before plating on the fibronectin-coated wells. 2 × 10^5 cells per well were allowed to adhere to the surface for 15 min at 37°C in 5% CO_2. The cells were stimulated with vehicle or fMLF (10 nM) for 5 min at 37 °C in 5% CO_2 incubator and then fixed with 4% PFA and 5% sucrose in ddH_2O for 15 min at RT, and blocked using 10% goat serum, 3% Fatty acid-free BSA, 0.05% Saponin in 0.2% PBST for 1 hr at RT. Subsequently, the cells were incubated with 1:100 P-MLC primary antibody prepared in 2% goat serum, 0.05% saponin in 0.1% PBST. The following day, the cells were washed with 0.05% saponin in 0.1% PBST for 10 min, three times, and incubated with anti-rabbit 488 secondary for 1 hr at RT and subsequently stained with DAPI. The cells were imaged in confocal mode with a 63× oil lens, and acquisition parameters were kept constant for all the experimental conditions. Three random fields were acquired per experiment, and images from three independent experiments were analyzed by counting the number of cells with asymmetric P-MLC staining and the total cells to determine % cells with asymmetric P-MLC distribution. Representative images were captured with a 100× oil lens.

3.3.11 Co-immunoprecipitation

3.5×10^5 A293 cells cultured in Dulbecco's modified Eagle's medium (DMEM), 10% (v/v) FBS and 1% P/S were plated on poly-D-lysine-coated 6-well tissue culture plates the day before transfection. 1 µg of each RASA cDNA were cotransfected with empty vector control, BioID2-$G\alpha_{i1}$ or BioID2-$G\alpha_{i1}$-QL using 1:3 DNA: Lipofectamine 2000 (Invitrogen) ratio. Proteins were expressed for 48 hr and cells were lysed in 500µL of 1% (v/v) Nonidet P-40 lysis buffer (10 mM Tris-Cl, pH 7.5, 50mM NaCl, 1% (v/v) Nonidet P-40) supplemented with 1× protease inhibitor (PI) cocktail (P8849, Sigma). After the supernatant was incubated overnight with 1 µL anti-FLAG antibody (F1804, Sigma) and 20 µL slurry of Protein G plus magnetic beads (88848, Thermo Scientific™) at 4 °C in an end-to-end rotator. Beads were centrifuged for 1 min at 16,000 g, washed twice with 1 mL of lysis buffer boiled in 30 µL of 2×SDS sample buffer, and resolved on SDS-PAGE followed by western blot.

3.3.12 Western blotting

Samples were resolved on 4-20% Mini-protean TGX™ Gels (4561094, Bio-Rad), were transferred to a nitrocellulose membrane (66485, Pall Corporation), and stained with Ponceau S (141194, Sigma). Membranes were blocked with 5% non-fat milk powder in TBST (0.1% Tween-20 in Tris-buffered saline) at RT for 1 hr with constant shaking. Membranes were probed with primary antibodies for 1 or 2 hr at RT or overnight at 4 °C. The membranes were washed with TBST, incubating with secondary antibody for 1 hr at RT, washed with TBST, and imaged using an Odyssey Infrared Imaging System (Li-Cor Biosciences).

3.3.13 Statistical analysis

All the experiments were performed at least three times. Data shown are expressed as mean ± SD or as a representative experiment with replicate data in the figure or the supplemental figures. Statistical significance between various conditions was assessed by determining P values using the Student's t-test, one-way or two-way ANOVA with Tukey's multiple comparisons test. (**P < 0.01, *** < 0.001, ****<0.0001). Western blot images were scanned using Licor and quantified using Image Studio Lite (Version 5.2). All data were analyzed using GraphPad Prism 7.0 (GraphPad; La Jolla, CA), and schematic representations of the figures were created with BioRender.com and Adobe illustrator.

3.4 Results

3.4.1 PRG selectively interacts with active $G\alpha_{i1}$

One protein of interest relevant to cell migration and significantly enriched in BioID2-$G\alpha_{i1}$-QL relative to BioID2-$G\alpha_{i1}$ samples was PDZ-RhoGEF (PRG) and also known as ARHGEF11), a Rho guanine nucleotide exchange factor. PRG biotin labeling by BioID2-$G\alpha_{i1}$ and BioID2-CaaX was similar based on the MS quantification, suggesting that labeling by inactive BioID2-$G\alpha_{i1}$ was primarily due to membrane proximity (Fig. 3.1 A). We decided to pursue PRG for several reasons. PRG was strongly enriched in the BioID2-$G\alpha_{i1}$-QL samples, and PRG has a role in the regulation of neutrophil migration downstream of Gi-coupled chemoattractant receptors [207, 266]. PRG localizes to the rear of migrating neutrophils and activates Rho and myosin-dependent tail retraction during migration in response to chemoattractants [207]. The abundance of endogenous PRG was similar in HT1080 cells transfected with BioID2-$G\alpha_{i1}$, BioID2-$G\alpha_{i1}$-QL, or BioID2-CaaX (Fig. 3.1 B), showing that the high PRG abundance in BioID2-$G\alpha_{i1}$-QL samples

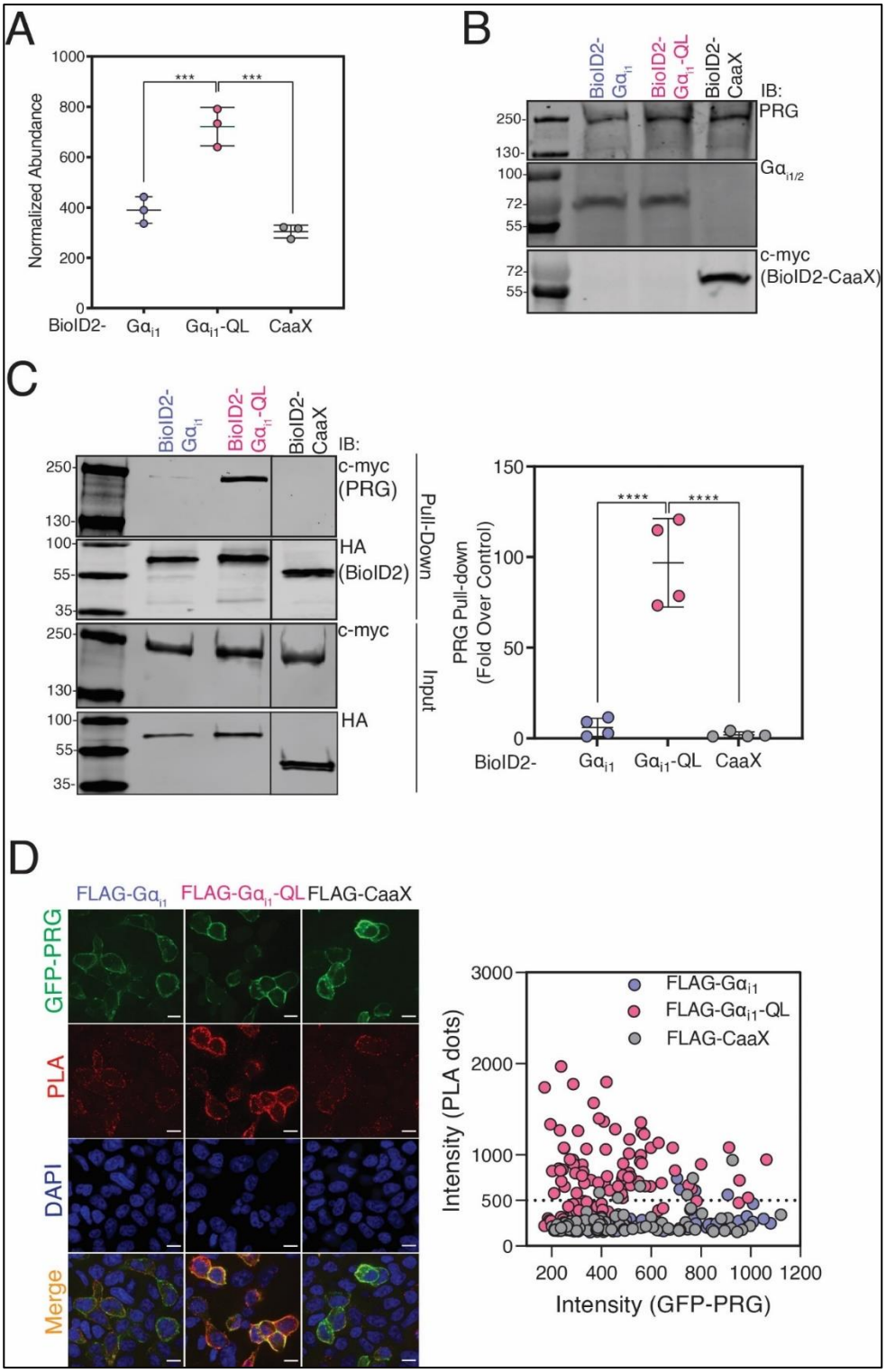

Figure 3.1: BioID2-Gα$_{i1}$-QL interacts with PRG in cells.
(A) Normalized abundance of PRG was quantified by MS in cells expressing BioID2-Gα$_{i1}$, BioID2-Gα$_{i1}$-QL, or BioID2-CaaX. The data represent the mean ± SD of three independent experiments. (****P<0.0001, one-way ANOVA with Tukey's multiple comparisons test). **(B)** HT1080 cells were transfected with the indicated constructs, and whole-cell lysates were resolved by Western blot. **(C)** A293 cells were transfected with PRG and BioID2-Gα$_{i1}$, BioID2-Gα$_{i1}$-QL, or BioID2-CaaX and labeled with biotin for 24 hr. Cell lysates were subjected to streptavidin pulldowns. Left: Representative Western blots of PRG in streptavidin pulldowns from cells expressing BioID2-Gα$_{i1}$, BioID2-Gα$_{i1}$-QL, or BioID2-CaaX. Right: Quantitation (shown as mean ± SD)

of three independent experiments normalized to total PRG. ***P < 0.001, ****<0.0001, one-way ANOVA with Tukey's multiple comparisons test). **(D)** PLAs were performed in cells transfected with GFP-PRG and APEX2-FLAG-tagged $G\alpha_{i1}$-WT, $G\alpha_{i1}$-QL, or CaaX. Left: Representative images from three randomly selected fields show GFP-PRG (green), PLA reaction (red), merge (orange) and DAPI (blue). Scale bar, 10μm. Right: The intensity of the PLA signal (y-axis) was plotted against GFP-PRG expression (x-axis). For each experiment, ~100 cells per condition were analyzed; the data are shown from one of three independent experiments that yielded similar results.

was not simply due to increased PRG expression.

To independently validate PRG enrichment in BioID2-$G\alpha_{i1}$-QL samples by MS, we labeled A293 cells co-expressing PRG with BioID2-$G\alpha_{i1}$, BioID2-$G\alpha_{i1}$-QL, or BioID2-CaaX with biotin and performed streptavidin affinity pulldowns. PRG was highly enriched in streptavidin pulldowns from BioID2-$G\alpha_{i1}$-QL-transfected cells compared to those transfected with BioID2-$G\alpha_{i1}$ or BioID2-CaaX (Fig. 3.1 C). Next, we used a proximity ligation assay (PLA) to test for interactions in A293 cells. A robust PLA signal in cells co-transfected with GFP-PRG and APEX-FLAG-$G\alpha_{i1}$-QL was observed. A low PLA signal observed between GFP-PRG and the controls APEX-FLAG-$G\alpha_{i1}$-WT or APEX-CaaX may be due to colocalization at the PM, resulting in background bystander proximity labeling (Fig. 3.1 D). These data further support selective interactions between $G\alpha_{i1}$-GTP and PRG (Fig. 3.1 D).

3.4.2 Gαi1 activates the RhoGEF activity of PRG

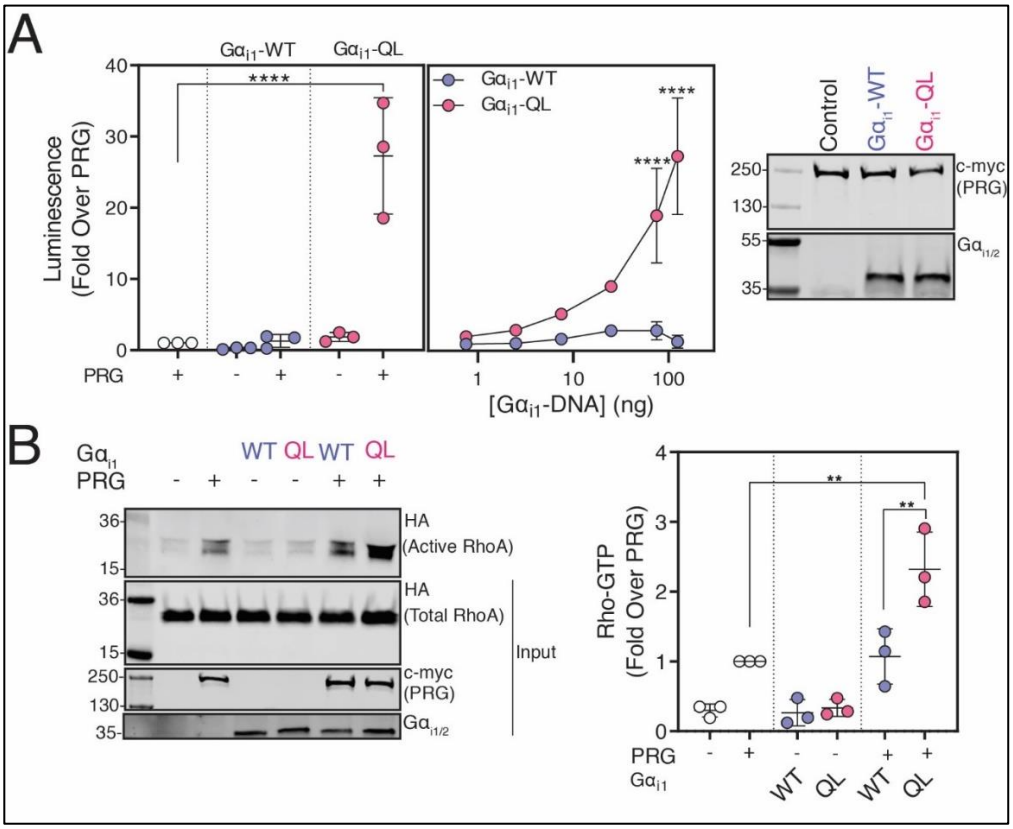

Figure 3.2: Gαi1-GTP activates PRG activity.
(A) A293 cells were transfected with cDNAs encoding SRE-Luciferase, PRG, and either Gαi1 or Gαi1-QL for 20 hr. Left and middle: Luminescence was measured in serum-starved cells 10 min after the addition of One-Glo™ reagent. The data represent the mean ± SD of three independent experiments. Right: Representative Western blots showing relative expression of various cDNA constructs in A293 cells. Data are representative of three independent experiments that yielded similar results. **(B)** A293 cells were transfected with the indicated cDNA constructs, and cell lysates were incubated with GST-Rhotekin beads. Left: Representative Western blots showing bound RhoA-GTP and relative expression of transfected constructs. Right: Quantification (shown as mean ± SD) of three independent experiments, normalized to total RhoA. (**P < 0.01, ****<0.0001, Panel A left and B: one-way ANOVA with Tukey's multiple comparisons test, Panel A middle: two-way ANOVA with Tukey's multiple comparisons test).

These findings prompted us to investigate whether Gαi1 could activate PRG. An SRE luciferase (SRE-Luc) reporter for Rho activation [358] was used to study PRG activation in A293 cells co-transfected with PRG and Gαi1-WT or Gαi1-QL. Strong synergistic activation of SRE-Luc was observed upon PRG and Gαi1-QL co-transfection, but not upon transfection of either component alone (Fig. 3.2 A left), suggesting that Gαi1-QL activates PRG to stimulate Rho activation. Activation of PRG depended on the Gαi1 activation state because Gαi1-WT did not

significantly increase PRG activity (Fig. 3.2 A left). PRG activation by $G\alpha_{i1}$-QL was concentration-dependent (Fig. 3.2 A middle). $G\alpha_{i1}$-WT and $G\alpha_{i1}$-QL were expressed at comparable levels, and PRG expression was similar in all three conditions (Fig. 3.2 A, right).

To validate activation of PRG by active $G\alpha_{i1}$, we measured active RhoA (RhoA-GTP) with a Rhotekin pulldown assay, in which RhoA binds to Rhotekin-Glutathione S-transferase (GST) in an activation-dependent manner. PRG expression led to increased RhoA-GTP levels in Rhotekin-GST pulldowns compared to control conditions, and this enhancement was further significantly increased with co-expression of $G\alpha_{i1}$-QL but not of $G\alpha_{i1}$-WT (Fig. 3.2 B). These assays establish that GTP-bound $G\alpha_{i1}$ activates the RhoGEF activity of PRG.

3.4.3 PRG-dependent SRE-Luc activation is specific to $G\alpha_{i/o}$ proteins

Activation of PRG by $G\alpha_{i1}$ was unexpected, given that PRG is reported to be regulated by $G\alpha_{12/13}$ [185, 187]. We tested whether other families of Gα subunits activated PRG as measured by the SRE-Luc reporter assay. Transfection of both WT and QL versions of $G\alpha_q$, $G\alpha_{12}$, $G\alpha_{13}$ increased the activity of the SRE-Luc reporter compared to control conditions, likely due to activation of endogenous RhoGEFs in A293 cells (Fig. 3.3A), although, for reasons that are not clear, activation was equal for the WT and QL forms of these proteins. Under the conditions of this assay, $G\alpha_q$, $G\alpha_{12}$, $G\alpha_{13}$ co-expression with PRG did not increase PRG-dependent SRE-Luc activation.

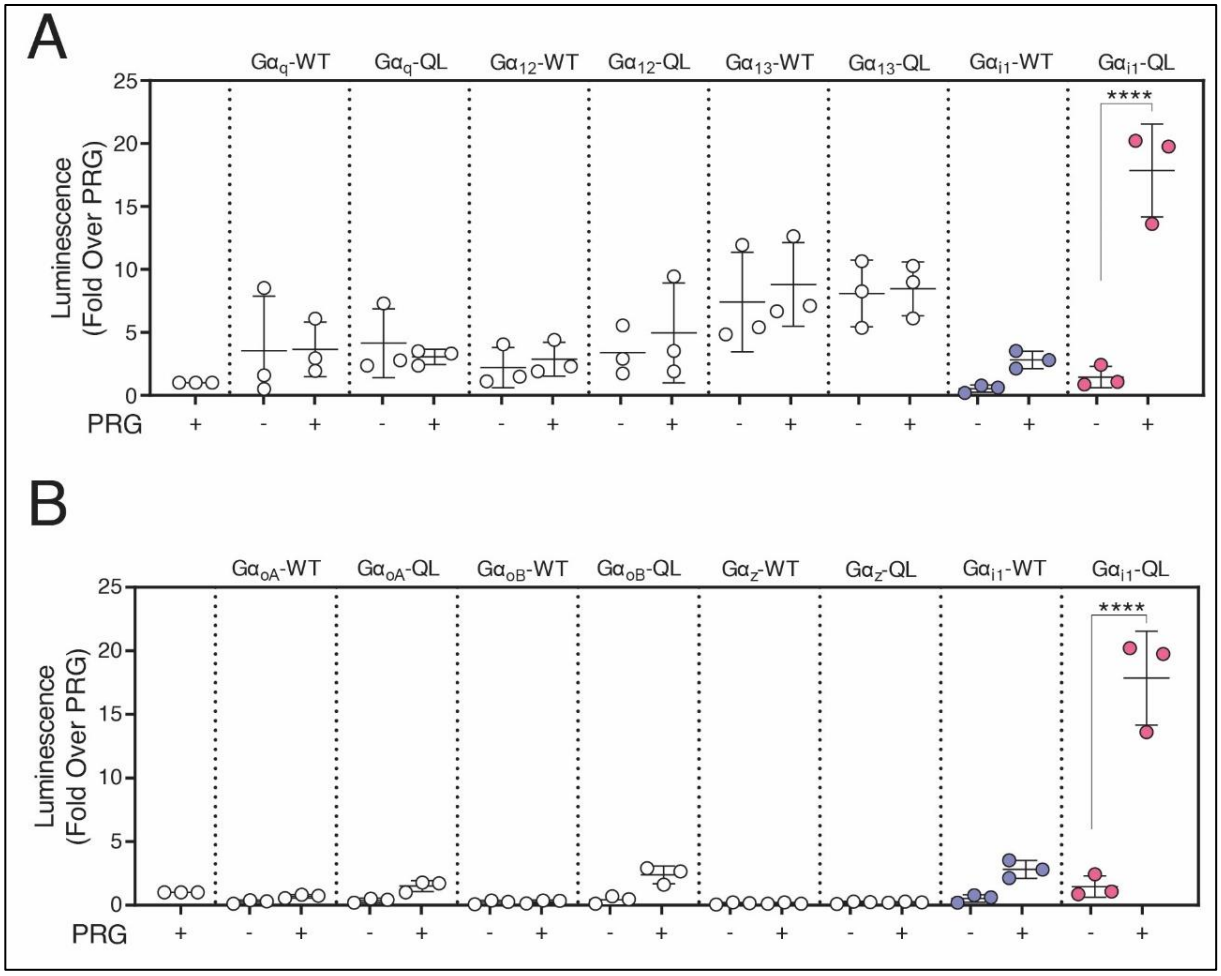

Figure 3.3: Specificity of PRG activation by different G protein subunit family members in the SRE-luciferase assay. **(A-B)** A293 cells were transfected with cDNAs encoding SRE-Luciferase, PRG, and the indicated Gα protein subunits. Luminescence was measured in serum-starved cells 10 min after the addition of One-Glo™ reagent. The data represent the mean ± SD of three independent experiments. (P****<0.0001, one-way ANOVA with Tukey's multiple comparisons test).

3.4.4 $G\alpha_{i1}$ and $G\alpha_{i3}$ strongly activate PRG, but $G\alpha_{i2}$ is a poor activator

We tested $G\alpha_i$ family member isoforms for their ability to activate PRG. $G\alpha_{oA}$-QL, $G\alpha_{oB}$-QL showed a small increase in PRG activation, whereas $G\alpha_z$ did not activate PRG (Fig. 3.3 B). The $G\alpha_i$ isoforms $G\alpha_{i1}$, $G\alpha_{i2}$, and $G\alpha_{i3}$ are highly homologous, with greater than 85% amino acid sequence identity [323].

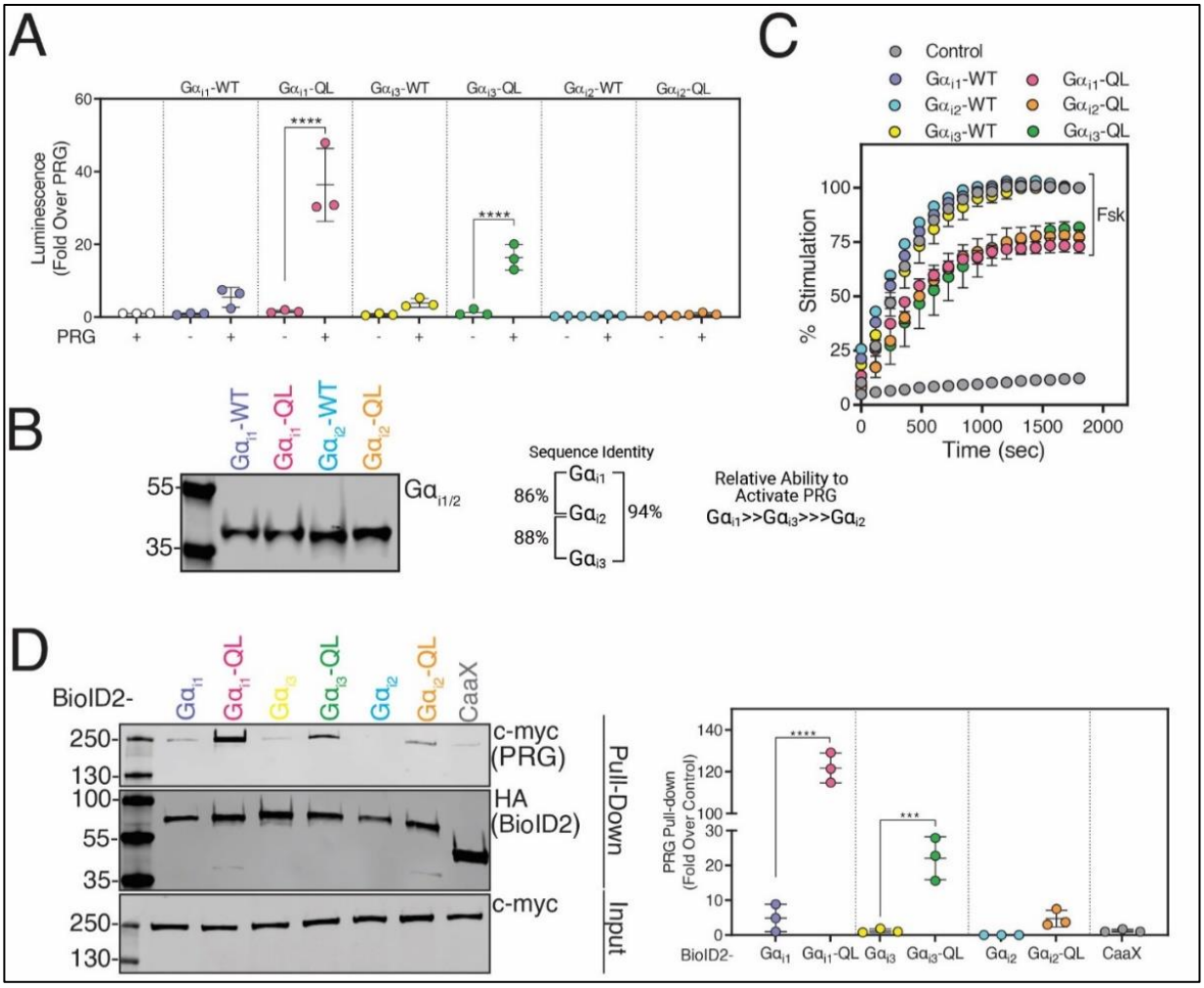

Figure 3.4: PRG activation is Gαi isoform-specific.
(A) A293 cells were transfected with cDNAs encoding SRE-Luciferase, PRG, and either Gαi1-QL, Gαi2-QL, or Gαi3-QL. Luminescence was measured in serum-starved cells 10 min after the addition of One-Glo™ reagent. The data represent the mean ± SD of three independent experiments. **(B)** Western blot showing relative expression of Gαi1 and Gαi2 constructs in A293 cells. Data are representative of three independent experiments that yielded similar results. **(C)** Cells were transfected with cAMP Glosensor™ and WT and QL versions of Gαi1, Gαi2, or Gαi3 for 24 hr. Luminescence was measured for 30 min (x-axis) after Forskolin (Fsk) stimulation and represented as % stimulation (y-axis) relative to the maximum signal in the respective WT group with 1 µM Fsk treatment. Data shown as mean ±SD are representative of three independent experiments. **(D)** A293 cells were transfected with PRG and BioID2-Gαi1-QL, BioID2-Gαi3-QL, or BioID2-Gαi2-QL and labeled with biotin for 24 hr. Cell lysates were subjected to streptavidin pulldowns. Left: Representative Western blots of PRG in streptavidin pulldowns as well as of expression of BioID2-Gαi1, Gαi1-QL and BioID2-CaaX. Right: Quantitation is shown as mean ± SD of three independent experiments normalized to total PRG. (***P <0.001, ****<0.0001, one-way ANOVA with Tukey's multiple comparisons test).

Gαi1-QL and Gαi3-QL strongly activated PRG, whereas Gαi2-QL did not (Fig. 3.4 A). Gαi1 and Gαi2 were expressed at approximately similar levels (Fig. 3.4 B), and Gαi3 expression could not be compared because the antibody does not recognize Gαi3. Gαi-QL versions of all three subtypes showed similar inhibition of Fsk-stimulated cAMP production (Fig. 3.4 C). To

corroborate this finding, we labeled A293 cells co-expressing PRG with BioID2-tagged WT and QL versions of the $G\alpha_i$ isoforms in A293 cells with biotin and streptavidin affinity pulldowns were performed. PRG was highly enriched in the streptavidin pulldown from BioID2-$G\alpha_{i1}$-QL-expressing cells (Fig. 3.4 D). Enrichment was lower in pulldown from BioID2-$G\alpha_{i3}$-QL-expressing cells and very low in those from BioID2-$G\alpha_{i2}$-QL-expressing cells (Fig. 3.4 D). Effector selectivity amongst these three highly related $G\alpha_i$ isoforms has not been previously reported.

3.4.5 $G\alpha_{i1}$-QL is specific for PRG mediated RhoA activation and does not require $G\alpha_{12/13}$

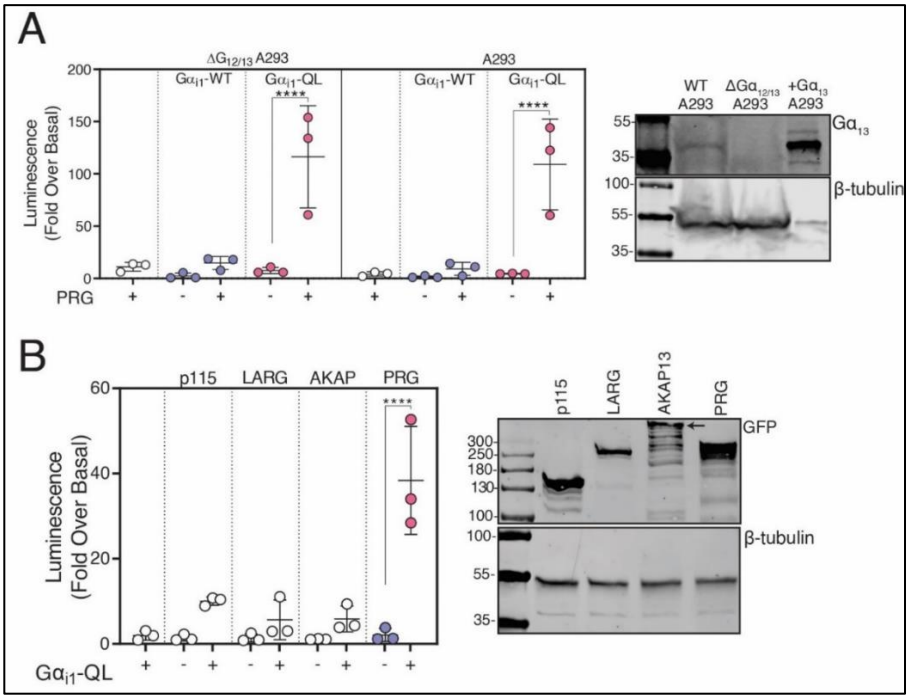

Figure 3.5: $G\alpha_{i1}$-QL is specific to PRG relative to other RhoGEFs and does not require $G\alpha_{12/13}$.
(A) Left: A293 or $\Delta G_{12/13}$ A293 cells were transfected with SRE-Luc and either $G\alpha_{i1}$ or $G\alpha_{i1}$-QL. Luminescence was measured in serum-starved cells 10 min after the addition of One-Glo™ reagent. Right: Western blot showing endogenous $G\alpha_{13}$ expression in both the cell lines and A293 cells transiently expressing $G\alpha_{13}$. β-tubulin was used as an internal control. **(B)** Left: A293 cells were transfected with SRE-Luc, the indicated RH-RhoGEF family members and either $G\alpha_{i1}$ or $G\alpha_{i1}$-QL. Luminescence was measured in serum-starved cells 10 min after the addition of One-Glo™ reagent. Right panel: Representative western blot showing relative expressions of various GFP tagged RhoGEFs in A293 cells. The data represent the mean ± SD of three independent experiments. (P****<0.0001, one-way ANOVA with Tukey's multiple comparisons test).

As mentioned above, $G\alpha_{12/13}$ is reported to bind to PRG [185, 187], leading us to investigate whether $G\alpha_{12/13}$ was required for $G\alpha_{i1}$-QL mediated PRG activation. $G\alpha_{i1}$-QL co-transfected with PRG robustly increased the activity of the SRE-Luc reporter, and knockout of $G\alpha_{12/13}$ by CRISPR/Cas9-mediated gene editing did not affect PRG activation (Fig. 3.5 A, left). Furthermore, $G\alpha_{13}$ KO was confirmed by Western blotting (Fig. 3.5 A, right). These findings demonstrate that $G\alpha_{i1}$-GTP can activate the RhoGEF activity of PRG in the absence of $G\alpha_{12}$ or $G\alpha_{13}$.

Next, we tested the ability of $G\alpha_{i1}$-QL to activate other members of the DH-PH family of RhoGEFs in the SRE-Luc reporter assay (Fig. 3.5 left). We co-transfected $G\alpha_{i1}$-QL with GFP-p115 RhoGEF (Lsc), GFP-LARG, GFP-AKAP13 (Proto-Lbc, ARHGEF13), and GFP-PRG. $G\alpha_{i1}$-QL robustly increased SRE-Luc reporter activity when co-transfected with PRG. $G\alpha_{i1}$-QL also activated p115RhoGEF, although to a much lesser extent as compared to PRG activation. $G\alpha_{i1}$-QL did not activate LARG or AKAP13 to a statistically significant extent. Western blotting demonstrated expression of the RhoGEFs at varying levels (Fig. 3.5 right).

3.4.6 The formyl peptide receptor 1 (FPR1) activates PRG through $G\alpha_{i1}$

To determine whether PRG could be activated by $G\alpha_i$ downstream of a Gi-coupled receptor, we assayed PRG activation with the SRE-Luc reporter. In A293 cells stably expressing FPR1 (A293-FPR1), fMLF activated SRE-Luc reporter activity in a concentration-dependent fashion only when PRG and $G\alpha_{i1}$-WT were co-transfected and not when PRG or $G\alpha_{i1}$-WT were transfected alone (Fig. 3.6).

In contrast, fMLF did not increase reporter activity in cells co-transfected with $G\alpha_{i2}$-WT and PRG (Fig. 3.6), confirming that $G\alpha_{i2}$-QL poorly activates PRG. Application of the $G\alpha_i$ blocker PTX significantly inhibited the fMLF-dependent increase in PRG activation in cells expressing

FPR1, $G\alpha_{i1}$ and PRG (Fig. 3.6), thus providing further evidence that FPR1 activation of PRG depends on $G\alpha_i$.

RhoA is a major regulator of cytoskeletal rearrangement and can induce peripheral protrusions [359, 360]. As an alternate measure of RhoA activation, we examined fMLF-stimulated dynamic protrusion formation in FPR1-A293 cells (Fig. 3.6 C left). The percentage of cells that formed protrusions in cells transfected with PRG alone was slightly but significantly higher than in cells transfected with vector control and was not affected by PTX treatment (Fig. 3. 6 C right). Co-expression of $G\alpha_{i1}$-WT with PRG significantly increased the percentage of cells with dynamic protrusions only when cells were stimulated with fMLF, and the activation was inhibited by PTX. Together, these data support the hypothesis that PRG RhoGEF activity can be activated downstream of Gi-coupled GPCRs through $G\alpha_{i1}$.

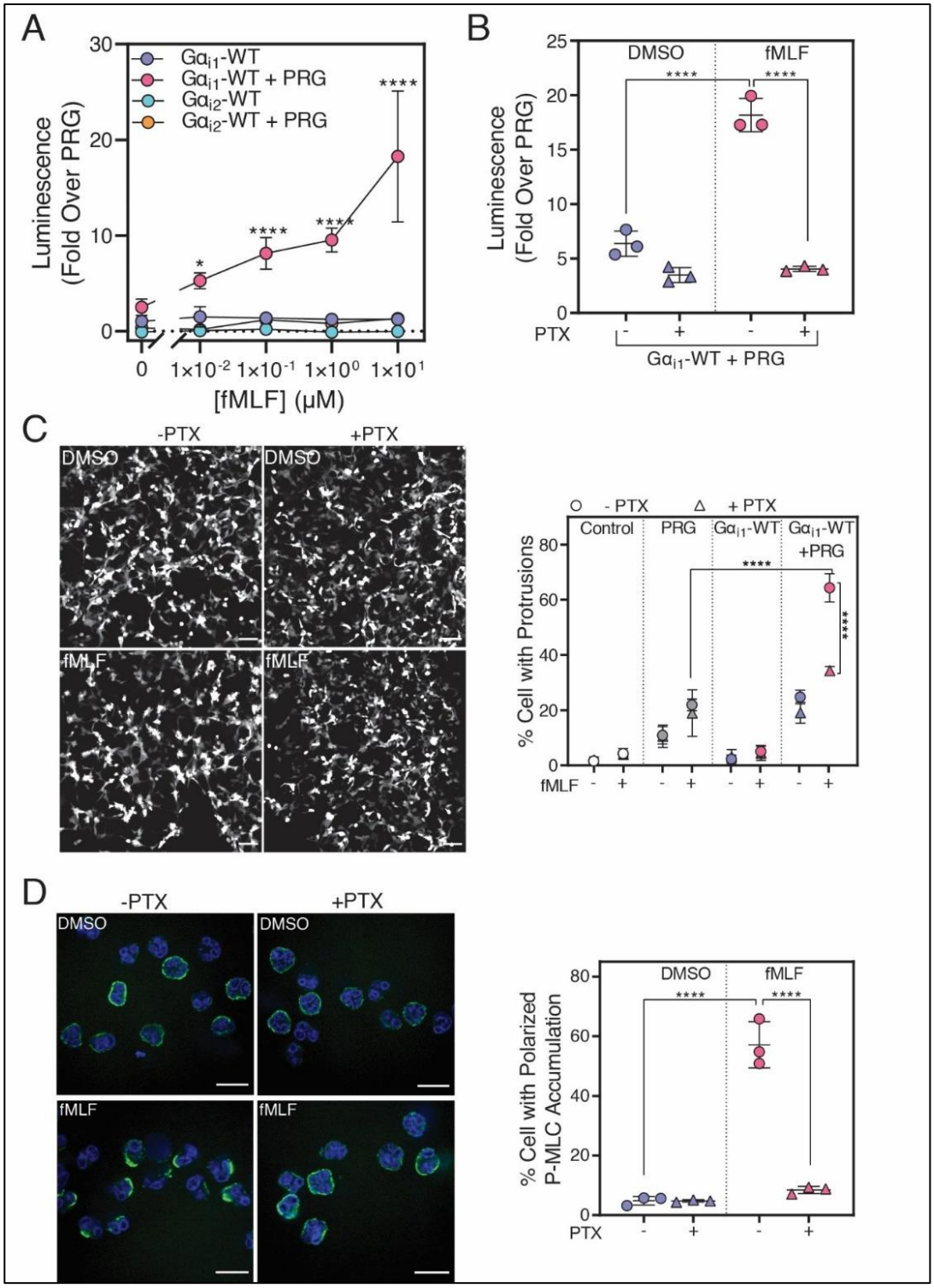

Figure 3.6: Activation of PRG downstream of Gα$_i$-coupled receptor FPR1.
(A) A293 cells stably expressing FPR1 (A293-FPR1) were transfected with cDNAs encoding SRE-Luc, PRG, and Gα$_{i1}$-WT or Gα$_{i2}$-WT and incubated for 12 hr in serum-free media containing fMLF (0.01, 0.1, 1 and 10 μM) or DMSO. Data from three independent experiments were plotted as mean ± SD. (**B)** A293-FPR1 cells were transfected and incubated for 12 hours in serum-free media containing PTX (100 ng/mL) and fMLF (10 μM). Luminescence was measured 10 min after the addition of the One-Glo^{TM} reagent. The data combined data (mean ± SD) of three independent experiments. **(C)** A293-FPR1 cells were transfected with PRG, Gα$_{i1}$-WT, and YFP for 36 hr. 24 hr after transfection, cells were treated with PTX (100 ng/mL) for 12 hr. Cells were stimulated with 100 nM fMLF and live-cell video microscopy was performed for 40 min. Left: Representative images

of A293-FPR1 cells expressing PRG + $G\alpha_{i1}$-WT and treated with fMLF or DMSO are shown. Scale bar, 100 μm. Right: Quantitative analysis of the percentage of cells with dynamic protrusions shown as mean ± SD from three independent experiments. For each experiment, >500 cells per condition were analyzed in a blinded manner. **(D)** Human neutrophils were pretreated or not with PTX (500 ng/mL) for 2 hr, allowed to adhere to the fibronectin-coated surface for 15 min, and stimulated with 10 nM fMLF for 5 min. The cells were stained with a P-MLC antibody and DAPI and imaged with confocal microscopy. Left: Representative images from three randomly selected fields of view are shown. Right: Total number of cells and cells with asymmetric P-MLC localization were counted in a field, and the % cells with polarized P-MLC localization (mean ± SD) from three independent experiments were plotted. (****P < 0.0001, Panel A: Two-way ANOVA with Tukey's multiple comparisons test, Panel B, C, D: One-way ANOVA with Tukey's multiple comparison test). Scale bar, 10 μm.

3.4.7 Evidence for the involvement of $G\alpha_i$ in fMLF-dependent PRG activation in human neutrophils

To understand the physiological relevance of the $G\alpha_i$-dependent mechanism for Rho regulation, we examined the role of Gi signaling in human neutrophils. Of the multiple G protein activated RhoGEFs expressed in neutrophils, PRG mediates Rho-dependent polarized accumulation of phosphorylated (at Ser^{19})-myosin light chain (P-MLC) at the trailing edge of migrating neutrophils [207, 266]. This effect has been proposed to result from FPR1-dependent $G\alpha_{13}$ activation [266] in part because PTX treatment of the neutrophil-like cell line HL60 only partially inhibits fMLF-dependent Rho activation and asymmetric localization of P-MLC [266]. To determine if $G\alpha_i$ activates endogenous PRG in human neutrophils, we examined polarized P-MLC staining after stimulation with a physiologically relevant concentration of fMLF. In DMSO treated neutrophils, P-MLC was uniformly distributed at the surface of cells. Stimulation with 10 nM fMLF promoted strong polarized P-MLC accumulation (Fig. 3.6 D left). In cells pretreated with PTX, fMLF failed to promote the polarized accumulation of P-MLC (Fig. 3.6 D right). Because PRG mediates the Rho-dependent polarization of P-MLC, this finding suggests that at physiological concentrations of fMLF, PRG activation in human neutrophils occurs through a $G\alpha_i$-dependent mechanism.

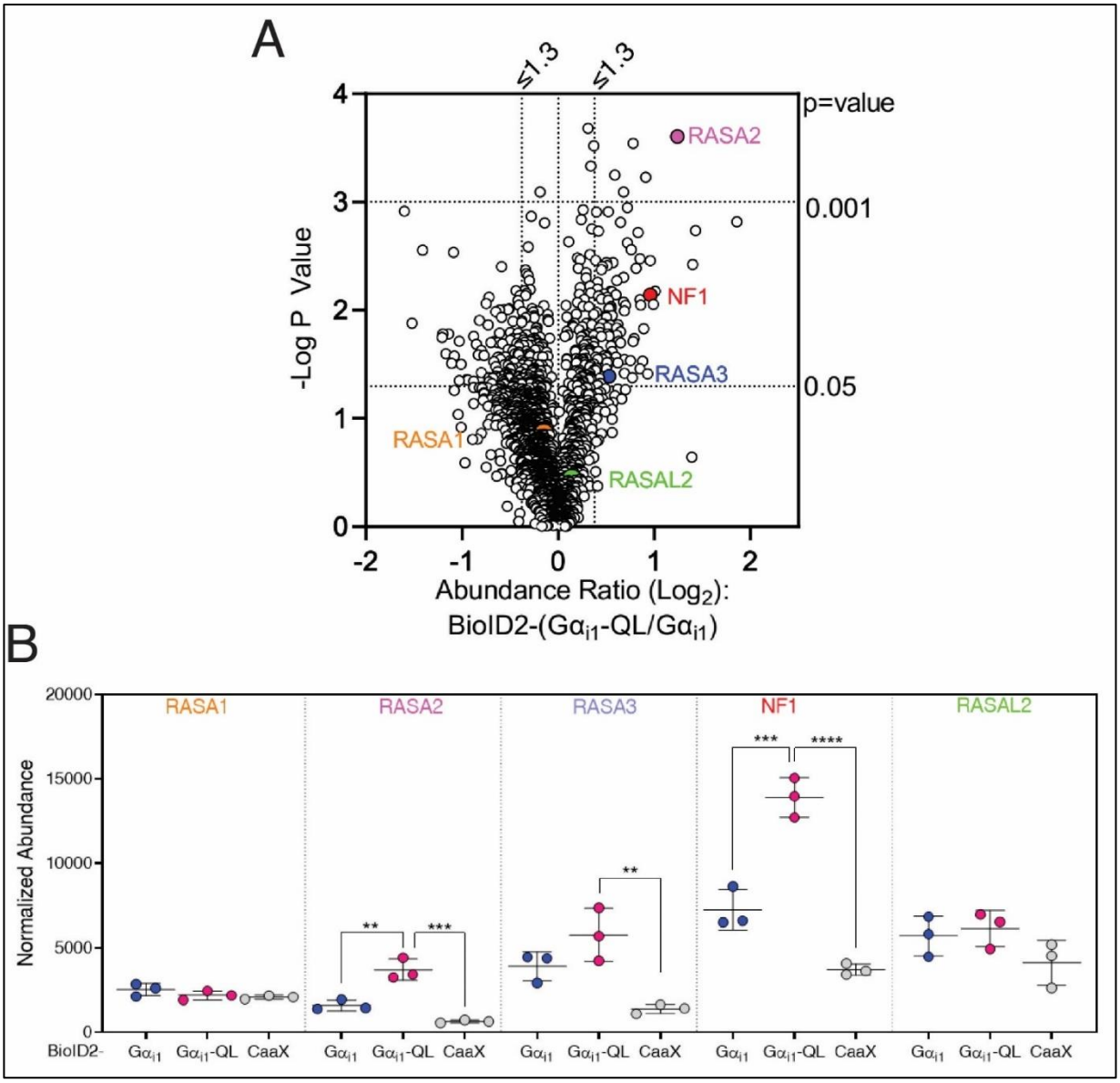

Figure 3.7: Selectively labeling of RASA family members by BioID2-Gαi1-QL identified by MS.
(A) Volcano plot showing relative changes in abundance of RASA subtypes along with all other high confidence proteins that were identified in the MS analysis **(B)** Normalized abundance of RASA members quantified by MS in cells expressing BioID2-Gαi1, BioID2-Gαi1-QL, or BioID2-CaaX. The data represent the mean ± SD of three independent experiments. (****P<0.0001, one-way ANOVA with Tukey's multiple comparisons test).

3.4.8 Multiple RasGAP family members were selectively enriched by Gαi1-QL biotin proximity labeling

Multiple members of RasGAPs were identified and, RASA2 and NF1 were selectively enriched in BioID2-Gαi1-QL samples compared to BioID2-Gαi1 and BioID2-CaaX (Fig. 3.7 A

and B). We decided to pursue RasGAPs for several reasons. RasGAP proteins are known to regulate Ras, but individual isoforms don't have redundant functions. Selective enrichment of BioID2-Gα_{i1}-QL might lead to an understanding of the differential functional regulation of RasGAPs by Gα_{i1}. In addition, there is a very limited literature precedent for G protein α subunit mediated RasGAP regulation [162, 355].

3.4.9 RASA1, RASA2, RASA3 and NF1 selectively interact with active Gα_{i1}

The expression of RASA1, RASA2, RASA3 and NF1 were unchanged in the presence of BioID2-Gα_{i1}, BioID2-Gα_{i1}-QL. To independently validate RASA enrichment in BioID2-Gα_{i1}-QL samples by MS, we performed co-immunoprecipitation in A293 cells co-expressing each RASA member with a control vector, BioID2-Gα_{i1}, or BioID2-Gα_{i1}-QL. All four proteins were enriched in co-IPs only when co-transfected with BioID2-Gα_{i1}-QL. However, weaker co-IP of RasGAPs was observed with BioID2-Gα_{i} transfected cells as compared with BioID2-Gα_{i1}-QL transfected cells (Fig. 3.8). No RasGAP was detected in empty vector-transfected cells, indicating no nonspecific binding of the proteins to the antibody or the beads. These data further support selective interactions between Gα_{i1}-GTP and RASA family members.

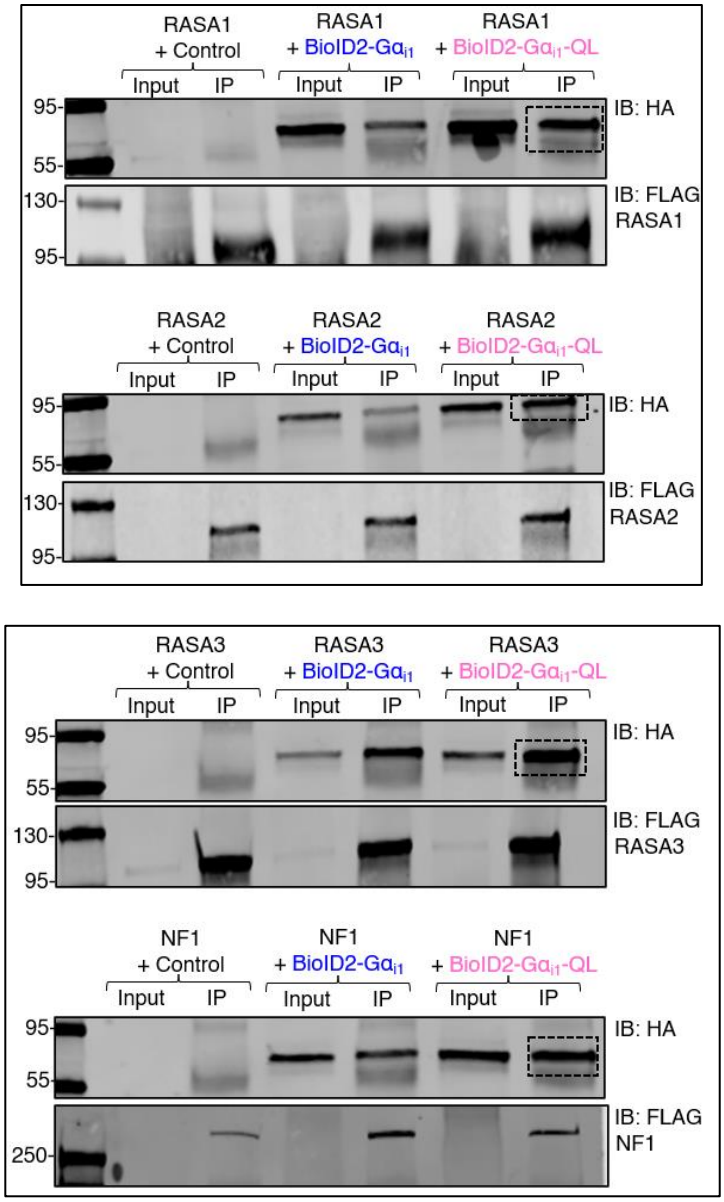

Figure 3.8: RASA1, RASA1, RASA1, and NF1 interacts with active $G\alpha_{i1}$ in transfected A293 cells.
A293 cells were transfected with RASA1 alone or RASA1 with BioID2-$G\alpha_{i1}$ or BioID2-$G\alpha_{i1}$-QL. Cells were lysed and immunoprecipitated with anti-FLAG specific antibody. Lysates were probed for RASA and BioID2-$G\alpha_{i1}$ using anti-FLAG and anti-HA antibodies, respectively. Each experiment was repeated twice with similar results.

3.5 Discussion

We used an unbiased approach to identify effectors of $G\alpha_i$ by the proximity labeling method and focused on identifying proteins involved in chemoattractant-dependent cell migration. From the proteins identified, we focused on PRG, a RhoGEF with well-established roles in cell

migration. We systematically characterized PRG as a novel effector of $G\alpha_i$ regulating cell migration and found its role in physiologically relevant cells, human neutrophils. It is the first mechanistic demonstration of Gαi regulation of the RhoA via PRG. PRG is known to regulate a variety of biological processes; therefore, this interaction can have implications in multiple biological processes beyond immune cells, such as cancer cell migration and metastasis and tissue repair, neuronal growth cone development and so on.

We demonstrated that $G\alpha_{i1}$ strongly activated PRG in a GTP and concentration-dependent manner in intact cells. We also demonstrated $G\alpha_i$-dependent PRG regulation downstream of the Gi-coupled chemoattractant receptor, FPR1, in A293 cells. In differentiated HL60 neutrophil-like cells, activation of FPR1 leads to PRG and Rho-dependent accumulation of P-MLC at the trailing edge, where it is responsible for tail retraction as the cell moves forward [207, 266], a process that has been proposed to be mediated by $G\alpha_{13}$. In our experiments, stimulation of primary human neutrophils with a physiological concentration fMLF promoted polarized P-MLC accumulation that was inhibited by PTX, suggesting this phenotype depends on $G\alpha_i$ signaling. In the previous work performed with 100 nM fMLF, PTX partially affected P-MLC polarization, and fMLF dependent RhoA activation was partially inhibited by PTX [266]. In contrast to this study, we used primary neutrophils and a physiological concentration of fMLF (10 nM). Our data suggest that at a low physiological concentration of chemoattractant, $G\alpha_i$ regulation of PRG is critical for tail retraction during cell migration, and we propose that $G\alpha_{13}$ may perform a more dominant role in migrating neutrophils at higher concentrations of chemotactic ligands.

It is accepted that $G\alpha_{13}$ activates RH-RhoGEFs such as PRG, and evidence shows that PRG activity is regulated downstream of $G\alpha_{12/13}$ [187, 205]. Strong data has demonstrated G_{13} binding to PRG, and a clear regulation of PRG by $G_{12/13}$ coupled GRCRs in physiological settings [361],

but we did not observe activation of PRG by $G\alpha_{12}$ or $G\alpha_{13}$ in our SRE based co-transfection experiments. $G\alpha_{12}$ and $G\alpha_{13}$ activated endogenous RhoGEFs in our assays because they promoted SRE activation without PRG co-transfection, but surprisingly the activation was not different between WT and constitutively active forms. The reasons for these discrepancies are unclear, but the demonstration of $G\alpha_{12/13}$ -dependent regulation of PRG in cell-based assays, similar to those used in our studies are limited [191, 362]. Nevertheless, we observed a clear activation of PRG by $G\alpha_i$ that was strongly dependent on the activation state of $G\alpha_i$, lending confidence to our results. Additionally, there is precedence for regulation of PRG by G proteins other than $G_{12/13}$. $G\alpha_s$-mediated activation of Cdc42 has been reported to require PRG [210].

From our studies, we cannot conclude whether the mechanism for $G\alpha_i$-dependent regulation of PDZ-RhoGEF involves direct PPI, if a higher order complex is involved. The strong stimulation of RhoGEF activity of PRG by $G\alpha_i$ suggests direct interactions, but further *in vitro* reconstitution experiments with purified components will be required to demonstrate direct PRG regulation by $G\alpha_i$.

Of the three highly homologous $G\alpha_i$ isoforms, $G\alpha_{i1}$ and $G\alpha_{i3}$ activated PRG, but $G\alpha_{i2}$ was a poor activator [160]. $G\alpha_{i1}$-QL shares 86% amino acid identity with $G\alpha_{i2}$ [363, 364], and the three $G\alpha_i$ isoforms inhibit AC with similar potency and efficacy [323]. These three $G\alpha_i$ isoforms have been studied for nearly three decades [363], and no molecular differences with respect to effector regulation have been demonstrated. Mouse neutrophils express $G\alpha_{i2}$ and $G\alpha_{i3}$ at similar amounts, and neutrophils from $G\alpha_{i3}$ KO mice showed reduced ability to migrate toward a chemotactic stimulus, whereas $G\alpha_{i2}$ KO resulted in loss of their ability to arrest [169, 365]. Therefore, this divergent role could be attributed to differential effector regulation by different $G\alpha_i$ subtypes.

PRG regulates various biological processes, including neurite retraction [198], cell migration, and proliferation of mouse embryonic fibroblasts [366]. Thus, these findings have broad implications for signaling by Gi-coupled receptors. Overall, identification of signaling pathways and networks regulated by G_i-coupled GPCRs has the potential to affect our understanding of the biology regulated by these ubiquitous and pharmacologically important receptors.

Previous reports show that active-$G\alpha_{i2}$ can regulate Ras, c-Jun N-terminal kinase (JNK) and extracellular signal-regulated kinase (ERK), causing oncogenic transformation of Rat-1 fibroblast cells [327]. Active $G\alpha_{i2}$ has also been reported to increase cell proliferation and anchorage-independent growth in NIH3T3 cells [328]. Ras is classically associated with the activation of ERK and JNK signaling pathways. However, only two reports have shown RASA1 and RAS3 downstream of GPCRs, the dopamine (D2S) and FPR receptors, respectively [162, 355]. Identification and differential enrichment of multiple RASA proteins by MS and co-immunoprecipitation studies indicates that Ras regulation by Gi dependent via RASA may be a more widespread process downstream of multiple Gi-coupled receptors.

Identification of proteins from multiple functional families indicates that Gi proteins likely play a central role in several biological processes through signaling networks that do not involve AC inhibition. Therefore, detailed characterization of individual candidate interactions or networks is warranted to validate and understand the roles of these interactions in Gi-coupled GPCR biology. Ultimately, discovery of new GPCR biology will lead to a greater understanding of disease pathologies, identification of new therapeutic targets, and development of innovative therapeutic strategies.

Chapter-4

Summary and Future Directions

4.1 Significance statement

Heterotrimeric G proteins activated by GPCRs shape some of the most fundamental cellular processes in health and disease. G protein family Gi subunits, $G\alpha_i$ and $G\beta\gamma$, are expressed in virtually all cell types. Multiple $G\beta\gamma$ effectors have been identified; however, relatively few $G\alpha_i$ interacting proteins are known. Identification of novel interaction partners of $G\alpha_i$-GTP downstream of chemokine GPCRs will be a step forward in expanding our understanding of the role of $G\alpha_i$ in chemokine signaling mediated cell adhesion at the molecular level. Moreover, enzyme-catalyzed proximity labeling has never been utilized for G proteins. Using this method, we identified novel candidate binding proteins of active $G\alpha_i$ using proximity labeling-coupled MS that have not been previously linked to Gi signaling. Systematic characterization of PRG, as a novel Gi effector, is the first mechanistic demonstration of RhoA activation downstream of active $G\alpha_i$. In addition, preliminary studies show that $G\alpha_i$ may potentially regulate a whole class of RasGAP proteins. Identification of a set of novel interacting proteins, conformationally specific for the active $G\alpha_{i1}$, provides a potential for revealing new signaling pathways for GPCRs and, consequently, new potential targets for therapeutic intervention. In addition, it provides a methodological blueprint for identifying interacting proteins for other $G\alpha$ subunits using the proximity-labeling coupled proteomics approach, which can unravel novel GPCR biology. We extended this method for another type of G protein subtype, $G\alpha_q$, identified classic effectors and potential novel, exciting interactors by MS. Further characterization of these effectors will improve our understanding of

biological and pathophysiological processes regulated by these pharmacologically important receptors and aid in identifying novel therapeutic targets.

4.2 Discussion and future directions

4.2.1 Knowns and unknowns of $G\alpha_i$ and $G\alpha_q$ interactors

$G\alpha_i$-coupled GPCRs regulate a plethora of physiological processes in the cardiovascular, nervous, sensory, endocrine, and immune systems. Cell adhesion and migration regulation through $G\alpha_i$-coupled GPCRs are important for developmental morphogenesis, leukocyte migration to lymphatic organs during antigen surveillance or to sites of infection or inflammation, and cancer cell motility. For many years, immune cell migration regulated by $G\alpha_i$-coupled GPCRs has been attributed solely to $G\beta\gamma$ mediated signaling, and the $G\alpha_i$ subunit is thought to passively function through the release of $G\beta\gamma$ [154, 159, 367]. However, most of the studies are based on PTX treatment or $G\alpha_i$ knockout studies, and both the approaches completely disrupt signaling by both $G\beta\gamma$ and $G\alpha_i$. The lack of tools to selectively interrogate $G\alpha_i$ signaling hindered the identification of roles for $G\alpha_i$ independent of $G\beta\gamma$ signaling.

Recent reports from our laboratory identified novel roles for $G\alpha_i$-GTP in cell adhesion and migration, but the direct effector regulated by $G\alpha_i$ responsible for this has not been identified [160, 161]. In addition, in the past several years, $G\alpha_i$ has been shown to bind multiple effectors including, mIns binding to the inactive form [155] and Dock180/Elmo1, Homer3 and Rap1-GAP to the active form [152, 153, 163]. These proteins regulate multiple aspects of cytoskeletal reorganization. However, the exact role of $G\alpha_i$-GTP, its downstream effectors, and dynamic activity during cell migration hasn't been explored. Accumulating evidence suggests novel roles of $G\alpha_i$ in chemokine signaling, but full mechanistic details remain to be discovered.

4.2.2 Choosing the "right" method

In addition to understanding directed cell migration, these observations motivated us to explore novel, AC independent interactors of $G\alpha_i$ subtypes regardless of the receptor and cellular processes. The interactome can be identified; either by testing all pairwise combinations of proteins or by a co-complex approach. Both these methods are hypothesis-generating or discovery-based, and as no hypothesis is being tested, except that novel interactors of $G\alpha_i$ involved in cell migration may exist, and the outcome is unpredictable. Thus, these are sometimes referred to as "fishing expeditions". But these methods can provide opportunities to identify unexpected, novel, unexplored, unrelated mechanisms that relate to biology and diseases.

The overall goal of the study was to adopt an unbiased approach to identify novel effector(s) and functions of $G\alpha_{i.}$ We adopted a proximity-based labeling approach that consists of biotin proximity labeling followed by AP-MS, which can identify neighboring and directly interacting proteins. BioID2 or APEX based proximity labeling has not been utilized for G proteins previously. We chose BioID2, a promiscuous biotin ligase enzyme, for our $G\alpha_i$ screen as it is relatively widely used compared to the APEX based approach and doesn't require H_2O_2 for labeling. H_2O_2 is a signaling molecule in neutrophils [368] and sometimes can be toxic to the cells [369]. By the time we initiated the $G\alpha_q$ screen, TurboID was engineered using directed evolution which takes as little as 10 min to produce sufficient labelled material for identification by MS [294]. We, therefore, used TurboID for the subsequent $G\alpha_q$ screen. BioID2 and TurboID can biotinylate proteins that come within the vicinity (<20 nm) of $G\alpha_i$ and subsequent proteomic analysis has the potential to identify direct binding interactions. In addition, proteins that do not interact directly, but are part of the same multiprotein complex, interactome, can also be identified, which may be necessary for signaling complex formation.

4.2.3 Choosing the "right" system

An essential component behind the success of these methods is choosing the right system. An important factor is choosing the cells which endogenously express potential protein interactors or signaling components. For example, the novel role of $G\alpha_i$ was identified in HT1080 as well as neutrophils and neutrophil-like HL60 cells; and proximity labeling in those cells increases the chances of finding novel interactors relevant to the cell biology of those cells. Since HT1080 cells are relatively easy to transfect and genetically manipulate as compared to human neutrophils and HL60 cells, we performed the $G\alpha_i$ screen in HT1080 cells. Another factor is identifying the right controls to weed out the background labeling from *bona fide* interactors. There are approximately 2-4 million proteins per cubic micron in mammalian cells [267]. Comparing binary protein states, for example, active vs. inactive or stimulated vs. unstimulated samples, can aid in filtering out the proteins which were labeled only because of the abundance or colocalization at the PM and not true interactions. The switchable nature of the inactive and active states of G proteins provided an ideal system for applying this method to enrich proteins that are specifically regulated by these two states.

BioID2 requires a longer labeling period and, therefore, is known to be associated with higher background labeling. However, with both BioID2 (24 hr labeling) and TurboID (1 hr labeling) screen, we ended up with only ~100 proteins that passed the filtering criteria described in chapter 2. This is because we are comparing active and inactive forms of $G\alpha_i$, which allows selection of the proteins selectively enriched in the active form of $G\alpha_i$ and filtering out the proteins equally labeled in both the active and inactive samples. Proteins which are differentially enriched in the inactive form of $G\alpha_i$ might be equally interesting. A caveat is that proteins enriched by active

$G\alpha_i$ may not necessarily be direct interactors. If active and inactive G proteins localize to different microdomains at the PM, enrichment might solely be based on the proximity in that compartment. For example, $G\alpha_o$ is shown to translocate to the membrane rafts of the rat cerebellum after activation [370]. And therefore, a detailed characterization of potential novel interactions is required.

As an additional control, we used a PM targeted control, CaaX tagged BioID2 and TurboID. $G\alpha_i$ is myristoylated and palmitoylated, whereas $G\alpha_q$ is palmitoylated at multiple residues. In contrast, CaaX moiety gets farnesylated. It has been shown that type of lipid modification affects the localization of the proteins in the subdomains of the PM. For instance, it is postulated that dual saturated acylation, myristoylation and palmitoylation, allows $G\alpha_o$ translocation to the lipid rafts after activation. In contrast, prenylation, which contains unsaturated bonds, on $G\gamma$ excludes from the lipid rafts [146]. Therefore, the membrane-targeted control might be localized to a compartment different from the $G\alpha$ subunit at the PM and could complicate the results. As an alternative, the Lyn tag, which gets mono myristoylated and palmitoylated, could be fused with the biotin ligase to ensure it is in the same submembrane compartment as the $G\alpha$ subunit.

4.2.4 Functional classification of candidate interacting proteins identified by MS

PANTHER analysis of the proteins, sorted by criteria described in chapter 2, showed the classification of proteins in various functional groups (Fig. 4.1) [371]. Surprisingly, in addition to cell adhesion, cytoskeleton, and cell junction proteins, many nuclear proteins were identified and classified as gene-specific transcription regulators, nuclei acid metabolism proteins, etc. GPCRs and G proteins are known to be present in the nucleus, and changes in the transcriptome by nuclear-

localized GPCR activation has been investigated. However, knowledge of molecular details and physiological relevance is of nuclear receptor signaling is not understood [3, 372, 373]. Investigation of the roles of $G\alpha_i$ and $G\alpha_q$ in regulating nuclear proteins and perhaps transcription may unveil important biological processes.

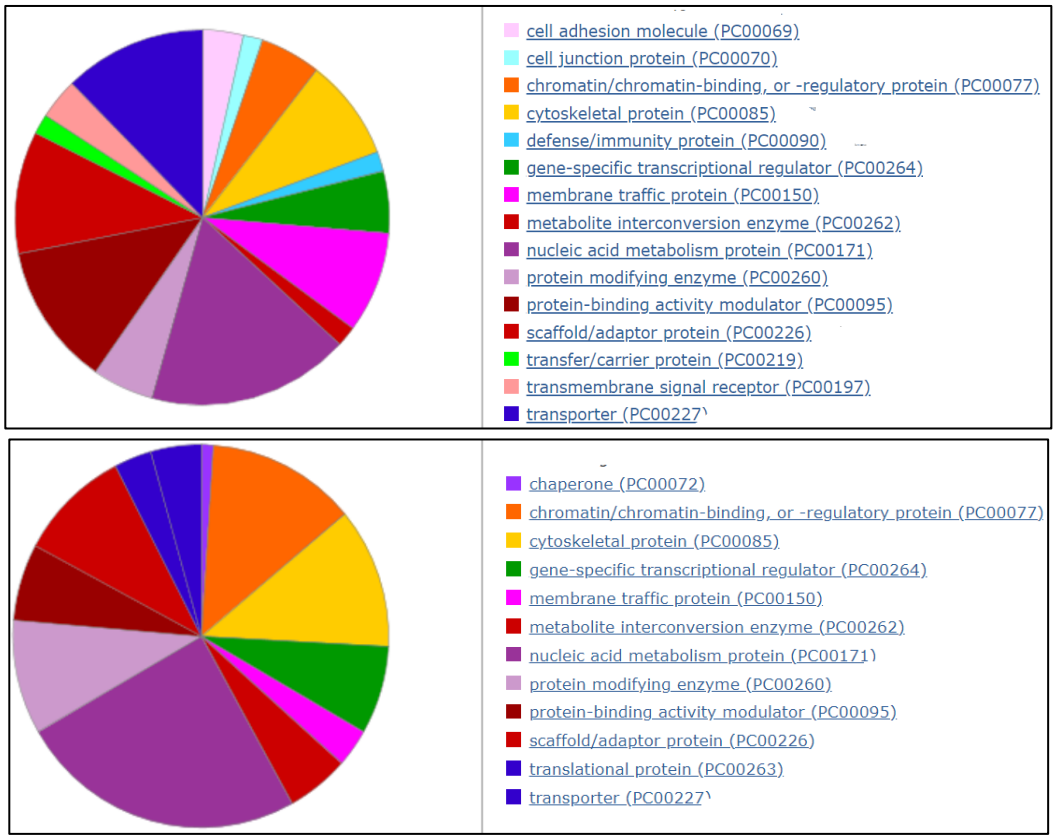

Figure 4.1: Pie chart showing the classification of 104 (top) and 141 (bottom) proteins in different protein classes from $G\alpha_{i1}$ and $G\alpha_q$ MS screen, respectively.
The graphs were generated using PANTHER [371].

4.2.5 Validation and characterization of PRG

Among the proteins we identified by MS, we have done partial characterization of RasGAP proteins and full functional interaction between PRG and active $G\alpha_{i1}$. The reasons we investigated PRG are manifold: 1) PRG was one of the four proteins enriched in BioID2-$G\alpha_{i1}$-Q204L with a P-value <0.001. 2) Both $G\alpha_{i1}$ and PRG are known to regulate immune and cancer cell migration

[161, 207]. Furthermore, perturbations of all three proteins, RhoA, PRG, and $G\alpha_{i1}$, have been shown to have the same phenotype; RhoA inhibition by C3 toxin in primary monocytes [374], PRG knockdown in Rat2 cells [206] and absence of active-$G\alpha_{i1}$ signaling in dHL60 cells showed cell elongation and tail retraction defect [161]. 3) $G\alpha_{i1}$ regulation of cell-deadhesion was shown to be dependent on Rho signaling, and inhibition of ROCK leads to reversal of the phenotype [161]. 4) PRG is one the most abundant, ubiquitously expressed RhoGEFs, but the G protein, which directly activates PRG downstream in neutrophils, hasn't been unambiguously identified. Therefore, we investigated the functional interaction between PRG and active $G\alpha_{i1}$ using multiple approaches.

Consistent with the MS data in HT1080 cells, we confirmed proximity between PRG and $G\alpha_{i1}$-QL using two methods; biotin labeling followed by streptavidin pulldown and a proximity ligation assay in A293 cells. Through SRE-luciferase reporter and Rhotekin pulldown assays, we showed for the first time that active-$G\alpha_{i1}$ activates PRG leading to RhoA activation. However, transfection of $G\beta\gamma$ in the assay didn't activate PRG (data not shown). The strong observed activation of PRG is surprising given that previous studies have indicated that $G\alpha_{12/13}$ regulates PRG. The previous study has shown that PRG forms a stable complex with both $G\alpha_{12}$ and $G\alpha_{13}$, and the RGS domain of PRG has been co-crystallized with $G\alpha_{13}$ [185]. Evidence in cell-based assays indirectly suggested that PRG is downstream of $G\alpha_{12/13}$ [187, 205]. Despite strong, $G\alpha_{12/13}$ didn't activate PRG *in vitro* assays under the assay conditions used or in in-cell co-transfection experiments [191, 362]. This indicates that additional factors likely exist in cell content-specific manner to regulate the activity of RhoGEF by $G\alpha_{12/13}$ [362], which remain to be discovered. For LARG, another member of the same RhoGEF family member, phosphorylation by a non-receptor tyrosine kinase, Tec, is required for its activation by $G\alpha_{12}$ [189]. A similar mechanism can likely

be in place for PRG activation by $G\alpha_{12/13}$. In this study, only $G\alpha_{i1}$-QL but not $G\alpha_q$, $G\alpha_{12}$, and $G\alpha_{13}$ activated PRG in an SRE-Luc assay under the assay conditions used, which is consistent with the previous findings. To rule out the need for $G\alpha_{12/13}$ in $G\alpha_{i1}$-QL mediated PRG activation, the SRE-Luc assay was performed in A293 cells with a $G_{12/13}$ null background where $G\alpha_{i1}$-QL was still able to activate PRG.

In the future, *in vitro* binding and GEF activation assays with full-length PRG and $G\alpha_{i1}$ would be required to comment about the direct interaction and activation of PRG by $G\alpha_{i1}$. A common method used to identify direct PPI includes *in vitro* purified protein pulldown. However, our preliminary tests to identify direct interaction between GST-PRG and myr-His-$G\alpha_{i1}$ proteins were unsuccessful (Data not shown). We, therefore, proposed that the interaction between $G\alpha_{i1}$-QL and PRG is transient or may require additional factors, such as proteins involved in post-translational modification. The advantage of the proximity labelling method is that it can label transient interactions and the biotin marks remain on the protein even after the interaction has ceased. Therefore, we were able to detect the hitherto unknown $G\alpha_{i1}$ effector, PRG, which was not detected by conventional immunoprecipitation-based methods.

In the future, other *in vitro* methods like Biolayer interferometry (BLI), Time-resolved Förster resonance energy transfer (TR-FRET) or bioluminescence resonance energy transfer (BRET) could be employed to investigate direct PPIs. BLI is a label free technology optical technique to measure macromolecular interactions by analyzing interference patterns of white light reflected from a biosensor chip. In addition to confirming a direct interaction, this method can provide on and off rates of the binding and thus affinity. TR FRET is a method where the energy transfer through the proximity of donor and acceptor fluorophores corresponds to the amount of binding. In FRET and BRET based studies, the assay

window is very small. As the binding is expected to be dependent on the nucleotide-bound stage of Gα subunits, comparing binding with GDP and GTPγS bound $G\alpha_i$ would serve as a perfect control. Assuming PRG binds to the same site as Gβγ on the $G\alpha_{i1}$ subunit, use of an excess of Gβγ would be another great control to ensure the specificity of the interaction. In addition, a conventional control, untagged/labelled-PRG, could be used to inhibit PRG-$G\alpha_{i1}$ interaction.

In addition, studies investigating direct activation of PRG by purified $G\alpha_i$ would be important to confirm the functional relevance of the binding studies. A kinetic FRET-based study is a widely used method to investigate the effect of a GEF on small GTPases using a MANT-fluorophore [375]. Activation of RhoA leads to an exchange of mant-GTP for GDP, and results increase FRET between tryptophan 58 (W58) on RhoA and mant-GTP. If $G\alpha_{i1}$ directly activates PRG, the addition of increasing concentrations of $G\alpha_{i1}$-GTPγS to this assay should result in a concentration-dependent increase in nucleotide exchange on RhoA. The $G\alpha_{i1}$-GTPγS loaded subunits can't bind mant-GTP, so any binding observed would be because of the binding to RhoA. Translocation of RhoGEFs to the PM where its substrate Rho is present is an important mechanism for regulating RhoGEF activity. However, the subcellular distribution of PRG varies depending on the cell type [198, 199, 207, 376]. Therefore, if the activation of PRG is not observed, the *in vitro* assay could be performed in the presence of phospholipid vesicles that would provide a membrane surface to bind both lipid modified $G\alpha_i$ and Rho. $G\alpha_i$-GTPγS-dependent recruitment of PRG to the membrane surface could be sufficient to activate membrane-bound Rho.

A co-crystal structure of rgRGS domain of PRG with $G\alpha_{13}$ has been solved, but not with full-length PRG. A co-crystal structure or cryo-EM structure of PRG bound to GTPγS-$G\alpha_{i1}$ would give a deeper insight into the details of the interaction.

4.2.6 Evolutionary conservation- G protein subtypes and differential regulation of PRG

To explore if activation of PRG extends to different families of Gα subunits, WT or QL versions $G\alpha_q$, $G\alpha_{12}$, $G\alpha_{13}$ as well as members of the $G\alpha_i$ family subunits $G\alpha_{oA}$, $G\alpha_{oB}$ and $G\alpha_z$ were tested, and only $G\alpha_{i1}$ showed strong activation. Out of three $G\alpha_i$ isoforms, $G\alpha i_1$, $G\alpha i_2$ and $G\alpha i_3$; we used $G\alpha_{i1}$ for all the experiments because $G\alpha_i$'s role in cell migration was first identified using the $G\alpha_{i1}$ isoform [160]. $G\alpha_{i1}$-QL has 88% and 94% amino acid sequence identity to $G\alpha_{i2}$ and $G\alpha_{i3}$, respectively [363, 364], and all three inhibit AC with similar potencies and to similar extents [323]. Given such a high degree of structural similarity, it is hypothesized that the cell uses all of them interchangeably. There is no direct evidence of selective activation of downstream effector (s). However, $G\alpha_{i1}$ is 98% identical among humans, rats, mice, and cows [165, 377]. This evolutionary conservation suggests that the differences between isoforms must be important to be conserved and argues against functional redundancy. We compared the ability of $G\alpha i_1$, $G\alpha i_2$ and $G\alpha i_3$ to activate PRG in the SRE-Luc assay. Surprisingly, $G\alpha_{i1}$-QL and $G\alpha_{i3}$-QL activated PRG, but $G\alpha_{i2}$-QL did not. $G\alpha_i$ isoforms have been known for almost three decades [363], but this is the first demonstration of selective activation of a downstream effector by a specific $G\alpha_i$ isoform.

Investigating the regions of $G\alpha_{i1}$ and $G\alpha_{i2}$, which confer effector specificity, is important to understand the mode of interaction and the mechanism of differential activation of PRG. Designing $G\alpha_{i1}/G\alpha_{i2}$ chimeras, followed by site-directed mutagenesis could elucidate the molecular basis of subtype specificity.

As for the Gi subfamily, no functional differences between different $G\alpha_q$ family members $G\alpha_q$, $G\alpha_{11}$, $G\alpha_{14}$, $G\alpha_{15/16}$ are identified yet. PBL-MS screen to identify isoform-specific interactors for Gαq subtypes would surely be a rewarding research direction to follow up.

4.2.7 Physiological relevance of PRG-Gα$_i$ interaction and agreement/disagreement with the previous reports

In neutrophil-like cells, dHL60s, activation of the formyl peptide receptor (FPR) by fMLF leads to Rho-dependent accumulation of phosphorylated-myosin light chain (P-MLC) at the trailing edge [266], and PRG has been shown to mediate this RhoA dependent response [207]. In our experiments, stimulation of primary human neutrophils with 10 nM fMLF promoted polarized P-MLC accumulation that was inhibited by PTX, confirming this phenotype to be dependent on Gα$_i$ signaling. Previous reports have shown in dHL60s, 100nM fMLF stimulation led to ~56% of cells showed asymmetric P-MLC accumulation, and PTX inhibited the response to ~38% [266]. In addition, fMLF has been shown to increase in RhoA-GTP, and PTX stimulation inhibited it by ~30% [266]. If we compare our data with this previously published data, it supports a model where at physiological concentrations of chemoattractant, activation of PRG/Rho is through Gα$_i$-GTP rather than Gα$_{13}$ in primary human neutrophils. Furthermore, PRG is known to regulate a gamut of biological processes, including neurite retraction through Rho-dependent signaling [198]. PRG regulates cell migration, and proliferation of mouse embryonic fibroblasts [366]. It is possible that Gα$_i$ signaling is also involved in these processes. In addition to chemokine receptors, these data has implications for the whole class of Gi-coupled GPCRs, which includes numerous receptors for neurotransmitters, including dopaminergic, serotonergic, α-adrenergic, muscarinic, GABA receptors, as well as opioid and cannabinoid receptors.

4.2.8 Validation and characterization of RasGAPs

Another set of PPIs we have begun to investigate is between the RasGAPs and active Gα$_{i1.}$ RASA3 has been shown to interact with Gα$_{i2}$ and Gα$_{i3}$ to mediate D2S-induced inactivation of

Ras-ERK1/2 pathway in neuroendocrine cells [171]. Ras GTPase activating protein RASA1, p120-GAP, is inhibited by FPR receptor activation in neutrophils by fMLF [162]. Ras proteins are a key the signaling hub and a major regulator of cell transformation, and RasGAPs are major regulators of Ras. Therefore, exploring the effect of different $G\alpha_{i1,2,3}$ isoforms on different members of the RasGAP family would increase our understanding of the complex regulation of Ras proteins. To determine the effect of $G\alpha_{i1}$ on RasGAP activity and test whether the effect of $G\alpha_{i}$ on RasGAP activity depends on RasGAP isoform, we decided to pursue different members of the RasGAP proteins. A preliminary co-immunoprecipitation study shows that $G\alpha_{i}$-QL binds to RASA1,2,3 and NF1. In future, *in vitro* activation studies using purified proteins would provide direct evidence of RasGAP regulation by $G\alpha_{i.}$

Buoyed by the successful identification and characterization of potential new targets of $G\alpha_{i}$, we extended this method to $G\alpha_{q}$ subtypes using TurboID. Currently, we are validating potential interactors identified by MS.

4.3 Final remarks

These studies have led to the discovery of potential novel interactors of $G\alpha_{i1}$ and $G\alpha_{q}$ that represent diverse classes of proteins not previously associated with Gi and Gq signaling. In addition to the identification and characterization of a few interaction partners, which would affect a wide range of biology and physiology, the MS data could be further utilized for validation and functional characterization of unexplored data by the scientific community. An essential component of understanding a biological system is to understand the network of possible PPIs that can ultimately lead to the identification of novel signaling pathways related to disease, identification of novel drug targets and, hopefully, better treatments for numerous human diseases.

Several avenues for investigation remain to understand better the dynamic interaction among proteins of a single protein interactome. Moreover, this method can be expanded to more complex analysis, comparing the role of individual protein interactome in normal biology and disease physiology to understand the perturbed signaling components and pathways (Fig. 4.2).

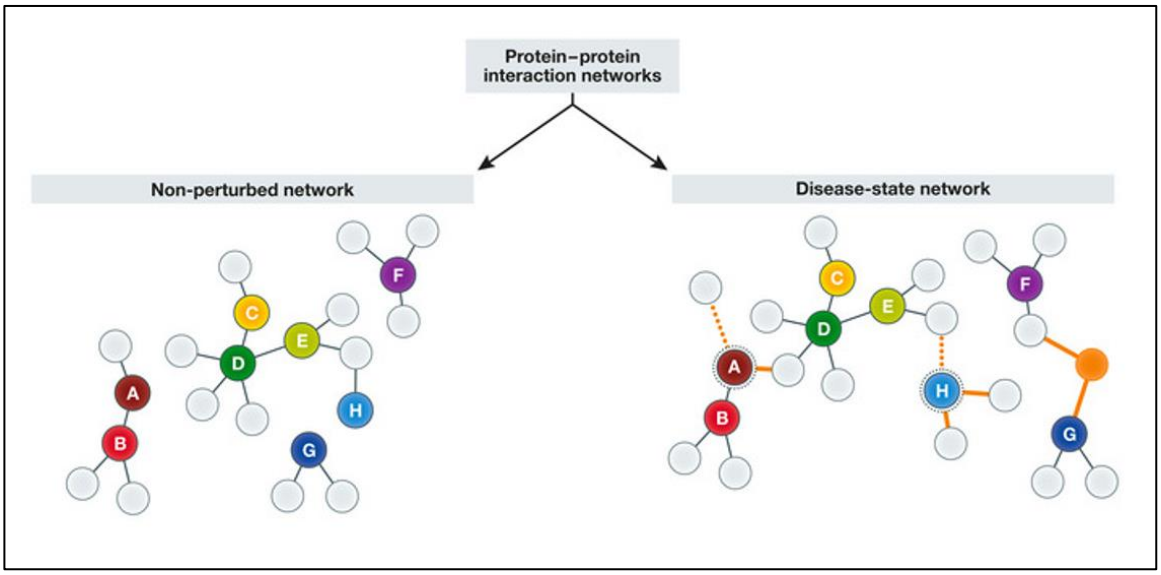

Figure 4.2: Schematic illustration of PPI network in normal physiology and disease.
Comparisons of those can help in the identification of aberrant changes and signaling pathways to devise novel therapeutic interventions. Adapted from [303].

References

1. Raymon, L.P., *Pharmacology and Mechanism of Action of Drugs*, in *Encyclopedia of Forensic Sciences (Second Edition)*, J.A. Siegel, P.J. Saukko, and M.M. Houck, Editors. 2013, Academic Press: Waltham. p. 210-217.
2. Sever, R. and C.K. Glass, *Signaling by nuclear receptors.* Cold Spring Harb Perspect Biol, 2013. **5**(3): p. a016709.
3. Jong, Y.I., S.K. Harmon, and K.L. O'Malley, *GPCR signalling from within the cell.* Br J Pharmacol, 2018. **175**(21): p. 4026-4035.
4. Eichel, K. and M. von Zastrow, *Subcellular Organization of GPCR Signaling.* Trends Pharmacol Sci, 2018. **39**(2): p. 200-208.
5. Alberts, B., *Molecular biology of the cell*. 2015.
6. Takeda, S., et al., *Identification of G protein-coupled receptor genes from the human genome sequence.* FEBS Lett, 2002. **520**(1-3): p. 97-101.
7. Sommer, M.E., et al., *The European Research Network on Signal Transduction (ERNEST): Toward a Multidimensional Holistic Understanding of G Protein-Coupled Receptor Signaling.* ACS Pharmacol Transl Sci, 2020. **3**(2): p. 361-370.
8. Schoneberg, T. and I. Liebscher, *Mutations in G Protein-Coupled Receptors: Mechanisms, Pathophysiology and Potential Therapeutic Approaches.* Pharmacol Rev, 2021. **73**(1): p. 89-119.
9. Hermans, E., *Biochemical and pharmacological control of the multiplicity of coupling at G-protein-coupled receptors.* Pharmacol Ther, 2003. **99**(1): p. 25-44.
10. Hauser, A.S., et al., *Trends in GPCR drug discovery: new agents, targets and indications.* Nat Rev Drug Discov, 2017. **16**(12): p. 829-842.
11. Fang, Y., T. Kenakin, and C. Liu, *Editorial: Orphan GPCRs As Emerging Drug Targets.* Front Pharmacol, 2015. **6**: p. 295.
12. Bar-Shavit, R., et al., *G Protein-Coupled Receptors in Cancer.* Int J Mol Sci, 2016. **17**(8).
13. Heng, B.C., D. Aubel, and M. Fussenegger, *An overview of the diverse roles of G-protein coupled receptors (GPCRs) in the pathophysiology of various human diseases.* Biotechnol Adv, 2013. **31**(8): p. 1676-94.
14. Haak, A.J., et al., *Targeting GPCR Signaling for Idiopathic Pulmonary Fibrosis Therapies.* Trends Pharmacol Sci, 2020. **41**(3): p. 172-182.
15. Rehman, A., et al., *Targeting of G-protein coupled receptors in sepsis.* Pharmacol Ther, 2020. **211**: p. 107529.
16. Alhosaini, K., et al., *GPCRs: The most promiscuous druggable receptor of the mankind.* Saudi Pharm J, 2021. **29**(6): p. 539-551.
17. Gacasan, S., D. Baker, and A. Parrill, *G protein-coupled receptors: The evolution of structural insight.* AIMS Biophysics, 2017. **4**: p. 491-527.
18. Fredriksson, R., et al., *The G-protein-coupled receptors in the human genome form five main families. Phylogenetic analysis, paralogon groups, and fingerprints.* Mol Pharmacol, 2003. **63**(6): p. 1256-72.

19. Leach, K., P.M. Sexton, and A. Christopoulos, *Allosteric GPCR modulators: taking advantage of permissive receptor pharmacology.* Trends Pharmacol Sci, 2007. **28**(8): p. 382-9.
20. Rajagopal, S. and S.K. Shenoy, *GPCR desensitization: Acute and prolonged phases.* Cell Signal, 2018. **41**: p. 9-16.
21. Lohse, M.J., et al., *Receptor-specific desensitization with purified proteins. Kinase dependence and receptor specificity of beta-arrestin and arrestin in the beta 2-adrenergic receptor and rhodopsin systems.* J Biol Chem, 1992. **267**(12): p. 8558-64.
22. Pitcher, J.A., N.J. Freedman, and R.J. Lefkowitz, *G protein-coupled receptor kinases.* Annu Rev Biochem, 1998. **67**: p. 653-92.
23. Lohse, M.J., et al., *beta-Arrestin: a protein that regulates beta-adrenergic receptor function.* Science, 1990. **248**(4962): p. 1547-50.
24. Goodman, O.B., Jr., et al., *Beta-arrestin acts as a clathrin adaptor in endocytosis of the beta2-adrenergic receptor.* Nature, 1996. **383**(6599): p. 447-50.
25. Gurevich, V.V., et al., *Arrestin interactions with G protein-coupled receptors. Direct binding studies of wild type and mutant arrestins with rhodopsin, beta 2-adrenergic, and m2 muscarinic cholinergic receptors.* J Biol Chem, 1995. **270**(2): p. 720-31.
26. Goodman, O.B., Jr., et al., *Role of arrestins in G-protein-coupled receptor endocytosis.* Adv Pharmacol, 1998. **42**: p. 429-33.
27. Lefkowitz, R.J., *G protein-coupled receptors. III. New roles for receptor kinases and beta-arrestins in receptor signaling and desensitization.* J Biol Chem, 1998. **273**(30): p. 18677-80.
28. Pitcher, J.A., et al., *The G-protein-coupled receptor phosphatase: a protein phosphatase type 2A with a distinct subcellular distribution and substrate specificity.* Proc Natl Acad Sci U S A, 1995. **92**(18): p. 8343-7.
29. Krueger, K.M., et al., *The role of sequestration in G protein-coupled receptor resensitization. Regulation of beta2-adrenergic receptor dephosphorylation by vesicular acidification.* J Biol Chem, 1997. **272**(1): p. 5-8.
30. Zhang, J., et al., *A central role for beta-arrestins and clathrin-coated vesicle-mediated endocytosis in beta2-adrenergic receptor resensitization. Differential regulation of receptor resensitization in two distinct cell types.* J Biol Chem, 1997. **272**(43): p. 27005-14.
31. Delom, F. and D. Fessart, *Role of Phosphorylation in the Control of Clathrin-Mediated Internalization of GPCR.* Int J Cell Biol, 2011. **2011**: p. 246954.
32. Krupnick, J.G. and J.L. Benovic, *The role of receptor kinases and arrestins in G protein-coupled receptor regulation.* Annu Rev Pharmacol Toxicol, 1998. **38**: p. 289-319.
33. Tsao, P. and M. von Zastrow, *Downregulation of G protein-coupled receptors.* Curr Opin Neurobiol, 2000. **10**(3): p. 365-9.
34. Collins, S., M.G. Caron, and R.J. Lefkowitz, *Regulation of adrenergic receptor responsiveness through modulation of receptor gene expression.* Annu Rev Physiol, 1991. **53**: p. 497-508.
35. Bouvier, M., et al., *Two distinct pathways for cAMP-mediated down-regulation of the beta 2-adrenergic receptor. Phosphorylation of the receptor and regulation of its mRNA level.* J Biol Chem, 1989. **264**(28): p. 16786-92.

36. Campbell, P.T., et al., *Mutations of the human beta 2-adrenergic receptor that impair coupling to Gs interfere with receptor down-regulation but not sequestration.* Mol Pharmacol, 1991. **39**(2): p. 192-8.
37. Strader, C.D., D.R. Sibley, and R.J. Lefkowitz, *Association of sequestered beta-adrenergic receptors with the plasma membrane: a novel mechanism for receptor down regulation.* Life Sci, 1984. **35**(15): p. 1601-10.
38. Wettschureck, N. and S. Offermanns, *Mammalian G proteins and their cell type specific functions.* Physiol Rev, 2005. **85**(4): p. 1159-204.
39. Amatruda, T.T., 3rd, et al., *The 35- and 36-kDa beta subunits of GTP-binding regulatory proteins are products of separate genes.* J Biol Chem, 1988. **263**(11): p. 5008-11.
40. Bourne, H.R., *GTPases: a family of molecular switches and clocks.* Philos Trans R Soc Lond B Biol Sci, 1995. **349**(1329): p. 283-9.
41. Downes, G.B. and N. Gautam, *The G protein subunit gene families.* Genomics, 1999. **62**(3): p. 544-52.
42. Gautam, N., et al., *G protein diversity is increased by associations with a variety of gamma subunits.* Proc Natl Acad Sci U S A, 1990. **87**(20): p. 7973-7.
43. Bourne, H.R., D.A. Sanders, and F. McCormick, *The GTPase superfamily: conserved structure and molecular mechanism.* Nature, 1991. **349**(6305): p. 117-27.
44. Gilman, A.G., *G proteins: transducers of receptor-generated signals.* Annu Rev Biochem, 1987. **56**: p. 615-49.
45. Oldham, W.M. and H.E. Hamm, *Heterotrimeric G protein activation by G-protein-coupled receptors.* Nat Rev Mol Cell Biol, 2008. **9**(1): p. 60-71.
46. Neubig, R.R., R.D. Gantzos, and W.J. Thomsen, *Mechanism of agonist and antagonist binding to alpha 2 adrenergic receptors: evidence for a precoupled receptor-guanine nucleotide protein complex.* Biochemistry, 1988. **27**(7): p. 2374-84.
47. Strange, P.G., *Signaling mechanisms of GPCR ligands.* Curr Opin Drug Discov Devel, 2008. **11**(2): p. 196-202.
48. Ross, E.M. and T.M. Wilkie, *GTPase-activating proteins for heterotrimeric G proteins: regulators of G protein signaling (RGS) and RGS-like proteins.* Annu Rev Biochem, 2000. **69**: p. 795-827.
49. Malbon, C.C., *G proteins in development.* Nat Rev Mol Cell Biol, 2005. **6**(9): p. 689-701.
50. Druey, K.M., et al., *Inhibition of G-protein-mediated MAP kinase activation by a new mammalian gene family.* Nature, 1996. **379**(6567): p. 742-6.
51. Watson, N., et al., *RGS family members: GTPase-activating proteins for heterotrimeric G-protein alpha-subunits.* Nature, 1996. **383**(6596): p. 172-5.
52. Dohlman, H.G. and J. Thorner, *RGS proteins and signaling by heterotrimeric G proteins.* J Biol Chem, 1997. **272**(7): p. 3871-4.
53. De Vries, L., et al., *The regulator of G protein signaling family.* Annu Rev Pharmacol Toxicol, 2000. **40**: p. 235-71.
54. Blumer, J.B., A.V. Smrcka, and S.M. Lanier, *Mechanistic pathways and biological roles for receptor-independent activators of G-protein signaling.* Pharmacol Ther, 2007. **113**(3): p. 488-506.
55. Cismowski, M.J., et al., *Genetic screens in yeast to identify mammalian nonreceptor modulators of G-protein signaling.* Nat Biotechnol, 1999. **17**(9): p. 878-83.
56. Takesono, A., et al., *Receptor-independent activators of heterotrimeric G-protein signaling pathways.* J Biol Chem, 1999. **274**(47): p. 33202-5.

57. Blumer, J.B., et al., *AGS proteins: receptor-independent activators of G-protein signaling.* Trends Pharmacol Sci, 2005. **26**(9): p. 470-6.
58. Blumer, J.B. and S.M. Lanier, *Activators of G-Protein Signaling (AGS)*, in *Encyclopedia of Signaling Molecules*, S. Choi, Editor. 2018, Springer International Publishing: Cham. p. 133-140.
59. Cismowski, M.J., et al., *Activation of heterotrimeric G-protein signaling by a ras-related protein. Implications for signal integration.* J Biol Chem, 2000. **275**(31): p. 23421-4.
60. Siderovski, D.P., M. Diverse-Pierluissi, and L. De Vries, *The GoLoco motif: a Galphai/o binding motif and potential guanine-nucleotide exchange factor.* Trends Biochem Sci, 1999. **24**(9): p. 340-1.
61. Bernard, M.L., et al., *Selective interaction of AGS3 with G-proteins and the influence of AGS3 on the activation state of G-proteins.* J Biol Chem, 2001. **276**(2): p. 1585-93.
62. Chan, P., et al., *Molecular chaperoning function of Ric-8 is to fold nascent heterotrimeric G protein alpha subunits.* Proc Natl Acad Sci U S A, 2013. **110**(10): p. 3794-9.
63. Gabay, M., et al., *Ric-8 proteins are molecular chaperones that direct nascent G protein alpha subunit membrane association.* Sci Signal, 2011. **4**(200): p. ra79.
64. Hinrichs, M.V., et al., *Ric-8: different cellular roles for a heterotrimeric G-protein GEF*. J Cell Biochem, 2012. **113**(9): p. 2797-805.
65. Tall, G.G., *Ric-8 regulation of heterotrimeric G proteins.* J Recept Signal Transduct Res, 2013. **33**(3): p. 139-43.
66. Mixon, M.B., et al., *Tertiary and quaternary structural changes in Gi alpha 1 induced by GTP hydrolysis.* Science, 1995. **270**(5238): p. 954-60.
67. Lambright, D.G., et al., *Structural determinants for activation of the alpha-subunit of a heterotrimeric G protein.* Nature, 1994. **369**(6482): p. 621-8.
68. Noel, J.P., H.E. Hamm, and P.B. Sigler, *The 2.2 A crystal structure of transducin-alpha complexed with GTP gamma S.* Nature, 1993. **366**(6456): p. 654-63.
69. Coleman, D.E., et al., *Structures of active conformations of Gi alpha 1 and the mechanism of GTP hydrolysis.* Science, 1994. **265**(5177): p. 1405-12.
70. Hamm, H.E. and A. Gilchrist, *Heterotrimeric G proteins.* Curr Opin Cell Biol, 1996. **8**(2): p. 189-96.
71. Bourne, H.R., *How receptors talk to trimeric G proteins.* Curr Opin Cell Biol, 1997. **9**(2): p. 134-42.
72. Wall, M.A., et al., *The structure of the G protein heterotrimer Gi alpha 1 beta 1 gamma 2.* Cell, 1995. **83**(6): p. 1047-58.
73. Smrcka, A.V., et al., *Regulation of polyphosphoinositide-specific phospholipase C activity by purified Gq.* Science, 1991. **251**(4995): p. 804-7.
74. Strathmann, M.P. and M.I. Simon, *G alpha 12 and G alpha 13 subunits define a fourth class of G protein alpha subunits.* Proc Natl Acad Sci U S A, 1991. **88**(13): p. 5582-6.
75. Fukuhara, S., H. Chikumi, and J.S. Gutkind, *RGS-containing RhoGEFs: the missing link between transforming G proteins and Rho?* Oncogene, 2001. **20**(13): p. 1661-8.
76. Dutt, P., N. Nguyen, and D. Toksoz, *Role of Lbc RhoGEF in Galpha12/13-induced signals to Rho GTPase.* Cell Signal, 2004. **16**(2): p. 201-9.
77. Meyer, B.H., et al., *Reversible translocation of p115-RhoGEF by G(12/13)-coupled receptors.* J Cell Biochem, 2008. **104**(5): p. 1660-70.

78. Diviani, D., J. Soderling, and J.D. Scott, *AKAP-Lbc anchors protein kinase A and nucleates Galpha 12-selective Rho-mediated stress fiber formation.* J Biol Chem, 2001. **276**(47): p. 44247-57.
79. Hepler, J.R. and A.G. Gilman, *G proteins.* Trends Biochem Sci, 1992. **17**(10): p. 383-7.
80. Siehler, S., *Regulation of RhoGEF proteins by G12/13-coupled receptors.* Br J Pharmacol, 2009. **158**(1): p. 41-9.
81. Kozasa, T., et al., *p115 RhoGEF, a GTPase activating protein for Galpha12 and Galpha13.* Science, 1998. **280**(5372): p. 2109-11.
82. Fredriksson, R. and H.B. Schioth, *The repertoire of G-protein-coupled receptors in fully sequenced genomes.* Mol Pharmacol, 2005. **67**(5): p. 1414-25.
83. Linder, M.E., et al., *Lipid modifications of G proteins: alpha subunits are palmitoylated.* Proc Natl Acad Sci U S A, 1993. **90**(8): p. 3675-9.
84. Kokame, K., et al., *Lipid modification at the N terminus of photoreceptor G-protein alpha-subunit.* Nature, 1992. **359**(6397): p. 749-52.
85. Neubert, T.A., et al., *The rod transducin alpha subunit amino terminus is heterogeneously fatty acylated.* J Biol Chem, 1992. **267**(26): p. 18274-7.
86. Wedegaertner, P.B., et al., *Palmitoylation is required for signaling functions and membrane attachment of Gq alpha and Gs alpha.* J Biol Chem, 1993. **268**(33): p. 25001-8.
87. Veit, M., et al., *The alpha-subunits of G-proteins G12 and G13 are palmitoylated, but not amidically myristoylated.* FEBS Lett, 1994. **339**(1-2): p. 160-4.
88. Gallego, C., et al., *Myristoylation of the G alpha i2 polypeptide, a G protein alpha subunit, is required for its signaling and transformation functions.* Proc Natl Acad Sci U S A, 1992. **89**(20): p. 9695-9.
89. Wilson, P.T. and H.R. Bourne, *Fatty acylation of alpha z. Effects of palmitoylation and myristoylation on alpha z signaling.* J Biol Chem, 1995. **270**(16): p. 9667-75.
90. Wedegaertner, P.B., *Lipid modifications and membrane targeting of G alpha.* Biol Signals Recept, 1998. **7**(2): p. 125-35.
91. Schmidt, C.J., et al., *Specificity of G protein beta and gamma subunit interactions.* J Biol Chem, 1992. **267**(20): p. 13807-10.
92. Sondek, J., et al., *Crystal structure of a G-protein beta gamma dimer at 2.1A resolution.* Nature, 1996. **379**(6563): p. 369-74.
93. Ray, K., et al., *Isolation of cDNA clones encoding eight different human G protein gamma subunits, including three novel forms designated the gamma 4, gamma 10, and gamma 11 subunits.* J Biol Chem, 1995. **270**(37): p. 21765-71.
94. Fletcher, J.E., et al., *The G protein beta5 subunit interacts selectively with the Gq alpha subunit.* J Biol Chem, 1998. **273**(1): p. 636-44.
95. Simon, M.I., M.P. Strathmann, and N. Gautam, *Diversity of G proteins in signal transduction.* Science, 1991. **252**(5007): p. 802-8.
96. von Weizsacker, E., M.P. Strathmann, and M.I. Simon, *Diversity among the beta subunits of heterotrimeric GTP-binding proteins: characterization of a novel beta-subunit cDNA.* Biochem Biophys Res Commun, 1992. **183**(1): p. 350-6.
97. Simon, M.I., M.P. Strathmann, and N. Gautam, *Diversity of G Proteins in Signal Transduction.* Science, 1991. **252**(5007): p. 802-808.
98. Neer, E.J., *Heterotrimeric G proteins: organizers of transmembrane signals.* Cell, 1995. **80**(2): p. 249-57.

99. Cabrera, J.L., et al., *Identification of the Gbeta5-RGS7 protein complex in the retina.* Biochem Biophys Res Commun, 1998. **249**(3): p. 898-902.
100. Makino, E.R., et al., *The GTPase activating factor for transducin in rod photoreceptors is the complex between RGS9 and type 5 G protein beta subunit.* Proc Natl Acad Sci U S A, 1999. **96**(5): p. 1947-52.
101. Smrcka, A.V., *G protein betagamma subunits: central mediators of G protein-coupled receptor signaling.* Cell Mol Life Sci, 2008. **65**(14): p. 2191-214.
102. Khan, S.M., et al., *The expanding roles of Gbetagamma subunits in G protein-coupled receptor signaling and drug action.* Pharmacol Rev, 2013. **65**(2): p. 545-77.
103. Clapham, D.E. and E.J. Neer, *G PROTEIN βγ SUBUNITS.* Annual Review of Pharmacology and Toxicology, 1997. **37**(1): p. 167-203.
104. Krapivinsky, G., et al., *G beta gamma binds directly to the G protein-gated K+ channel, IKACh.* J Biol Chem, 1995. **270**(49): p. 29059-62.
105. Wickman, K. and D.E. Clapham, *Ion channel regulation by G proteins.* Physiol Rev, 1995. **75**(4): p. 865-85.
106. Krapivinsky, G., et al., *Gbeta binding to GIRK4 subunit is critical for G protein-gated K+ channel activation.* J Biol Chem, 1998. **273**(27): p. 16946-52.
107. Zhang, F.L. and P.J. Casey, *Protein prenylation: molecular mechanisms and functional consequences.* Annu Rev Biochem, 1996. **65**: p. 241-69.
108. Ueda, N., et al., *G protein beta gamma subunits. Simplified purification and properties of novel isoforms.* J Biol Chem, 1994. **269**(6): p. 4388-95.
109. Iniguez-Lluhi, J.A., et al., *G protein beta gamma subunits synthesized in Sf9 cells. Functional characterization and the significance of prenylation of gamma.* J Biol Chem, 1992. **267**(32): p. 23409-17.
110. Mumby, S.M., et al., *G protein gamma subunits contain a 20-carbon isoprenoid.* Proc Natl Acad Sci U S A, 1990. **87**(15): p. 5873-7.
111. Myung, C.S., et al., *Role of isoprenoid lipids on the heterotrimeric G protein gamma subunit in determining effector activation.* J Biol Chem, 1999. **274**(23): p. 16595-603.
112. Higgins, J.B. and P.J. Casey, *In vitro processing of recombinant G protein gamma subunits. Requirements for assembly of an active beta gamma complex.* J Biol Chem, 1994. **269**(12): p. 9067-73.
113. Ikeda, S.R., *Voltage-dependent modulation of N-type calcium channels by G-protein beta gamma subunits.* Nature, 1996. **380**(6571): p. 255-8.
114. Welch, H.C., *Regulation and function of P-Rex family Rac-GEFs.* Small GTPases, 2015. **6**(2): p. 49-70.
115. Stephens, L., et al., *A novel phosphoinositide 3 kinase activity in myeloid-derived cells is activated by G protein beta gamma subunits.* Cell, 1994. **77**(1): p. 83-93.
116. Logothetis, D.E., et al., *The beta gamma subunits of GTP-binding proteins activate the muscarinic K+ channel in heart.* Nature, 1987. **325**(6102): p. 321-6.
117. Clapham, D.E. and E.J. Neer, *G protein beta gamma subunits.* Annu Rev Pharmacol Toxicol, 1997. **37**: p. 167-203.
118. Moss, J. and M. Vaughan, *ADP-ribosylation of guanyl nucleotide-binding regulatory proteins by bacterial toxins.* Adv Enzymol Relat Areas Mol Biol, 1988. **61**: p. 303-79.
119. Katada, T. and M. Ui, *ADP ribosylation of the specific membrane protein of C6 cells by islet-activating protein associated with modification of adenylate cyclase activity.* J Biol Chem, 1982. **257**(12): p. 7210-6.

120. Mangmool, S. and H. Kurose, *G(i/o) protein-dependent and -independent actions of Pertussis Toxin (PTX).* Toxins (Basel), 2011. **3**(7): p. 884-99.
121. Katada, T., *The inhibitory G protein G(i) identified as pertussis toxin-catalyzed ADP-ribosylation.* Biol Pharm Bull, 2012. **35**(12): p. 2103-11.
122. Sprang, S.R., *G PROTEIN MECHANISMS: Insights from Structural Analysis.* Annual Review of Biochemistry, 1997. **66**(1): p. 639-678.
123. Sternweis, P.C. and A.G. Gilman, *Aluminum: a requirement for activation of the regulatory component of adenylate cyclase by fluoride.* Proc Natl Acad Sci U S A, 1982. **79**(16): p. 4888-91.
124. Stadel, J.M. and S.T. Crooke, *Differential effects of fluoride on adenylate cyclase activity and guanine nucleotide regulation of agonist high-affinity receptor binding.* Biochem J, 1988. **254**(1): p. 15-20.
125. Raw, A.S., et al., *Structural and Biochemical Characterization of the GTPγS-, GDP·Pi-, and GDP-Bound Forms of a GTPase-Deficient Gly42 → Val Mutant of Giα1.* Biochemistry, 1997. **36**(50): p. 15660-15669.
126. Masters, S.B., et al., *Mutations in the GTP-binding site of GS alpha alter stimulation of adenylyl cyclase.* J Biol Chem, 1989. **264**(26): p. 15467-74.
127. Osawa, S., et al., *G alpha i-G alpha s chimeras define the function of alpha chain domains in control of G protein activation and beta gamma subunit complex interactions.* Cell, 1990. **63**(4): p. 697-706.
128. Bray, P., et al., *Human cDNA clones for four species of G alpha s signal transduction protein.* Proc Natl Acad Sci U S A, 1986. **83**(23): p. 8893-7.
129. Gilman, A.G., *G proteins and dual control of adenylate cyclase.* Cell, 1984. **36**(3): p. 577-9.
130. Sternweis, P.C., et al., *The regulatory component of adenylate cyclase. Purification and properties.* J Biol Chem, 1981. **256**(22): p. 11517-26.
131. Vallar, L., A. Spada, and G. Giannattasio, *Altered Gs and adenylate cyclase activity in human GH-secreting pituitary adenomas.* Nature, 1987. **330**(6148): p. 566-8.
132. Ross, E.M., et al., *Reconstitution of hormone-sensitive adenylate cyclase activity with resolved components of the enzyme.* J Biol Chem, 1978. **253**(18): p. 6401-12.
133. Pfeuffer, T., *GTP-binding proteins in membranes and the control of adenylate cyclase activity.* J Biol Chem, 1977. **252**(20): p. 7224-34.
134. Ahn, S., et al., *A dominant-negative inhibitor of CREB reveals that it is a general mediator of stimulus-dependent transcription of c-fos.* Mol Cell Biol, 1998. **18**(2): p. 967-77.
135. Kozasa, T., et al., *Isolation and characterization of the human Gs alpha gene.* Proc Natl Acad Sci U S A, 1988. **85**(7): p. 2081-5.
136. Mattera, R., et al., *Splice variants of the alpha subunit of the G protein Gs activate both adenylyl cyclase and calcium channels.* Science, 1989. **243**(4892): p. 804-7.
137. Sunahara, R.K., C.W. Dessauer, and A.G. Gilman, *Complexity and diversity of mammalian adenylyl cyclases.* Annu Rev Pharmacol Toxicol, 1996. **36**: p. 461-80.
138. Klemke, M., et al., *Characterization of the extra-large G protein alpha-subunit XLalphas. II. Signal transduction properties.* J Biol Chem, 2000. **275**(43): p. 33633-40.
139. Berridge, M.J., *Inositol trisphosphate and diacylglycerol: two interacting second messengers.* Annu Rev Biochem, 1987. **56**: p. 159-93.

140. Hazeki, O. and M. Ui, *Modification by islet-activating protein of receptor-mediated regulation of cyclic AMP accumulation in isolated rat heart cells.* J Biol Chem, 1981. **256**(6): p. 2856-62.
141. Katada, T., T. Amano, and M. Ui, *Modulation by islet-activating protein of adenylate cyclase activity in C6 glioma cells.* J Biol Chem, 1982. **257**(7): p. 3739-46.
142. Bokoch, G.M., et al., *Identification of the predominant substrate for ADP-ribosylation by islet activating protein.* J Biol Chem, 1983. **258**(4): p. 2072-5.
143. Bokoch, G.M., et al., *Purification and properties of the inhibitory guanine nucleotide-binding regulatory component of adenylate cyclase.* J Biol Chem, 1984. **259**(6): p. 3560-7.
144. Codina, J., et al., *Pertussis toxin substrate, the putative Ni component of adenylyl cyclases, is an alpha beta heterodimer regulated by guanine nucleotide and magnesium.* Proc Natl Acad Sci U S A, 1983. **80**(14): p. 4276-80.
145. Hildebrandt, J.D., et al., *Stimulation and inhibition of adenylyl cyclases mediated by distinct regulatory proteins.* Nature, 1983. **302**(5910): p. 706-9.
146. Blumer, J.B. and G.G. Tall, *G Protein α i/o/z*, in *Encyclopedia of Signaling Molecules*, S. Choi, Editor. 2018, Springer International Publishing: Cham. p. 1927-1940.
147. Solis, G.P., et al., *Golgi-Resident Galphao Promotes Protrusive Membrane Dynamics.* Cell, 2017. **170**(5): p. 939-955 e24.
148. Offermanns, S., *G-proteins as transducers in transmembrane signalling.* Prog Biophys Mol Biol, 2003. **83**(2): p. 101-30.
149. de Oliveira, P.G., et al., *Gi/o-Protein Coupled Receptors in the Aging Brain.* Front Aging Neurosci, 2019. **11**: p. 89.
150. Thelen, M., *Dancing to the tune of chemokines.* Nat Immunol, 2001. **2**(2): p. 129-34.
151. Kamakura, S., et al., *The cell polarity protein mInsc regulates neutrophil chemotaxis via a noncanonical G protein signaling pathway.* Dev Cell, 2013. **26**(3): p. 292-302.
152. Li, H., et al., *Association between Galphai2 and ELMO1/Dock180 connects chemokine signalling with Rac activation and metastasis.* Nat Commun, 2013. **4**: p. 1706.
153. Wu, J., et al., *Homer3 regulates the establishment of neutrophil polarity.* Mol Biol Cell, 2015. **26**(9): p. 1629-39.
154. Neptune, E.R., T. Iiri, and H.R. Bourne, *Galphai is not required for chemotaxis mediated by Gi-coupled receptors.* J Biol Chem, 1999. **274**(5): p. 2824-8.
155. Kamakura, S., et al., *The cell polarity protein mInsc regulates neutrophil chemotaxis via a noncanonical G protein signaling pathway.* Developmental cell, 2013. **26 3**: p. 292-302.
156. Wang, Y., H. Li, and F. Li, *ELMO2 association with Galphai2 regulates pancreatic cancer cell chemotaxis and metastasis.* PeerJ, 2020. **8**: p. e8910.
157. Kremer, K.N., A. Kumar, and K. Hedin, *J±i2 and ZAP-70 Mediate RasGRP1 Membrane Localization and Activation of SDF-1 Induced T Cell Functions.* The Journal of Immunology, 2011. **187**: p. 3177 - 3185.
158. Ma, Y.C., et al., *Src tyrosine kinase is a novel direct effector of G proteins.* Cell, 2000. **102**(5): p. 635-46.
159. Surve, C.R., D. Lehmann, and A.V. Smrcka, *A chemical biology approach demonstrates G protein betagamma subunits are sufficient to mediate directional neutrophil chemotaxis.* J Biol Chem, 2014. **289**(25): p. 17791-801.

160. Surve, C.R., et al., *Dynamic regulation of neutrophil polarity and migration by the heterotrimeric G protein subunits Galphai-GTP and Gbetagamma.* Sci Signal, 2016. **9**(416): p. ra22.
161. To, J.Y. and A.V. Smrcka, *Activated heterotrimeric G protein alphai subunits inhibit Rap-dependent cell adhesion and promote cell migration.* J Biol Chem, 2018. **293**(5): p. 1570-1578.
162. Nafisi, H., et al., *GAP1(IP4BP)/RASA3 mediates Galphai-induced inhibition of mitogen-activated protein kinase.* J Biol Chem, 2008. **283**(51): p. 35908-17.
163. Mochizuki, N., et al., *Activation of the ERK/MAPK pathway by an isoform of rap1GAP associated with G alpha(i).* Nature, 1999. **400**(6747): p. 891-4.
164. Kalogriopoulos, N.A., et al., *Receptor tyrosine kinases activate heterotrimeric G proteins via phosphorylation within the interdomain cleft of Galphai.* Proc Natl Acad Sci U S A, 2020. **117**(46): p. 28763-28774.
165. Lochrie, M.A. and M.I. Simon, *G protein multiplicity in eukaryotic signal transduction systems.* Biochemistry, 1988. **27**(14): p. 4957-65.
166. Cui, Z., et al., *Expression of a G protein subunit, alpha i-1, in Balb/c 3T3 cells leads to agonist-specific changes in growth regulation.* J Biol Chem, 1991. **266**(30): p. 20276-82.
167. Carty, D.J., et al., *Distinct guanine nucleotide binding and release properties of the three Gi proteins.* J Biol Chem, 1990. **265**(11): p. 6268-73.
168. Linder, M.E., et al., *Purification and characterization of Go alpha and three types of Gi alpha after expression in Escherichia coli.* J Biol Chem, 1990. **265**(14): p. 8243-51.
169. Kuwano, Y., et al., *Galphai2 and Galphai3 Differentially Regulate Arrest from Flow and Chemotaxis in Mouse Neutrophils.* J Immunol, 2016. **196**(9): p. 3828-33.
170. Laliberte, B., et al., *TNFAIP8: a new effector for Galpha(i) coupling to reduce cell death and induce cell transformation.* J Cell Physiol, 2010. **225**(3): p. 865-74.
171. Ghahremani, M.H., C. Forget, and P.R. Albert, *Distinct roles for Galpha(i)2 and Gbetagamma in signaling to DNA synthesis and Galpha(i)3 in cellular transformation by dopamine D2S receptor activation in BALB/c 3T3 cells.* Mol Cell Biol, 2000. **20**(5): p. 1497-506.
172. Whitehead, I.P., et al., *Dbl family proteins.* Biochim Biophys Acta, 1997. **1332**(1): p. F1-23.
173. Rossman, K.L., C.J. Der, and J. Sondek, *GEF means go: turning on RHO GTPases with guanine nucleotide-exchange factors.* Nat Rev Mol Cell Biol, 2005. **6**(2): p. 167-80.
174. Yamada, T., et al., *Physical and functional interactions of the lysophosphatidic acid receptors with PDZ domain-containing Rho guanine nucleotide exchange factors (RhoGEFs).* J Biol Chem, 2005. **280**(19): p. 19358-63.
175. Chikumi, H., et al., *Homo- and hetero-oligomerization of PDZ-RhoGEF, LARG and p115RhoGEF by their C-terminal region regulates their in vivo Rho GEF activity and transforming potential.* Oncogene, 2004. **23**(1): p. 233-40.
176. Hart, M.J., et al., *Direct stimulation of the guanine nucleotide exchange activity of p115 RhoGEF by Galpha13.* Science, 1998. **280**(5372): p. 2112-4.
177. Suzuki, N., N. Hajicek, and T. Kozasa, *Regulation and physiological functions of G12/13-mediated signaling pathways.* Neurosignals, 2009. **17**(1): p. 55-70.
178. Sternweis, P.C., et al., *Regulation of Rho guanine nucleotide exchange factors by G proteins.* Adv Protein Chem, 2007. **74**: p. 189-228.

179. Tanabe, S., et al., *Regulation of RGS-RhoGEFs by Galpha12 and Galpha13 proteins.* Methods Enzymol, 2004. **390**: p. 285-94.
180. Buhl, A.M., et al., *G alpha 12 and G alpha 13 stimulate Rho-dependent stress fiber formation and focal adhesion assembly.* J Biol Chem, 1995. **270**(42): p. 24631-4.
181. Strathmann, M. and M.I. Simon, *G protein diversity: a distinct class of alpha subunits is present in vertebrates and invertebrates.* Proc Natl Acad Sci U S A, 1990. **87**(23): p. 9113-7.
182. Dhanasekaran, N. and J.M. Dermott, *Signaling by the G12 class of G proteins.* Cell Signal, 1996. **8**(4): p. 235-45.
183. Mao, J., et al., *Guanine nucleotide exchange factor GEF115 specifically mediates activation of Rho and serum response factor by the G protein alpha subunit Galpha13.* Proc Natl Acad Sci U S A, 1998. **95**(22): p. 12973-6.
184. Chen, Z., et al., *Activation of p115-RhoGEF requires direct association of Galpha13 and the Dbl homology domain.* J Biol Chem, 2012. **287**(30): p. 25490-500.
185. Chen, Z., et al., *Recognition of the activated states of Galpha13 by the rgRGS domain of PDZRhoGEF.* Structure, 2008. **16**(10): p. 1532-43.
186. Wang, Q., et al., *Thrombin and lysophosphatidic acid receptors utilize distinct rhoGEFs in prostate cancer cells.* J Biol Chem, 2004. **279**(28): p. 28831-4.
187. Fukuhara, S., et al., *A novel PDZ domain containing guanine nucleotide exchange factor links heterotrimeric G proteins to Rho.* J Biol Chem, 1999. **274**(9): p. 5868-79.
188. Fukuhara, S., H. Chikumi, and J.S. Gutkind, *Leukemia-associated Rho guanine nucleotide exchange factor (LARG) links heterotrimeric G proteins of the G(12) family to Rho.* FEBS Lett, 2000. **485**(2-3): p. 183-8.
189. Suzuki, N., et al., *Galpha 12 activates Rho GTPase through tyrosine-phosphorylated leukemia-associated RhoGEF.* Proc Natl Acad Sci U S A, 2003. **100**(2): p. 733-8.
190. Yuan, J., L.W. Slice, and E. Rozengurt, *Activation of protein kinase D by signaling through Rho and the alpha subunit of the heterotrimeric G protein G13.* J Biol Chem, 2001. **276**(42): p. 38619-27.
191. Wells, C.D., et al., *Mechanisms for reversible regulation between G13 and Rho exchange factors.* J Biol Chem, 2002. **277**(2): p. 1174-81.
192. Hart, M.J., et al., *Identification of a novel guanine nucleotide exchange factor for the Rho GTPase.* J Biol Chem, 1996. **271**(41): p. 25452-8.
193. Fromm, C., et al., *The small GTP-binding protein Rho links G protein-coupled receptors and Galpha12 to the serum response element and to cellular transformation.* Proc Natl Acad Sci U S A, 1997. **94**(19): p. 10098-103.
194. Chen, Z., et al., *Structure of the p115RhoGEF rgRGS domain-Galpha13/i1 chimera complex suggests convergent evolution of a GTPase activator.* Nat Struct Mol Biol, 2005. **12**(2): p. 191-7.
195. Rumenapp, U., et al., *Rho-specific binding and guanine nucleotide exchange catalysis by KIAA0380, a dbl family member.* FEBS Lett, 1999. **459**(3): p. 313-8.
196. Longenecker, K.L., et al., *Structure of the RGS-like domain from PDZ-RhoGEF: linking heterotrimeric g protein-coupled signaling to Rho GTPases.* Structure, 2001. **9**(7): p. 559-69.
197. Zheng, M., et al., *On the mechanism of autoinhibition of the RhoA-specific nucleotide exchange factor PDZRhoGEF.* BMC Struct Biol, 2009. **9**: p. 36.

198. Togashi, H., et al., *Functions of a rho-specific guanine nucleotide exchange factor in neurite retraction. Possible role of a proline-rich motif of KIAA0380 in localization.* J Biol Chem, 2000. **275**(38): p. 29570-8.
199. Banerjee, J. and P.B. Wedegaertner, *Identification of a novel sequence in PDZ-RhoGEF that mediates interaction with the actin cytoskeleton.* Mol Biol Cell, 2004. **15**(4): p. 1760-75.
200. Perrot, V., J. Vazquez-Prado, and J.S. Gutkind, *Plexin B regulates Rho through the guanine nucleotide exchange factors leukemia-associated Rho GEF (LARG) and PDZ-RhoGEF.* J Biol Chem, 2002. **277**(45): p. 43115-20.
201. Pascoe, H.G., et al., *Secondary PDZ domain-binding site on class B plexins enhances the affinity for PDZ-RhoGEF.* Proc Natl Acad Sci U S A, 2015. **112**(48): p. 14852-7.
202. Lin, M.Y., et al., *PDZ-RhoGEF ubiquitination by Cullin3-KLHL20 controls neurotrophin-induced neurite outgrowth.* J Cell Biol, 2011. **193**(6): p. 985-94.
203. Swiercz, J.M., et al., *Plexin-B1 directly interacts with PDZ-RhoGEF/LARG to regulate RhoA and growth cone morphology.* Neuron, 2002. **35**(1): p. 51-63.
204. Chang, Y.J., et al., *The Rho-guanine nucleotide exchange factor PDZ-RhoGEF governs susceptibility to diet-induced obesity and type 2 diabetes.* Elife, 2015. **4**.
205. Jackson, M., et al., *Modulation of the neuronal glutamate transporter EAAT4 by two interacting proteins.* Nature, 2001. **410**(6824): p. 89-93.
206. Iwanicki, M.P., et al., *FAK, PDZ-RhoGEF and ROCKII cooperate to regulate adhesion movement and trailing-edge retraction in fibroblasts.* J Cell Sci, 2008. **121**(Pt 6): p. 895-905.
207. Wong, K., A. Van Keymeulen, and H.R. Bourne, *PDZRhoGEF and myosin II localize RhoA activity to the back of polarizing neutrophil-like cells.* J Cell Biol, 2007. **179**(6): p. 1141-8.
208. Longhurst, D.M., et al., *Interaction of PDZRhoGEF with microtubule-associated protein 1 light chains: link between microtubules, actin cytoskeleton, and neuronal polarity.* J Biol Chem, 2006. **281**(17): p. 12030-40.
209. Ding, Z., et al., *PDZ-RhoGEF Is a Signaling Effector for TROY-Induced Glioblastoma Cell Invasion and Survival.* Neoplasia, 2018. **20**(10): p. 1045-1058.
210. Castillo-Kauil, A., et al., *Galphas directly drives PDZ-RhoGEF signaling to Cdc42.* J Biol Chem, 2020. **295**(50): p. 16920-16928.
211. Jaffe, A.B. and A. Hall, *Rho GTPases: biochemistry and biology.* Annu Rev Cell Dev Biol, 2005. **21**: p. 247-69.
212. Aktories, K. and J. Frevert, *ADP-ribosylation of a 21-24 kDa eukaryotic protein(s) by C3, a novel botulinum ADP-ribosyltransferase, is regulated by guanine nucleotide.* Biochem J, 1987. **247**(2): p. 363-8.
213. Aktories, K., et al., *Botulinum ADP-ribosyltransferase C3. Purification of the enzyme and characterization of the ADP-ribosylation reaction in platelet membranes.* Eur J Biochem, 1988. **172**(2): p. 445-50.
214. Aktories, K., C. Wilde, and M. Vogelsgesang, *Rho-modifying C3-like ADP-ribosyltransferases.* Rev Physiol Biochem Pharmacol, 2004. **152**: p. 1-22.
215. Narumiya, S., T. Ishizaki, and N. Watanabe, *Rho effectors and reorganization of actin cytoskeleton.* FEBS Lett, 1997. **410**(1): p. 68-72.
216. Miralles, F., et al., *Actin dynamics control SRF activity by regulation of its coactivator MAL.* Cell, 2003. **113**(3): p. 329-42.

217. Dubash, A.D., et al., *A novel role for Lsc/p115 RhoGEF and LARG in regulating RhoA activity downstream of adhesion to fibronectin.* J Cell Sci, 2007. **120**(Pt 22): p. 3989-98.
218. Kimura, K., et al., *Regulation of myosin phosphatase by Rho and Rho-associated kinase (Rho-kinase).* Science, 1996. **273**(5272): p. 245-8.
219. Amano, M., et al., *Phosphorylation and activation of myosin by Rho-associated kinase (Rho-kinase).* J Biol Chem, 1996. **271**(34): p. 20246-9.
220. Goode, B.L. and M.J. Eck, *Mechanism and function of formins in the control of actin assembly.* Annu Rev Biochem, 2007. **76**: p. 593-627.
221. Narumiya, S., M. Tanji, and T. Ishizaki, *Rho signaling, ROCK and mDia1, in transformation, metastasis and invasion.* Cancer Metastasis Rev, 2009. **28**(1-2): p. 65-76.
222. Reiner, D.J. and E.A. Lundquist, *Small GTPases.* WormBook, 2018. **2018**: p. 1-65.
223. Ueda, T., et al., *Purification and characterization from bovine brain cytosol of a novel regulatory protein inhibiting the dissociation of GDP from and the subsequent binding of GTP to rhoB p20, a ras p21-like GTP-binding protein.* J Biol Chem, 1990. **265**(16): p. 9373-80.
224. Resat, H., et al., *The arginine finger of RasGAP helps Gln-61 align the nucleophilic water in GAP-stimulated hydrolysis of GTP.* Proc Natl Acad Sci U S A, 2001. **98**(11): p. 6033-8.
225. Boguski, M.S. and F. McCormick, *Proteins regulating Ras and its relatives.* Nature, 1993. **366**(6456): p. 643-54.
226. Van Aelst, L. and C. D'Souza-Schorey, *Rho GTPases and signaling networks.* Genes Dev, 1997. **11**(18): p. 2295-322.
227. Maertens, O. and K. Cichowski, *An expanding role for RAS GTPase activating proteins (RAS GAPs) in cancer.* Adv Biol Regul, 2014. **55**: p. 1-14.
228. Scheffzek, K. and G. Shivalingaiah, *Ras-Specific GTPase-Activating Proteins-Structures, Mechanisms, and Interactions.* Cold Spring Harb Perspect Med, 2019. **9**(3).
229. Harrell Stewart, D.R. and G.J. Clark, *Pumping the brakes on RAS - negative regulators and death effectors of RAS.* J Cell Sci, 2020. **133**(3).
230. Bellazzo, A. and L. Collavin, *Cutting the Brakes on Ras-Cytoplasmic GAPs as Targets of Inactivation in Cancer.* Cancers (Basel), 2020. **12**(10).
231. Trahey, M. and F. McCormick, *A cytoplasmic protein stimulates normal N-ras p21 GTPase, but does not affect oncogenic mutants.* Science, 1987. **238**(4826): p. 542-5.
232. Trahey, M., et al., *Molecular cloning of two types of GAP complementary DNA from human placenta.* Science, 1988. **242**(4886): p. 1697-700.
233. Vogel, U.S., et al., *Cloning of bovine GAP and its interaction with oncogenic ras p21.* Nature, 1988. **335**(6185): p. 90-3.
234. Marchuk, D.A., et al., *cDNA cloning of the type 1 neurofibromatosis gene: complete sequence of the NF1 gene product.* Genomics, 1991. **11**(4): p. 931-40.
235. Zhang, G., et al., *Structure of the adenylyl cyclase catalytic core.* Nature, 1997. **386**(6622): p. 247-53.
236. Tesmer, J.J., et al., *Crystal structure of the catalytic domains of adenylyl cyclase in a complex with Gsalpha.GTPgammaS.* Science, 1997. **278**(5345): p. 1907-16.
237. Smigel, M.D., *Purification of the catalyst of adenylate cyclase.* J Biol Chem, 1986. **261**(4): p. 1976-82.
238. Krupinski, J., et al., *Adenylyl cyclase amino acid sequence: possible channel- or transporter-like structure.* Science, 1989. **244**(4912): p. 1558-64.

239. Chen, Y., et al., *Soluble adenylyl cyclase as an evolutionarily conserved bicarbonate sensor.* Science, 2000. **289**(5479): p. 625-8.
240. Kamenetsky, M., et al., *Molecular details of cAMP generation in mammalian cells: a tale of two systems.* J Mol Biol, 2006. **362**(4): p. 623-39.
241. Premont, R.T., et al., *Identification and characterization of a widely expressed form of adenylyl cyclase.* J Biol Chem, 1996. **271**(23): p. 13900-7.
242. Gao, B.N. and A.G. Gilman, *Cloning and expression of a widely distributed (type IV) adenylyl cyclase.* Proc Natl Acad Sci U S A, 1991. **88**(22): p. 10178-82.
243. Houslay, M.D. and G. Milligan, *Tailoring cAMP-signalling responses through isoform multiplicity.* Trends Biochem Sci, 1997. **22**(6): p. 217-24.
244. Rodbell, M., *Signal transduction: evolution of an idea.* Environ Health Perspect, 1995. **103**(4): p. 338-45.
245. Taussig, R. and A.G. Gilman, *Mammalian membrane-bound adenylyl cyclases.* J Biol Chem, 1995. **270**(1): p. 1-4.
246. Gilman, A.G., *Nobel Lecture. G proteins and regulation of adenylyl cyclase.* Biosci Rep, 1995. **15**(2): p. 65-97.
247. Harwood, J.P., H. Low, and M. Rodbell, *Stimulatory and inhibitory effects of guanyl nucleotides on fat cell adenylate cyclase.* J Biol Chem, 1973. **248**(17): p. 6239-45.
248. Londos, C. and J. Wolff, *Two distinct adenosine-sensitive sites on adenylate cyclase.* Proc Natl Acad Sci U S A, 1977. **74**(12): p. 5482-6.
249. Tang, W.J. and A.G. Gilman, *Type-specific regulation of adenylyl cyclase by G protein beta gamma subunits.* Science, 1991. **254**(5037): p. 1500-3.
250. Smit, M.J. and R. Iyengar, *Mammalian adenylyl cyclases.* Adv Second Messenger Phosphoprotein Res, 1998. **32**: p. 1-21.
251. Simonds, W.F., *G protein regulation of adenylate cyclase.* Trends Pharmacol Sci, 1999. **20**(2): p. 66-73.
252. Cooper, D.M., N. Mons, and J.W. Karpen, *Adenylyl cyclases and the interaction between calcium and cAMP signalling.* Nature, 1995. **374**(6521): p. 421-4.
253. Mons, N., et al., *Ca2+-sensitive adenylyl cyclases, key integrators of cellular signalling.* Life Sci, 1998. **62**(17-18): p. 1647-52.
254. Defer, N., M. Best-Belpomme, and J. Hanoune, *Tissue specificity and physiological relevance of various isoforms of adenylyl cyclase.* Am J Physiol Renal Physiol, 2000. **279**(3): p. F400-16.
255. Nathan, C., *Neutrophils and immunity: challenges and opportunities.* Nature Reviews Immunology, 2006. **6**(3): p. 173-182.
256. Rabiet, M.J., E. Huet, and F. Boulay, *The N-formyl peptide receptors and the anaphylatoxin C5a receptors: an overview.* Biochimie, 2007. **89**(9): p. 1089-106.
257. Le, Y., et al., *Chemokines and chemokine receptors: their manifold roles in homeostasis and disease.* Cell Mol Immunol, 2004. **1**(2): p. 95-104.
258. Sun, L. and R.D. Ye, *Role of G protein-coupled receptors in inflammation.* Acta Pharmacol Sin, 2012. **33**(3): p. 342-50.
259. Migeotte, I., D. Communi, and M. Parmentier, *Formyl peptide receptors: a promiscuous subfamily of G protein-coupled receptors controlling immune responses.* Cytokine Growth Factor Rev, 2006. **17**(6): p. 501-19.

260. Ye, R.D., et al., *International Union of Basic and Clinical Pharmacology. LXXIII. Nomenclature for the formyl peptide receptor (FPR) family.* Pharmacol Rev, 2009. **61**(2): p. 119-61.
261. Bao, L., et al., *Mapping of genes for the human C5a receptor (C5AR), human FMLP receptor (FPR), and two FMLP receptor homologue orphan receptors (FPRH1, FPRH2) to chromosome 19.* Genomics, 1992. **13**(2): p. 437-40.
262. He, H.Q., et al., *Structural determinants for the interaction of formyl peptide receptor 2 with peptide ligands.* J Biol Chem, 2014. **289**(4): p. 2295-306.
263. Dorward, D.A., et al., *The role of formylated peptides and formyl peptide receptor 1 in governing neutrophil function during acute inflammation.* Am J Pathol, 2015. **185**(5): p. 1172-84.
264. Devosse, T., et al., *Formyl peptide receptor-like 2 is expressed and functional in plasmacytoid dendritic cells, tissue-specific macrophage subpopulations, and eosinophils.* J Immunol, 2009. **182**(8): p. 4974-84.
265. Wen, X., et al., *G-protein-coupled formyl peptide receptors play a dual role in neutrophil chemotaxis and bacterial phagocytosis.* Mol Biol Cell, 2019. **30**(3): p. 346-356.
266. Xu, J., et al., *Divergent signals and cytoskeletal assemblies regulate self-organizing polarity in neutrophils.* Cell, 2003. **114**(2): p. 201-14.
267. Milo, R., *What is the total number of protein molecules per cell volume? A call to rethink some published values.* Bioessays, 2013. **35**(12): p. 1050-5.
268. Ngounou Wetie, A.G., et al., *Proteomics and Non-proteomics Approaches to Study Stable and Transient Protein-Protein Interactions.* Adv Exp Med Biol, 2019. **1140**: p. 121-142.
269. Wang, E.T., et al., *Alternative isoform regulation in human tissue transcriptomes.* Nature, 2008. **456**(7221): p. 470-6.
270. Pan, Q., et al., *Deep surveying of alternative splicing complexity in the human transcriptome by high-throughput sequencing.* Nat Genet, 2008. **40**(12): p. 1413-5.
271. Cusick, M.E., et al., *Interactome: gateway into systems biology.* Hum Mol Genet, 2005. **14 Spec No. 2**: p. R171-81.
272. De Las Rivas, J. and C. Fontanillo, *Protein-protein interactions essentials: key concepts to building and analyzing interactome networks.* PLoS Comput Biol, 2010. **6**(6): p. e1000807.
273. Liddington, R.C., *Structural basis of protein-protein interactions.* Methods Mol Biol, 2015. **1278**: p. 3-22.
274. Droit, A., G.G. Poirier, and J.M. Hunter, *Experimental and bioinformatic approaches for interrogating protein-protein interactions to determine protein function.* J Mol Endocrinol, 2005. **34**(2): p. 263-80.
275. Galperin, M.Y. and E.V. Koonin, *Who's your neighbor? New computational approaches for functional genomics.* Nat Biotechnol, 2000. **18**(6): p. 609-13.
276. De Las Rivas, J. and C. Fontanillo, *Protein-protein interaction networks: unraveling the wiring of molecular machines within the cell.* Brief Funct Genomics, 2012. **11**(6): p. 489-96.
277. Snider, J., et al., *Fundamentals of protein interaction network mapping.* Mol Syst Biol, 2015. **11**(12): p. 848.
278. Fields, S. and O. Song, *A novel genetic system to detect protein-protein interactions.* Nature, 1989. **340**(6230): p. 245-6.
279. Wagemans, J. and R. Lavigne, *Identification of protein-protein interactions by standard gal4p-based yeast two-hybrid screening.* Methods Mol Biol, 2015. **1278**: p. 409-31.

280. Koegl, M. and P. Uetz, *Improving yeast two-hybrid screening systems.* Brief Funct Genomic Proteomic, 2007. **6**(4): p. 302-12.
281. von Mering, C., et al., *Comparative assessment of large-scale data sets of protein-protein interactions.* Nature, 2002. **417**(6887): p. 399-403.
282. Huang, H., B.M. Jedynak, and J.S. Bader, *Where have all the interactions gone? Estimating the coverage of two-hybrid protein interaction maps.* PLoS Comput Biol, 2007. **3**(11): p. e214.
283. Saraon, P., et al., *Detecting Membrane Protein-protein Interactions Using the Mammalian Membrane Two-hybrid (MaMTH) Assay.* Curr Protoc Chem Biol, 2017. **9**(1): p. 38-54.
284. Snider, J., et al., *Detecting interactions with membrane proteins using a membrane two-hybrid assay in yeast.* Nat Protoc, 2010. **5**(7): p. 1281-93.
285. Stagljar, I., et al., *A genetic system based on split-ubiquitin for the analysis of interactions between membrane proteins in vivo.* Proc Natl Acad Sci U S A, 1998. **95**(9): p. 5187-92.
286. *Genetics of Breast and Gynecologic Cancers (PDQ®)—Health Professional Version - National Cancer Institute.* https://www.cancer.gov/types/breast/hp/breast-ovarian-genetics-pdq#link/_113_toc, 2017.
287. Sokolina, K., et al., *Systematic protein-protein interaction mapping for clinically relevant human GPCRs.* Mol Syst Biol, 2017. **13**(3): p. 918.
288. Bontinck, M., et al., *Recent Trends in Plant Protein Complex Analysis in a Developmental Context.* Front Plant Sci, 2018. **9**: p. 640.
289. Gingras, A.C., K.T. Abe, and B. Raught, *Getting to know the neighborhood: using proximity-dependent biotinylation to characterize protein complexes and map organelles.* Curr Opin Chem Biol, 2019. **48**: p. 44-54.
290. Chapman-Smith, A. and J.E. Cronan, Jr., *Molecular biology of biotin attachment to proteins.* J Nutr, 1999. **129**(2S Suppl): p. 477S-484S.
291. Choi-Rhee, E., H. Schulman, and J.E. Cronan, *Promiscuous protein biotinylation by Escherichia coli biotin protein ligase.* Protein Sci, 2004. **13**(11): p. 3043-50.
292. Roux, K.J., *Marked by association: techniques for proximity-dependent labeling of proteins in eukaryotic cells.* Cell Mol Life Sci, 2013. **70**(19): p. 3657-64.
293. Kim, D.I., et al., *An improved smaller biotin ligase for BioID proximity labeling.* Mol Biol Cell, 2016. **27**(8): p. 1188-96.
294. Branon, T.C., et al., *Efficient proximity labeling in living cells and organisms with TurboID.* Nat Biotechnol, 2018. **36**(9): p. 880-887.
295. Minamihata, K., M. Goto, and N. Kamiya, *Protein heteroconjugation by the peroxidase-catalyzed tyrosine coupling reaction.* Bioconjug Chem, 2011. **22**(11): p. 2332-8.
296. Martell, J.D., et al., *Engineered ascorbate peroxidase as a genetically encoded reporter for electron microscopy.* Nat Biotechnol, 2012. **30**(11): p. 1143-8.
297. Rees, J.S., et al., *Protein Neighbors and Proximity Proteomics.* Mol Cell Proteomics, 2015. **14**(11): p. 2848-56.
298. Lambert, J.P., et al., *Proximity biotinylation and affinity purification are complementary approaches for the interactome mapping of chromatin-associated protein complexes.* J Proteomics, 2015. **118**: p. 81-94.
299. Loh, K.H., et al., *Proteomic Analysis of Unbounded Cellular Compartments: Synaptic Clefts.* Cell, 2016. **166**(5): p. 1295-1307 e21.

300. Wilkins, M.R., et al., *Progress with proteome projects: why all proteins expressed by a genome should be identified and how to do it.* Biotechnol Genet Eng Rev, 1996. **13**: p. 19-50.
301. Shevchenko, A., et al., *Mass spectrometric sequencing of proteins silver-stained polyacrylamide gels.* Anal Chem, 1996. **68**(5): p. 850-8.
302. Rosenfeld, J., et al., *In-gel digestion of proteins for internal sequence analysis after one- or two-dimensional gel electrophoresis.* Anal Biochem, 1992. **203**(1): p. 173-9.
303. Richards, A.L., M. Eckhardt, and N.J. Krogan, *Mass spectrometry-based protein-protein interaction networks for the study of human diseases.* Mol Syst Biol, 2021. **17**(1): p. e8792.
304. Washburn, M.P., D. Wolters, and J.R. Yates, 3rd, *Large-scale analysis of the yeast proteome by multidimensional protein identification technology.* Nat Biotechnol, 2001. **19**(3): p. 242-7.
305. Yates Iii, J.R., *A century of mass spectrometry: from atoms to proteomes.* Nature Methods, 2011. **8**(8): p. 633-637.
306. Karas, M. and F. Hillenkamp, *Laser desorption ionization of proteins with molecular masses exceeding 10,000 daltons.* Anal Chem, 1988. **60**(20): p. 2299-301.
307. Fenn, J.B., et al., *Electrospray ionization for mass spectrometry of large biomolecules.* Science, 1989. **246**(4926): p. 64-71.
308. Sokolowska, I., et al., *Applications of Mass Spectrometry in Proteomics.* Australian Journal of Chemistry, 2013. **66**.
309. Miller, P.E. and M.B. Denton, *The quadrupole mass filter: Basic operating concepts.* Journal of Chemical Education, 1986. **63**(7): p. 617.
310. Graves, P.R. and T.A. Haystead, *Molecular biologist's guide to proteomics.* Microbiol Mol Biol Rev, 2002. **66**(1): p. 39-63; table of contents.
311. Liu, H., R.G. Sadygov, and J.R. Yates, 3rd, *A model for random sampling and estimation of relative protein abundance in shotgun proteomics.* Anal Chem, 2004. **76**(14): p. 4193-201.
312. Petyuk, V.A., et al., *Elimination of systematic mass measurement errors in liquid chromatography-mass spectrometry based proteomics using regression models and a priori partial knowledge of the sample content.* Anal Chem, 2008. **80**(3): p. 693-706.
313. Strittmatter, E.F., et al., *Proteome analyses using accurate mass and elution time peptide tags with capillary LC time-of-flight mass spectrometry.* J Am Soc Mass Spectrom, 2003. **14**(9): p. 980-91.
314. Pagala, V.R., et al., *Quantitative protein analysis by mass spectrometry.* Methods Mol Biol, 2015. **1278**: p. 281-305.
315. Shiio, Y. and R. Aebersold, *Quantitative proteome analysis using isotope-coded affinity tags and mass spectrometry.* Nat Protoc, 2006. **1**(1): p. 139-45.
316. Wiese, S., et al., *Protein labeling by iTRAQ: a new tool for quantitative mass spectrometry in proteome research.* Proteomics, 2007. **7**(3): p. 340-50.
317. Ong, S.E. and M. Mann, *Stable isotope labeling by amino acids in cell culture for quantitative proteomics.* Methods Mol Biol, 2007. **359**: p. 37-52.
318. Chandan, N.R., et al., *Identification of G Protein α_i Signaling Partners by Proximity Labeling Reveals a Network of Interactions that Includes PDZ-RhoGEF*. bioRxiv, 2021: p. 2021.07.15.452545.
319. Hepler, J.R. and A.G. Gilman, *G proteins.* Trends Biochem.Sci., 1992. **17**: p. 383-387.

320. Gilman, A.G., *G proteins: transducers of receptor-generated signals.* Annu Rev Biochem, 1987. **56**: p. 615-649.
321. Oldham, W.M. and E. Hamm, *Structural basis of function in heterotrimeric G proteins.* Quarterly Reviews of Biophysics, 2006. **39**(02): p. 117-166.
322. Smrcka, A.V., *G protein βγ subunits: Central mediators of G protein-coupled receptor signaling*, in *Cell. Mol. Life Sci.* 2008. p. 2191-2214.
323. Taussig, R., J.A. Iniguez-Lluhi, and A.G. Gilman, *Inhibition of adenylyl cyclase by Gi alpha.* Science, 1993. **261**(5118): p. 218-21.
324. Murphy, P.M., *The molecular biology of leukocyte chemoattractant receptors.* Annu Rev Immunol, 1994. **12**: p. 593-633.
325. Bendall, L., *Chemokines and their receptors in disease.* Histol Histopathol, 2005. **20**(3): p. 907-26.
326. Smrcka, A.V. and I. Fisher, *G-protein betagamma subunits as multi-functional scaffolds and transducers in G-protein-coupled receptor signaling.* Cell Mol Life Sci, 2019. **76**(22): p. 4447-4459.
327. Pace, A.M., Y.H. Wong, and H.R. Bourne, *A mutant alpha subunit of Gi2 induces neoplastic transformation of Rat-1 cells.* Proc Natl Acad Sci U S A, 1991. **88**(16): p. 7031-5.
328. Hermouet, S., et al., *Activating and inactivating mutations of the alpha subunit of Gi2 protein have opposite effects on proliferation of NIH 3T3 cells.* Proc Natl Acad Sci U S A, 1991. **88**(23): p. 10455-9.
329. Tall, G.G., A.M. Krumins, and A.G. Gilman, *Mammalian Ric-8A (synembryn) is a heterotrimeric Galpha protein guanine nucleotide exchange factor.* J Biol Chem, 2003. **278**(10): p. 8356-62.
330. Solis, G.P., et al., *Golgi-Resident Galphao Promotes Protrusive Membrane Dynamics.* Cell, 2017. **170**(6): p. 1258.
331. Roux, K.J., et al., *A promiscuous biotin ligase fusion protein identifies proximal and interacting proteins in mammalian cells.* J Cell Biol, 2012. **196**(6): p. 801-10.
332. Lutz, S., et al., *The guanine nucleotide exchange factor p63RhoGEF, a specific link between Gq/11-coupled receptor signaling and RhoA.* J Biol Chem, 2005. **280**(12): p. 11134-9.
333. Rojas, R.J., et al., *Galphaq directly activates p63RhoGEF and Trio via a conserved extension of the Dbl homology-associated pleckstrin homology domain.* J Biol Chem, 2007. **282**(40): p. 29201-10.
334. Lutz, S., et al., *Structure of Galphaq-p63RhoGEF-RhoA complex reveals a pathway for the activation of RhoA by GPCRs.* Science, 2007. **318**(5858): p. 1923-7.
335. Golebiewska, U. and S. Scarlata, *Galphaq binds two effectors separately in cells: evidence for predetermined signaling pathways.* Biophys J, 2008. **95**(5): p. 2575-82.
336. Yeh, H.W., et al., *PSPC1 mediates TGF-beta1 autocrine signalling and Smad2/3 target switching to promote EMT, stemness and metastasis.* Nat Cell Biol, 2018. **20**(4): p. 479-491.
337. Rosonina, E., et al., *Role for PSF in mediating transcriptional activator-dependent stimulation of pre-mRNA processing in vivo.* Mol Cell Biol, 2005. **25**(15): p. 6734-46.
338. Chen, X., J. Shen, and R. Prywes, *The luminal domain of ATF6 senses endoplasmic reticulum (ER) stress and causes translocation of ATF6 from the ER to the Golgi.* J Biol Chem, 2002. **277**(15): p. 13045-52.

339. Zhang, Q., et al., *Impaired Dendritic Development and Memory in Sorbs2 Knock-Out Mice.* J Neurosci, 2016. **36**(7): p. 2247-60.
340. Mumby, S.M. and A.G. Gilman, *[19] Synthetic peptide antisera with determined specificity for G protein α or β subunits*, in *Methods in Enzymology*. 1991, Academic Press. p. 215-233.
341. Hesketh, G.G., et al., *Parallel Exploration of Interaction Space by BioID and Affinity Purification Coupled to Mass Spectrometry.* Methods Mol Biol, 2017. **1550**: p. 115-136.
342. McAlister, G.C., et al., *MultiNotch MS3 enables accurate, sensitive, and multiplexed detection of differential expression across cancer cell line proteomes.* Anal Chem, 2014. **86**(14): p. 7150-8.
343. Perez-Riverol, Y., et al., *The PRIDE database and related tools and resources in 2019: improving support for quantification data.* Nucleic Acids Res, 2019. **47**(D1): p. D442-D450.
344. Gibson, S.K. and A.G. Gilman, *Gialpha and Gbeta subunits both define selectivity of G protein activation by alpha2-adrenergic receptors.* Proc Natl Acad Sci U S A, 2006. **103**(1): p. 212-7.
345. Coleman, D.E., et al., *Crystallization and preliminary crystallographic studies of Gi alpha 1 and mutants of Gi alpha 1 in the GTP and GDP-bound states.* J Mol Biol, 1994. **238**(4): p. 630-4.
346. Ahmed, S.M., et al., *G protein betagamma subunits regulate cell adhesion through Rap1a and its effector Radil.* J Biol Chem, 2010. **285**(9): p. 6538-51.
347. Chen, L.T., A.G. Gilman, and T. Kozasa, *A candidate target for G protein action in brain.* J Biol Chem, 1999. **274**(38): p. 26931-8.
348. Huang da, W., B.T. Sherman, and R.A. Lempicki, *Systematic and integrative analysis of large gene lists using DAVID bioinformatics resources.* Nat Protoc, 2009. **4**(1): p. 44-57.
349. Huang, C., et al., *Persistent membrane association of activated and depalmitoylated G protein α subunits.* Proceedings of the National Academy of Sciences, 1999. **96**: p. 412-417.
350. Le-Niculescu, H., et al., *Identification and characterization of GIV, a novel Galpha i/s-interacting protein found on COPI, endoplasmic reticulum-Golgi transport vesicles.* J Biol Chem, 2005. **280**(23): p. 22012-20.
351. Navarro, G., et al., *Evidence for functional pre-coupled complexes of receptor heteromers and adenylyl cyclase.* (2041-1723 (Electronic)).
352. Ferré, S., *The GPCR heterotetramer: challenging classical pharmacology.* (1873-3735 (Electronic)).
353. Rebois, R.V., et al., *Heterotrimeric G proteins form stable complexes with adenylyl cyclase and Kir3.1 channels in living cells.* (0021-9533 (Print)).
354. Smrcka, A.V., *Molecular targeting of Galpha and Gbetagamma subunits: a potential approach for cancer therapeutics.* Trends Pharmacol Sci, 2013. **34**(5): p. 290-8.
355. Drugan, J.K., et al., *The Ras/p120 GTPase-activating protein (GAP) interaction is regulated by the p120 GAP pleckstrin homology domain.* J Biol Chem, 2000. **275**(45): p. 35021-7.
356. Guo, F., et al., *An in vitro recombination method to convert restriction- and ligation-independent expression vectors.* Biotechnol J, 2008. **3**(3): p. 370-7.
357. Cash, J.N., et al., *Discovery of Small Molecules That Target the Phosphatidylinositol (3,4,5) Trisphosphate (PIP3)-Dependent Rac Exchanger 1 (P-Rex1) PIP3-Binding Site*

and Inhibit P-Rex1-Dependent Functions in Neutrophils. Mol Pharmacol, 2020. **97**(3): p. 226-236.
358. Hill, C.S., J. Wynne, and R. Treisman, *The Rho family GTPases RhoA, Rac1, and CDC42Hs regulate transcriptional activation by SRF*. Cell, 1995. **81**(7): p. 1159-70.
359. Pertz, O., et al., *Spatiotemporal dynamics of RhoA activity in migrating cells.* Nature, 2006. **440**(7087): p. 1069-72.
360. Etienne-Manneville, S. and A. Hall, *Rho GTPases in cell biology*. Nature, 2002. **420**(6916): p. 629-35.
361. Struckhoff, A.P., et al., *PDZ-RhoGEF is essential for CXCR4-driven breast tumor cell motility through spatial regulation of RhoA.* J Cell Sci, 2013. **126**(Pt 19): p. 4514-26.
362. Carter, A.M., S. Gutowski, and P.C. Sternweis, *Regulated localization is sufficient for hormonal control of regulator of G protein signaling homology Rho guanine nucleotide exchange factors (RH-RhoGEFs).* J Biol Chem, 2014. **289**(28): p. 19737-46.
363. Itoh, H., et al., *Presence of three distinct molecular species of Gi protein alpha subunit. Structure of rat cDNAs and human genomic DNAs.* J Biol Chem, 1988. **263**(14): p. 6656-64.
364. Ko, E.M., Y.E. Leem, and H.T. Choi, *Purification and characterization of laccase isozymes from the white-rot basidiomycete Ganoderma lucidum.* Appl Microbiol Biotechnol, 2001. **57**(1-2): p. 98-102.
365. Zarbock, A., et al., *Galphai2 is required for chemokine-induced neutrophil arrest.* Blood, 2007. **110**(10): p. 3773-9.
366. Mikelis, C.M., et al., *PDZ-RhoGEF and LARG are essential for embryonic development and provide a link between thrombin and LPA receptors and Rho activation.* J Biol Chem, 2013. **288**(17): p. 12232-43.
367. Neptune, E.R. and H.R. Bourne, *Receptors induce chemotaxis by releasing the betagamma subunit of Gi, not by activating Gq or Gs.* Proc Natl Acad Sci U S A, 1997. **94**(26): p. 14489-94.
368. Strassheim, D., et al., *Modulation of bone marrow-derived neutrophil signaling by H2O2: disparate effects on kinases, NF-kappaB, and cytokine expression.* Am J Physiol Cell Physiol, 2004. **286**(3): p. C683-92.
369. Che, Y. and P.A. Khavari, *Research Techniques Made Simple: Emerging Methods to Elucidate Protein Interactions through Spatial Proximity.* J Invest Dermatol, 2017. **137**(12): p. e197-e203.
370. Yuyama, K., et al., *Translocation of activated heterotrimeric G protein Galpha(o) to ganglioside-enriched detergent-resistant membrane rafts in developing cerebellum.* J Biol Chem, 2007. **282**(36): p. 26392-400.
371. Mi, H., et al., *PANTHER version 7: improved phylogenetic trees, orthologs and collaboration with the Gene Ontology Consortium.* Nucleic Acids Res, 2010. **38**(Database issue): p. D204-10.
372. Boivin, B., et al., *G protein-coupled receptors in and on the cell nucleus: a new signaling paradigm?* J Recept Signal Transduct Res, 2008. **28**(1-2): p. 15-28.
373. Bhosle, V.K., J.C. Rivera, and S. Chemtob, *New insights into mechanisms of nuclear translocation of G-protein coupled receptors.* Small GTPases, 2019. **10**(4): p. 254-263.
374. Worthylake, R.A., et al., *RhoA is required for monocyte tail retraction during transendothelial migration.* J Cell Biol, 2001. **154**(1): p. 147-60.

375. Rojas, R.J., et al., *Established and emerging fluorescence-based assays for G-protein function: Ras-superfamily GTPases.* Comb Chem High Throughput Screen, 2003. **6**(4): p. 409-18.
376. Kuner, R., et al., *Characterization of the expression of PDZ-RhoGEF, LARG and G(alpha)12/G(alpha)13 proteins in the murine nervous system.* Eur J Neurosci, 2002. **16**(12): p. 2333-41.
377. Albert, P.R. and L. Robillard, *G protein specificity: traffic direction required.* Cell Signal, 2002. **14**(5): p. 407-18.